MUSCLE REGENERATION IN HYPOTHYROID CONTROL AND *MDX* DYSTROPHIC MICE

BY

LAURA MAUREEN McINTOSH

A Thesis
Submitted to the Faculty of Graduate Studies
in Partial Fulfillment of the Requirements
for the degree of

MASTER OF SCIENCE

Department of Anatomy
Faculty of Medicine
University of Manitoba
Winnipeg, Manitoba

ISBN 0-315-92257-5

Canada

Name LAURA MCINTOSH

Dissertation Abstracts International is arranged by broad, general subject categories. Please select the one subject which most nearly describes the content of your dissertation. Enter the corresponding four-digit code in the spaces provided.

ANATOMY

SUBJECT TERM

0287

SUBJECT CODE

U·M·I

Subject Categories

THE HUMANITIES AND SOCIAL SCIENCES

COMMUNICATIONS AND THE ARTS
Architecture 0729
Art History 0377
Cinema 0900
Dance 0378
Fine Arts 0357
Information Science 0723
Journalism 0391
Library Science 0399
Mass Communications 0708
Music 0413
Speech Communication 0459
Theater 0465

EDUCATION
General 0515
Administration 0514
Adult and Continuing 0516
Agricultural 0517
Art 0273
Bilingual and Multicultural 0282
Business 0688
Community College 0275
Curriculum and Instruction 0727
Early Childhood 0518
Elementary 0524
Finance 0277
Guidance and Counseling 0519
Health 0680
Higher 0745
History of 0520
Home Economics 0278
Industrial 0521
Language and Literature 0279
Mathematics 0280
Music 0522
Philosophy of 0998
Physical 0523
Psychology 0525
Reading 0535
Religious 0527
Sciences 0714
Secondary 0533
Social Sciences 0534
Sociology of 0340
Special 0529
Teacher Training 0530
Technology 0710
Tests and Measurements 0288
Vocational 0747

LANGUAGE, LITERATURE AND LINGUISTICS
Language
- General 0679
- Ancient 0289
- Linguistics 0290
- Modern 0291

Literature
- General 0401
- Classical 0294
- Comparative 0295
- Medieval 0297
- Modern 0298
- African 0316
- American 0591
- Asian 0305
- Canadian (English) 0352
- Canadian (French) 0355
- English 0593
- Germanic 0311
- Latin American 0312
- Middle Eastern 0315
- Romance 0313
- Slavic and East European 0314

PHILOSOPHY, RELIGION AND THEOLOGY
Philosophy 0422
Religion
- General 0318
- Biblical Studies 0321
- Clergy 0319
- History of 0320
- Philosophy of 0322

Theology 0469

SOCIAL SCIENCES
American Studies 0323
Anthropology
- Archaeology 0324
- Cultural 0326
- Physical 0327

Business Administration
- General 0310
- Accounting 0272
- Banking 0770
- Management 0454
- Marketing 0338

Canadian Studies 0385
Economics
- General 0501
- Agricultural 0503
- Commerce-Business 0505
- Finance 0508
- History 0509
- Labor 0510
- Theory 0511

Folklore 0358
Geography 0366
Gerontology 0351
History
- General 0578
- Ancient 0579
- Medieval 0581
- Modern 0582
- Black 0328
- African 0331
- Asia, Australia and Oceania 0332
- Canadian 0334
- European 0335
- Latin American 0336
- Middle Eastern 0333
- United States 0337

History of Science 0585
Law 0398
Political Science
- General 0615
- International Law and Relations 0616
- Public Administration 0617

Recreation 0814
Social Work 0452
Sociology
- General 0626
- Criminology and Penology 0627
- Demography 0938
- Ethnic and Racial Studies 0631
- Individual and Family Studies 0628
- Industrial and Labor Relations 0629
- Public and Social Welfare 0630
- Social Structure and Development 0700
- Theory and Methods 0344

Transportation 0709
Urban and Regional Planning 0999
Women's Studies 0453

THE SCIENCES AND ENGINEERING

BIOLOGICAL SCIENCES
Agriculture
- General 0473
- Agronomy 0285
- Animal Culture and Nutrition 0475
- Animal Pathology 0476
- Food Science and Technology 0359
- Forestry and Wildlife 0478
- Plant Culture 0479
- Plant Pathology 0480
- Plant Physiology 0817
- Range Management 0777
- Wood Technology 0746

Biology
- General 0306
- Anatomy 0287
- Biostatistics 0308
- Botany 0309
- Cell 0379
- Ecology 0329
- Entomology 0353
- Genetics 0369
- Limnology 0793
- Microbiology 0410
- Molecular 0307
- Neuroscience 0317
- Oceanography 0416
- Physiology 0433
- Radiation 0821
- Veterinary Science 0778
- Zoology 0472

Biophysics
- General 0786
- Medical 0760

EARTH SCIENCES
Biogeochemistry 0425
Geochemistry 0996
Geodesy 0370
Geology 0372
Geophysics 0373
Hydrology 0388
Mineralogy 0411
Paleobotany 0345
Paleoecology 0426
Paleontology 0418
Paleozoology 0985
Palynology 0427
Physical Geography 0368
Physical Oceanography 0415

HEALTH AND ENVIRONMENTAL SCIENCES
Environmental Sciences 0768
Health Sciences
- General 0566
- Audiology 0300
- Chemotherapy 0992
- Dentistry 0567
- Education 0350
- Hospital Management 0769
- Human Development 0758
- Immunology 0982
- Medicine and Surgery 0564
- Mental Health 0347
- Nursing 0569
- Nutrition 0570
- Obstetrics and Gynecology 0380
- Occupational Health and Therapy 0354
- Ophthalmology 0381
- Pathology 0571
- Pharmacology 0419
- Pharmacy 0572
- Physical Therapy 0382
- Public Health 0573
- Radiology 0574
- Recreation 0575
- Speech Pathology 0460
- Toxicology 0383

Home Economics 0386

PHYSICAL SCIENCES
Pure Sciences
Chemistry
- General 0485
- Agricultural 0749
- Analytical 0486
- Biochemistry 0487
- Inorganic 0488
- Nuclear 0738
- Organic 0490
- Pharmaceutical 0491
- Physical 0494
- Polymer 0495
- Radiation 0754

Mathematics 0405
Physics
- General 0605
- Acoustics 0986
- Astronomy and Astrophysics 0606
- Atmospheric Science 0608
- Atomic 0748
- Electronics and Electricity 0607
- Elementary Particles and High Energy 0798
- Fluid and Plasma 0759
- Molecular 0609
- Nuclear 0610
- Optics 0752
- Radiation 0756
- Solid State 0611

Statistics 0463

Applied Sciences
Applied Mechanics 0346
Computer Science 0984
Engineering
- General 0537
- Aerospace 0538
- Agricultural 0539
- Automotive 0540
- Biomedical 0541
- Chemical 0542
- Civil 0543
- Electronics and Electrical 0544
- Heat and Thermodynamics 0348
- Hydraulic 0545
- Industrial 0546
- Marine 0547
- Materials Science 0794
- Mechanical 0548
- Metallurgy 0743
- Mining 0551
- Nuclear 0552
- Packaging 0549
- Petroleum 0765
- Sanitary and Municipal 0554
- System Science 0790

Geotechnology 0428
Operations Research 0796
Plastics Technology 0795
Textile Technology 0994

PSYCHOLOGY
General 0621
Behavioral 0384
Clinical 0622
Developmental 0620
Experimental 0623
Industrial 0624
Personality 0625
Physiological 0989
Psychobiology 0349
Psychometrics 0632
Social 0451

MUSCLE REGNERATION IN HYPOTHROID CONTROL AND MDX DYSTROPHIC MICE

BY

LAURA MAUREEN MCINTOSH

A Thesis submitted to the Faculty of Graduate Studies of the University of Manitoba in partial fulfillment of the requirements of the degree of

MASTER OF SCIENCE

TABLE OF CONTENTS

ABSTRACT

The *mdx* mouse, a model for human Duchenne muscular dystrophy (DMD), is excellent for studying dystrophic processes and muscle regeneration dynamics. In order to devise treatments for DMD, it is important to decide what might promote or inhibit successful regeneration. Thus, the effects of hypothyroidism (created by 0.05% propylthiouracil-PTU in drinking water for 4 or 8 weeks) were studied in *mdx* and age-matched control mice. Histological, morphometric, immunocytochemical and autoradiographic (to detect DNA synthesis) techniques were used to study dystrophy in the *mdx* mouse, and muscle regeneration in control and *mdx* tibialis anterior muscle (TA) after a crush injury. Recovery after the crush injury progressed as previously reported, and was almost complete by 15 days post-injury in all groups. The remainder of the experiments were performed on mice allowed to recover for 4 days. Hypothyroidism worsened the phenotype of *mdx* mice to resemble DMD more closely. As well, muscle repair from crush injury in hypothyroid *mdx* mice exhibited decreased myotube formation and delayed debris removal. In contrast, control TA did not appear to be as affected by hypothyroidism. Double-immunocytochemical staining with anti-neural cell adhesion molecule and anti-basic fibroblast growth factor antibodies was not specific for muscle precursor cells in the injured TA, as initially hoped. Autoradiography results showed that the proportion of labelled myotube nuclei was less, but the proportion of total labelled cells was more, in treated compared to untreated animals. Results suggest that prolonged replication by precursor cells and delayed fusion produces fewer myotubes in regenerating hypothyroid *mdx* muscle.

ACKNOWLEDGEMENTS

There are so many people that have encouraged and helped me through my degree and I would like to attempt to thank each of them (not an easy task!). These advisors, colleagues, friends and family have made my experience as a Master's student very enjoyable, so much in fact that I have decided to stay on to do a PhD!

First, I would like to thank Dr. Judy Anderson, my advisor and friend, for her endless enthusiasm in my work and ideas. She took a person with no idea of what scientific research was and developed a person who passed a Master's degree. It never ceases to amaze me how she can concentrate on so many things at once and excel in them, while remaining to be a very approachable wonderful person! I feel fortunate to have had (and continue to have) such a remarkable advisor.

I would like to thank the Anatomy department for their support in the form of a travel allowance and scholarships. Also, thanks to the faculty members, support staff and students of the Anatomy department for their encouragement and helpful comments.

The members of my examining committee: Dr's Greenberg, Thliveris, and Paterson deserve a big thank-you for their very valuable comments and suggestions about my work. They managed to once again enthuse me about muscular dystrophy and about research in general.

I would like to thank the Medical Research Council of Canada (Studentship) and the Thyroid Foundation of Canada (Summer Student Scholarship) for their financial support which allowed me to study on a full-time basis.

With the expertise of Mr. Roy Simpson, photographs were made to look exceptional on a tight deadline and I am very grateful for his assistance.

Without the members of the lab, my days would have been much less exciting and I would like to thank each of them for their never ending words of encouragement and friendship. Thanks to Kerryn for her kind ear on all sorts of matters and advice on the technical aspects of the thesis experiments and writing (remember I expect a call from Australia). To Annyue for her always upbeat mood and cheering from the sidelines (we'll have to cheer and calm each other in Montreal before the talks!). To Andrea for technical assistance and thoughtful conversations about results. It was nice to have someone at the same stage in the game that appreciated what I was going through (don't panic about your transfer). Also I'd like to thank the previous members of the lab. To Karen for her coaching about "what to expect" and also for checking up on me every so often to make sure I was still writing (by the way, no more cats!). To Marianne for her words of encouragement, especially when I was trying to master that cryostat (congrats doc, we graduate at the same ceremony!). Finally, I'd like to thank Steven and Micheal.

Without the support of my family and my in-laws, life in the big city would have been much less enjoyable. Thanks to my Dad, Mom and sister Karen for their endless questions and interest in what exactly I was doing. I sure appreciated their support even when they didn't quite understand (and fell asleep!). My family allowed me to make my own decisions and grow, while giving me the quiet encouragement that I needed to do it.
I would also like to thank Mom and Dad Sims, Sherry & Brett, Roxy & Dale, Brad & Donna and Cam for their encouragement (I'm a "Scientist" not a mouse doctor). Also, thanks to Auntie Mary for the many meals that kept us going and for her interest in my studies.

Last, but not least, I'd like to thank my husband and "brick", Warren. If it wasn't for him, I'd still be making photographic plates, spell-checking and checking the bibliography. Thanks for your patience, tolerance and curiosity about what I was trying to do. You were always there for me at the end of the day (or early in the morning, after spending 24 hours at the computer) to offer a word of encouragement (and to make me a cup of tea!).

I would like to dedicate this work to my mother. I hope that I do make you proud mom.

LIST OF ABBREVIATIONS

bFGF	basic fibroblast growth factor
DMD	Duchenne muscular dystrophy
ECM	extracellular matrix
EGF	epidermal growth factor
IGF	insulin-like growth factor
MDGF	macrophage-derived growth factor
MHC	myosin heavy chain
mpc	muscle precursor cell
MRF	muscle regulatory factor
NCAM	neural cell adhesion molecule
NMJ	neuromuscular junction
PDGF	platelet-derived growth factor
poly	polymorphonuclear leukocyte
PTU	propylthiouracil
TA	tibialis anterior
TGF-ß	transforming growth factor-beta
TSH	thyroid stimulating hormone

1. INTRODUCTION

Skeletal muscle is the mechanically active part of the musculo-skeletal system and it is specifically organized for movement. It makes up the bulk of the adult human body, comprising about 45% of its total weight. The specific developmental pattern of skeletal muscle results in variety and uniqueness in each mature muscle. Much of what is known about the potential or capacity of skeletal muscle to repair itself after injury is based upon our knowledge of muscle development.

The focus of this study is on muscle regeneration in an animal model of Duchenne muscular dystrophy (DMD), the *mdx* mouse. The *mdx* mouse is genetically identical to DMD, in that both diseases are X-linked dystrophin-deficiencies. However, the ability for muscle regeneration is gradually lost in DMD, with subsequent replacement of muscle with fibrous and adipose tissue, while the *mdx* mouse maintains the capability for successful regeneration. Ultimately, DMD is fatal; *mdx* dystrophy is not.

It is of interest to characterize the factors imperative for successful muscle regeneration when considering treatment for DMD. The *mdx* mouse serves as a good model for this, particularly since negative changes in the regenerative capacity can be clearly observed without interference by fibrosis and adipose tissue formation. For instance, adequate levels of certain growth factors and hormones are required in order for muscle regeneration to progress normally.

Basic fibroblast growth factor (bFGF) plays a role in promoting proliferation and inhibiting fusion of muscle precursor cells (mpcs), and may be an important factor in promoting *mdx* regeneration, since it is found in higher amounts in *mdx* than control muscles. Neural cell adhesion molecule (NCAM) is another important factor, and probably helps in cell recognition and fusion in regenerating muscles.

Thyroid hormone is important in muscle development and maturation. However, its roles in regeneration are less well defined. It is suggested

that any change in the balance of thyroid hormone will change a muscle's response to damage. Excess thyroid hormone (hyperthyroidism) in *mdx* muscles worsens dystrophic damage and possibly repair. In this study, the consequences of lack of thyroid hormone (hypothyroidism) are examined in *mdx* and control mice.

2. REVIEW OF LITERATURE

2.1 SKELETAL MUSCLE STRUCTURE (ADULT)

The normal morphology of skeletal muscle, as seen through the light microscope, is considered in this section. It will become evident that in understanding muscle structure, a knowledge of muscle development is helpful (section 2.2).

2.1.1 Light microscopic histology of skeletal muscle

A mature muscle cell is termed a myofiber. It is a long cylindrical cell consisting of numerous ovoid peripheral nuclei, a sarcolemma (plasma membrane) and sarcoplasm (cytoplasm) which is occupied centrally by myofibrils and peripherally by organelles. Myofibers may extend for many centimeters (they may be as long as the entire muscle), and they insert into tendinous extensions or intersections within connective tissue.

In cross-section, myofibers are rounded or polygonal in shape. They are 10-100μm in diameter in the human. In normal adult muscle, up to 3% of all myofibers may be centrally nucleated (Swash & Schwartz, 1984). Satellite cells (see section 2.3.3) are important cells that are located between the external lamina and the sarcolemma of myofibers. They are hard to distinguish under the light microscope and may be mistaken for peripheral nuclei.

Each myofiber is independent and surrounded in a delicate network of connective tissue, the endomysium. Bundles of myofibers, or fascicles, are surrounded by stronger connective tissue layers called perimysium. The fascicles are surrounded by another thick connective tissue layer, the epimysium, and it is this layer that delineates each named muscle of gross anatomy. Almost every muscle is attached at 2 different bones by tendons, and bridges at least 1 joint.

Muscle tissue consists of more than just myofibers: many blood capillaries, lymphatics (not in the endomysium) and nerves run in the

fibroconnective tissue surrounding them. Each myofiber is surrounded by 2 to 5 capillaries, depending upon the type of fiber. One terminal motor nerve fiber joins a single myofiber at the neuromuscular junction (NMJ). One neuron may have an axon that branches to innervate hundreds of myofibers. Muscle spindles, the sensory (length-tension) receptors, are located in the perimysium of most human skeletal muscles, primarily muscles with fine motor control (Calpan et al., 1988).

Myofibers are composed of myofibrils which give the fiber its characteristic striated appearance. Skeletal muscle stained for light microscopic observation has a unique pattern of A- (dark or anisotropic) bands and I- (light or isotropic) bands. A Z-line bisects each I-band, and the functional unit of contraction, the sarcomere, lies between two Z-lines. Also, a lighter area is present in the A-band, called an H-band. Myofibrils are composed of myofilaments whose distribution results in a cross-banding pattern. Myofilaments are of three types: thick, thin and intermediate. The thick filaments consist mainly of myosin and form the A-bands. Thin filaments are composed of actin, tropomyosin and troponin, and extend from each side of the Z-line through the adjacent I-bands and part way into the A-band, interdigitating with the thick filaments. The H-band is simply the area in the centre of the A-band free of thin filaments. The thick filaments have bridge-like structures (the heads of myosin filaments) extending radially toward the thin filaments, and they "slide" upon each other in contraction. Discussion of other myofiber organelles and membranes (t-tubules, sarcoplasmic reticulum, ribosomes and mitochondria) is omitted since their small size precludes observation by typical light microscopy.

A sarcomere is the functional unit underlying contraction. The myofibrillar apparatus accomplishes force generation while the membrane components - transverse (T) tubules and sarcoplasmic reticulum (SR) - are responsible for its control. The arrangement of several thousand sarcomeres in series and their coordinated activation in response to a

stimulus from the motor neuron allow the rapid shortening and force generation of the muscle fiber (Flucher, 1992).

2.1.2 Fiber typing

Different skeletal muscles exhibit variations in structure, innervation, physiology, biochemistry and vascularity. These variations result from compositional differences in the myofibrils. There are many different fiber classification schemes (reviewed in Pette & Staron, 1990) - the one most widely accepted will be briefly outlined. It is important to realize that there is a multiplicity of fiber types and that the dynamic nature of muscle makes it difficult to categorize fibers into distinct units.

Basically, myofibers can be divided into two types: type I and type II (subtypes IIA, IIB, IIC, IIM and IIX). The content, biochemistry and energetics of myosin heavy chain (MHC) molecules and isoforms of many other muscle-specific molecules, account for the characteristics of individual fiber types. **Type** I myofibers are oxidative, slow-twitch, and fatigue resistant. They exhibit many mitochondria and have a low content of glycogen and glycolytic enzymes. Slow MHC isoforms are present. **Type IIA** myofibers are fast twitch, oxidative fibers. They contract faster than type I fibers, have more mitochondria and are more fatigue resistant than type IIB fibers. **Type IIB** fibers are fast contracting, but rely more on glycolytic than oxidative pathways for energy production. Both type IIA and IIB fibers have pure fast MHCs, but the isoforms are immunologically distinct. **Type IIC** fibers contain both fast MHCs and are thus termed intermediate fibers. They also are relatively primitive and have the capability of differentiating into type IIA or IIB. **Type IIM** fibers are found in mainly the jaw muscles of mammalian carnivores and are considered "superfast" fibers. **Type IIX** (sometimes referred to as type IID) fibers are also considered intermediate in character between type IIA and IIB fibers (Haemaelaeinen & Pette, 1993) and may be mistaken for type IIB

fibers. The motorneuron plays an important role in determining the fiber type of skeletal muscle (Pette & Staron, 1990).

2.2 DEVELOPMENT OF SKELETAL MUSCLE

The specific developmental pattern of skeletal muscle results in the variety and uniqueness of each mature muscle. Normal development of skeletal muscle in mammals occurs in three distinct phases: i) commitment (or determination) of cells to the muscle lineage, ii) proliferation of the myoblasts and iii) terminal differentiation of cells into a mature state. These events seem to be highly dependent on a group of muscle regulatory factors (MRFs) (section 2.2.5).

2.2.1 Commitment of muscle precursors

As defined by Stockdale et al. (1989), commitment is a heritable change in the genetic structure of a cell that irreversibly restricts the subsequent fate of the cell before it manifests a differentiated phenotype. The skeletal muscle lineage (reviewed by Stockdale, 1992) is committed from a group of mesodermal stem cells, and the committed cell is called a myoblast. The first muscle precursor cells (mpcs) are found in the somite of the developing embryo within a compartment called the myotome. Myoblasts migrate to invade future muscle territories while they divide, and ultimately form the majority of the limb and trunk musculature. Cervical and craniobulbar muscles arise from the branchial arches.

It is thought that the establishment of the muscle phenotype is dependent on myogenic "master" genes that control all later events (Pinney et al., 1990). A likely candidate is the recently identified family MRFs (section 2.2.5). Cells expressing these MRFs are first detected in the somite. As each stage of development progresses, groups of muscle-specific genes are activated that first determine and then regulate muscle function.

2.2.2 Proliferation of new myoblasts

Committed myoblasts undergo mitosis, amplifying the myoblast population. The main ingredients influencing proliferation *in vitro* are serum and embryo extract components, growth factors and oncogenic signals

(reviewed by Olson, 1992). Two of the most extensively characterized growth factors which stimulate proliferation in culture are bFGF (Clegg et al., 1987) (section 2.7) and insulin-like growth factors (IGF-I, IGF-II and insulin) (Florini & Magri, 1989). The *in vivo* role of these growth factors is less well-known.

It appears that there is rich diversity among the myoblast population. Many subtypes of myoblasts (such as somitic, embryonic and fetal) can be detected through characterization of MHC expression. Pin & Merrifield (1993) report that embryonic and fetal rat myoblasts express different phenotypes *in vitro* and they may represent distinct myoblast lineages. In contrast, Dusterhoft et al. (1990) find no evidence of satellite cell diversity *in vitro*.

2.2.3 Withdrawal from the cell cycle

Proliferation and differentiation are two distinct events. A myriad of opposing positive and negative signals help to determine whether a myoblast will remain in the cell cycle, or withdraw from it and begin to terminally differentiate (reviewed by Olson, 1992). These signals include growth factor expression, hormonal presence and the expression of the MRF family.

In culture, differentiation is repressed by serum and exogenous growth factors, such as bFGF (Clegg et al., 1987) and TGF-ß (Olson et al., 1986), held at a critical level. Recently, it has been suggested that endogenous bFGF promotes proliferation as well as exogenous bFGF (Moore et al., 1991). Basic FGF can block differentiation even when it is not mitogenic, and TGF-ß is probably not mitogenic, hence the inhibitory effects of these growth factors appear to be independent of their roles in proliferation (Olson et al., 1986). It appears that the MRF genes act as targets for growth factors, such that the stimulus to differentiate is modulated by the growth factor-MRF interaction (Moore et al., 1991). Myoblast fusion can also be inhibited by BrdU, calcium chelating agents and overexpression of certain proto-oncogenes (reviewed by Bishopric et

al., 1992).

At some point, the activators of differentiation override the inhibitory factors and cells differentiate rather than continuing to proliferate. Expression of bFGF is down-regulated at the transcriptional level during myogenic differentiation in cultured myocytes (Moore et al., 1991). Activation of the MRF family (Olson et al., 1991) and the disappearance or down-regulation of surface receptors for mitogens on myogenic cells (Moore et al., 1991; Olwin & Hauschka, 1988) also occurs. When expressed at very high levels, the MRF family can override mitogenic signals and cause growth arrest, independent of differentiation (Olson et al, 1991). IGFs are stimulators of terminal differentiation (Florini & Magri, 1989), and therefore the previous generalizations that mitogens inhibit differentiation are not valid (Florini & Magri, 1989). Increased expression of other proteins, such as desmin (an intermediate filament protein) and H36 (an integral membrane protein) in post-mitotic myoblasts (Kaufman, 1991), also stimulate differentiation. Differentiation can occur only when cells are growth arrested at the G0/G1 stage of the cell cycle.

2.2.4 Terminal differentiation of muscle fibers

After myoblasts have withdrawn from the cell cycle, they assemble in a row and fuse to form a long cell with central nuclei called a myotube. Fusion of mononuclear myoblasts to one another involves the expression of certain cell adhesion molecules which act in cell recognition and adhesion. Neural cell adhesion molecules (NCAM) play a role in fusion (section 2.4). A residual specialized population of myoblasts does not fuse, but remain as single cells positioned between the external lamina and the myotube periphery. These are myo-satellite cells. Satellite cells can be activated to replicate during regeneration and repair after birth (Kaufman, 1991) (section 2.3.3). Activation of certain muscle specific genes (Miller et al., 1993) allows the formation of the contractile machinery (reviewed by Bandman, 1992). The fusion of myoblasts is not a prerequisite for the early initial development of the contractile

machinery, however the transition of myoblast to myotube is accompanied by an enormous synthesis of proteins of the contractile system (Kaufman, 1991).

As myotubes mature, they undergo modulation. Modulation is defined as a reversible change in the phenotype of a cell, which occurs within limits set by the particular commitment of a cell, and which occurs after a cell differentiates (Stockdale et al., 1989). This modulation allows the manifestation of multiple phenotypes to be dependent upon a number of different stimuli. The diverse phenotypes of myofibers depend partly upon innervation, but nerve supply is not a prerequisite in all stages of muscle development. Other factors which influence muscle fiber type to various degrees are hormones (for example thyroid hormone, section 2.8), growth factors, isoforms of contractile proteins (myosin, actin, troponin, tropomyosin) (Bishopric et al., 1992) and functional demands. Some authors extend these features to suggest that the different fiber types may also be reflected in distinct subpopulations of myoblasts or muscle precursors (Pin & Merrifield, 1993; Miller et al., 1993; Kaufman, 1991).

Myotube formation is a crucial step in myogenesis. In small laboratory animals, such as rodents, myotube formation is biphasic. Ontell et al. (1987; 1988) have extensively characterized primary and secondary myotubes in the mouse soleus and extensor digitorum longus muscles. Primary myotubes, formed from the fusion of embryonic myoblasts, run from tendon to tendon in the muscle and provide a framework for subsequent formation of secondary myotubes. Primary myotubes appear to be densely innervated in the rat (Sheard et al., 1991), but their formation is nerve-independent. Secondary myotubes form when 2 mononucleate fetal myoblasts fuse in the vicinity of the endplate of the primary myotube. It is debatable as to whether initiation of secondary myotube formation is nerve-dependent (Draeger et al., 1987) or independent (Sheard et al., 1991). The secondary myotubes grow longitudinally along the surface of primary myotubes, acquiring more nuclei as myoblasts progressively fuse.

Secondary myotubes connect with tendons and separate laterally from the primary myotube. The number of fibers in an adult muscle depends on the number of primary myotubes first formed and the number of secondary myotubes that form around each primary (Wilson et al., 1992).

In larger mammals, such as sheep (Wilson et al., 1992) and humans (Draeger et al., 1987), it is suggested that the secondary generation of myotubes form at endplate sites in a series arrangement along the length of a single primary myotube, and that tertiary, and possibly later generations of myotubes in their turn, use the earlier generation of myotubes as a scaffold. The ratio of adult muscle fibers to primary myotubes is 70:1 in sheep (Wilson et al., 1992), thus it seems unlikely that every later generation myotube uses a primary myotube as a scaffold. Precise timing of NMJ formation and structural maturation has not been extensively investigated. However, the first embryonic movements probably reflect functionally active NMJs (Carpenter & Karpati, 1984) with spontaneous quantal transmitter release.

Fiber growth occurs by the addition of further mononucleated cells to the sides and ends of a fiber. As growth in diameter occurs, the central myotube nuclei move to the periphery, and myofibrils assume a central position. Ultimately, the formation of muscles requires the interplay and cooperation of many cell types: connective tissue, nervous system, bone, cartilage and vasculature. The molecular mechanisms by which the shape of whole muscle architecture is determined remains unknown, but connective tissue cells seem to direct patterning (Miller et al., 1993).

2.2.5 Muscle regulatory factors (MRFs)

MRFs are an intriguing group of proteins. When expressed, MRFs can generate a complete differentiated muscle phenotype which requires the activation of many genes. MRFs have the potential to convert fibroblasts and other non-myogenic cell types to cells that express muscle-specific genes *in vitro* (Olson et al., 1991). They are normally expressed exclusively in skeletal muscle and can induce myogenesis in transfected

10T1/2 cells (a clonal mouse embryo fibroblast cell line) (Stockdale, 1992; Olson, 1992). These amazing capabilities *in vitro* suggest that the typical development of skeletal muscle *in vivo* depends on characteristic sequences of functional expression of these genes.

The MRFs include four factors: MyoD; myogenin; Myf-5; and MRF-4 (reviewed by Miller et al., 1993). Another gene, *myd* (Pinney et al., 1988), is sometimes included with the MRFs, but few studies are reported. The MRFs form heterodimers in the nucleus and activate genes by binding (directly, or indirectly through other transcription factors) to a DNA region called the E-box (Olson et al., 1991). The regulatory factors have a homology region of 68 amino acids (called *myc*) responsible for DNA binding and mediation of dimerization (Olson et al., 1991). This region on its own appears to be capable of inducing the formation of myoblasts from 10T1/2 cells (Tapscott et al., 1988) and from other undetermined cell types.

It seems that each MRF has a specific function in myogenesis, although an overlapping redundancy in their functions is suggested. In the normal development of mouse muscle, Myf-5 mRNA is first detected in the dermomyotome of the cranial somites at day 8 of gestation (E8), prior to the expression of any known muscle marker protein or other MRFs. Myogenin expression occurs 12 hours later, with MRF-4 soon following (at about E9). At this time, some muscle specific-proteins can be recognized. Finally, MyoD and other contractile proteins appear in the differentiated myotomal cells. Myf-5 and MRF-4 occur transiently in early somites, and MRF-4 reappears later in the limb muscles of the fetus and adult (Bober et al., 1991). Myogenin and MyoD continue to be expressed at high levels throughout embryonic and fetal development, although in progressively more caudal and distal muscles, until their expression is downregulated in the postnatal period (reviewed by Braun et al., 1992).

Recent studies have explored the results of inactivating certain of the MRF genes in transgenic knockout mice. Surprisingly, the deficiencies

of Myf-5 (Braun et al., 1992) and MyoD (Rudnicki et al., 1992) result in mild abnormalities in the skeletal muscle of newborn mice. Mice missing MyoD are viable and fertile. However, the redundancy in the genome is illustrated since Myf-5 mRNA is found in greater amounts in MyoD knockouts than in controls. That overexpression also seems to compensate for the loss of MyoD. Also, the first appearance of muscle-specific markers is delayed in MyoD knockout mice. Although mutant mice lacking Myf-5 have apparently normal skeletal muscle structure at birth, they cannot breathe when born due to the absence of a major portion of the ribs, in that only the heads of each rib are present and attached to the vertebrae.

A genetic deficiency of myogenin in mice (Hasty et al., 1993; Nabeshima et al., 1993) results in much greater defects in skeletal muscle. The mutant animals survive fetal development, but die immediately after birth and show a severe reduction of skeletal muscle (although there are a few poorly formed muscle fibers), indicating that myogenin encourages terminal differentiation. Studies of double knockouts for MyoD and Myf-5 should prove interesting.

The above researchers and Smith et al. (1993) conclude that there is a spatio-temporal pattern of expression of Myf-5, myogenin, MRF-4 and MyoD. The spatio-temporal expression of MRFs suggests that they may subserve different aspects of muscle development during embryogenesis. We can only conclude that MRFs are part of a complex auto- and cross-regulatory network in which the activity of one member regulates its own expression and/or the expression of other MRFs. Other, as yet unidentified, tissue-specific factors are likely to act upstream, downstream or in parallel with the expression of members of the MRF family to regulate muscle commitment, proliferation and differentiation.

2.3 SKELETAL MUSCLE REGENERATION

Skeletal muscle has a remarkable capacity to repair itself. That process is termed regeneration, the formation of essentially normal tissue. Much of what is known about the potential for restoration of skeletal muscle following injury is based on our knowledge of muscle development, combined with investigations of the cellular and molecular events during muscle regeneration after various injuries. Thus, regeneration is much like embryonic development of muscle (section 2.2), but does not exactly recapitulate it. In order for skeletal muscle to regenerate, certain factors are required: myoblastic cells, adequate vascularity, adequate number and distribution of motor and sensory neurons, appropriate mechanical environment, a remnant external lamina, the presence of nonmyogenic repair cells, and a space occupying matrix that stimulates migration, proliferation and differentiation of myoblastic cells (Calpan et al., 1988).

The events in muscle regeneration will be discussed with special attention to human and mouse regeneration (reviewed by Grounds, 1991; Calpan et al., 1988; Allbrook, 1981; Carlson, 1973). Also, a specific technique for studying muscle regeneration will be highlighted (the crush injury). The essential process of regeneration is similar irrespective of the cause of injury, but the outcome and time course of regeneration vary according to type, severity and extent of injury, age of the animal, and in some cases, the species of animal.

2.3.1 Review of terms used in muscle regeneration

A "presumptive myoblast" refers to a suspected muscle precursor cell which lacks evidence of cytoplasmic filamentous muscle proteins. A "myoblast" is a muscle precursor cell confirmed by the presence of thick and thin myofilaments in the cytoplasm. It is spindle-shaped and often located between degenerating fibers and the external lamina. However, they are not reliably identified using light microscopy and routine staining. "Mononuclear muscle precursor cell (mpc)" is a general term which includes

satellite cells, presumptive myoblasts and myoblasts. "Myotubes" are centrally multinucleated young muscle fibers. The term "myogenic cells" includes mpcs, multinucleated myotubes and myofibers, the cells of the muscle lineage (from Robertson et al., 1990).

2.3.2 Degeneration and removal of injured muscle

After an insult to skeletal muscle, intrinsic degeneration occurs, characterized by membrane damage, disruption of sarcomeres at the Z-bands, mitochondrial swelling and nuclear pyknosis. Damage to the sarcolemma of the myofiber results in increased intracellular calcium and activation of complement (Orimo et al., 1991). These conditions disrupt the normal ionic balance of the myofibers and induce widespread necrosis. The sarcoplasm of the ruptured myofiber is then exposed to the extracellular matrix (ECM), and extracellular molecules enter the interior of the fiber (Grounds, 1991). Subsequently, active production of new sarcolemma occurs, which contributes to the formation of the part of the sarcolemma that demarcates the viable portion of the myofiber from the injured area (Papadimitriou et al., 1990). In experimental damage to mouse muscle, myofiber resealing is seen by 8 hours after injury and the majority of myofibers are resealed by 24 hours (Papadimitriou et al., 1990). Resealing is purely a function of local cells and is not dependent upon infiltrating leukocytes (Robertson et al., 1992).

Meanwhile, cell-mediated fragmentation of damaged myofibers occurs, mainly by phagocytic macrophages. The timing of phagocytic cell entry depends upon the vascularity of the damaged myofiber. Vascular sprouts grow into the degenerated mass, and not until this has occurred can phagocytes invade the area. Robertson et al. (1993) suggest that chemotactic factors from the damaged myofibers attract the phagocytic cells to the site of injury. Polymorphonuclear leukocytes (polys) play an immediate role in the removal of necrotic debris. If little damage occurs to the local blood supply, polys enter about 3 hours after injury in the mouse (Schmalbruch et al., 1976). The number of polys peak at about 12

hours after injury (Orimo et al., 1991), and by 24 hours post-injury they are no longer conspicuous (Schmalbruch, 1976). Macrophages enter by between 6 and 12 hours post-injury, with a maximum level at about 2 days (Orimo et al., 1991). Macrophages do not vacate the area until all contractile filament and other cytoplasmic debris is removed.

The efficiency of revascularization generally relates to the extent of fibrosis and calcification in the muscle after injury (Grounds, 1991). In areas far removed from the blood supply, necrosis sets in and degeneration occurs in the absence of an intracellular phagocytic reaction. Many factors stimulate revascularization, usually by increasing endothelial cell proliferation. Such angiogenic factors are bFGF (section 2.7), chemoattractants (like complement) in the area of damage, and prostaglandins. If no revascularization occurs, minimal regeneration results.

The integrity of the external lamina is important for muscle regeneration. The remaining external lamina acts as a scaffold for reconstruction of regenerating myofibers, maintains a microenvironment favorable for regeneration, and at the same time, excludes fibroblasts and the majority of newly forming collagen fibers from interfering with regrowth (Grounds, 1991).

2.3.3 The origin of myogenic repair cells

Once the removal of old myofibers is well underway, a population of activated spindle-shaped mpcs appear beneath the external lamina. The origin of these cells and their mode of activation in regenerating muscle fibers is of great interest and debate. No resolvable structural markers are available at the light microscopic level which can identify the source of the undifferentiated mpc proliferating *in vivo*, or which can positively distinguish early mpcs from other mononuclear cells present in regenerating tissue.

When deciding upon the **origin** of mpcs, one must consider 3 theories offered by Grounds (1991), each of which will be considered in turn: i)

myoblasts in regenerating muscle arise from myonuclei that separate off from dedifferentiated muscle fibers, ii) satellite cells are reserve cells with myogenic capacity and they become activated after muscle damage, and iii) mpcs are derived from circulating mononucleated cells produced in remote places from injured tissue. The question arises as to whether highly differentiated cells can act on their own behalf in repair (i.e. myonuclei) or whether an infusion or activation of new cells from a normally dormant population regulates repair (i.e. satellite cells).

Mpcs from myonuclei: Proponents of this idea (Naidoo, 1992; Mastaglia et al., 1975; Reznik, 1969) believe that peripheral nuclei break off from damaged myofibers, become completely invested with a cell membrane and serve as the cellular source of regenerating myofibers. In order to do this, the nuclei must dedifferentiate, because adult myonuclei are postmitotic and are incapable of DNA synthesis or mitosis. Naidoo (1992) feels that myonuclei are transformed into myoblasts during muscle regeneration, and that the presumptive myoblast produced from a myonucleus is a stage in the development of the satellite cell. However, in view of questionable electron micrographs, his conclusions are disregarded. Thus, currently there is little evidence that myonuclei can participate in regeneration, but the possibility has not been completely disproved.

Mpcs from satellite cells: Proponents of this idea (Snow, 1981; Schmalbruch, 1976; Moss & Leblond, 1971; Mauro, 1961) believe that the myonuclei of damaged muscle cannot reactivate their own synthetic or replicative processes, or even survive degeneration. Instead, a population of undifferentiated quiescent cells with myogenic potential (satellite cells) is activated to proliferate and forms a population of myoblasts which may subsequently fuse to form new myofibers.

Satellite cells are mononucleated, spindle-shaped cells with ovoid nuclei that are located between the external lamina and the sarcolemma of adult muscle tissue. Heterochromatin appears in the nucleus, there is scant cytoplasm, no sarcomeric myofilaments are present, but they contain

some actin and myosin and thus are probably capable of some migratory movement beneath the external lamina (Schultz et al., 1988). Upon activation, quiescent satellite cells re-enter the cell cycle, and their nuclear heterochromatin is reduced as an EM marker for the activation (Snow, 1981). When and from what source satellite cells are derived remains a mystery (Allen & Rankin, 1990). Dusterhoft and colleagues (1990) report that there is no evidence for the existence of satellite cell diversity among rat muscle of different fiber type composition *in vitro*. Other investigators (Feldman & Stockdale, 1991) report that satellite cells are of different types and that fast and slow muscles differ in the percentage of each type they contain.

Various studies have proven that satellite cells are the source of myoblasts in regenerating muscle. The simple fact that satellite cells are absent in cardiac muscle supports their role in regeneration, since cardiac muscle cells cannot proliferate or regenerate after they are mature. Snow (1977) reports that repeated trauma seems to increase the numbers of satellite cells at the trauma location and that as a result, regeneration occurs faster. Also, the number of satellite cells (Snow, 1977) and the proliferative potential of satellite cells (Mezzogiorno et al., 1993) in rats and mice decrease with advanced age, and this reduction appears to result in slower regeneration of old muscle after insult (Sadeh, 1988).

It is uncertain whether satellite cells originate within the region of damage or if they migrate from outside sources. Some researchers (Carlson, 1986; Hansen-Smith & Carlson, 1979) believe that after an injury, satellite cells remain in the area, withstanding the damaging environmental influence and ischemia, and directly and immediately contribute to regeneration. Others (Schultz et al., 1988) believe that satellite cells migrate from the ischemic core of an injury to more peripheral regions after insult, and are among the population of single cells that accompany ingrowing vasculature. It is also thought that

satellite cells from remote uninjured muscle can migrate to the area of repair upon focal injury (Grounds et al., 1992a; Allen & Rankin, 1990; Watt et al., 1987) and that the actual site of injury contributes relatively few cells (Grounds et al., 1992a). It could be that the survival of satellite cells in the injured area depends on the severity and extent of injury, but it appears that subsequent establishment of a growing population of mpcs requires the effective simultaneous growth of a blood supply.

Since Mauro's initial description of satellite cells in 1961, most researchers believe that satellite cells contribute to, and are necessary for, regeneration (Allbrook, 1981). However, the extent of the contribution remains to be elucidated. It may be that all satellite cells do not have the same potential to form muscle and that they may not be the only source of mpcs in injured mature muscle (Watt et al., 1987).

Mpcs from other areas: It has been suggested that a third source of mpcs is derived from circulating mononucleated cells produced in remote places from injured tissue (reviewed in Grounds, 1991). There are numerous reports that various cells of mesodermal (particularly fibroblasts and adipocytes) and neuroectodermal origin can give rise to mpcs under certain conditions (see Grounds, 1991). In particular, the thymus may be involved in producing mpcs (Grounds et al., 1992b). MyoD and myogenin genes are expressed in the thymus of adult mice, and this is the first report in higher vertebrates of MyoD and myogenin expression in a tissue other than skeletal muscle (Grounds et al., 1992b).

MRFs and identification of mpcs: The discovery of the MyoD family of MRFs (section 2.2.5) may be the key to identifying presumptive myoblasts and mpcs. MyoD and myogenin appear to be markers for the very early identification and study of activated mononuclear skeletal mpcs in muscle regenerating *in vivo* (Grounds et al., 1992a; Fuchtbauer & Westphal, 1992). Their expression in regeneration is very similar to the pattern shown in development (section 2.2.5). MyoD and myogenin are not detected

(Fuchtbauer & Westphal, 1992), or infrequently detected (Grounds et al. 1992a), in mononuclear cells of noninjured muscle. The use of in situ hybridization shows increased MyoD and myogenin mRNA sequences in mononuclear cells as early as 6 hours post-injury, a peak in mRNAs between 24 and 48 hours, and thereafter a decline to pre-injury levels at about 8 days (Grounds et al., 1992a). MyoD and myogenin mRNAs are located in mononuclear cells some distance from the site of crush and eventually migrate in toward the crush site as the inflammatory cells migrate inward. Grounds et al. (1992a) conclude that the positive cells are probably initiating replication at the same time as they are expressing MyoD and myogenin genes, and that the genes play a small part during fusion. The use of immunocytochemistry shows that 10-20% of nuclei are positive for both MyoD and myogenin in degenerating muscle fibers after grafting (Fuchtbauer & Westphal, 1992). In contrast to the findings of Grounds et al. (1992a), all nuclei in newly fused myotubes are positive, and positive nuclei persist for at least 2 weeks in regenerated myofibers (Fuchtbauer & Westphal, 1992). This could be due to the difference between protein and mRNA expression (Garrett & Anderson, personal communication). Fuchtbauer & Westphal (1992) suggest that MyoD and myogenin play active roles in terminal differentiation of muscle fibers, and that the other MRFs (MRF-4 and Myf-5) may be responsible for the commitment of myogenic cells in repairing adult skeletal muscle.

2.3.4 The proliferation of myogenic repair cells

Irrespective of their origin, mpcs must migrate to the damaged area and proliferate. It is thought that exudate macrophages induce a strong positive chemotactic response in myogenic cells by secretion of certain growth factors (Robertson et al., 1993). Before, during and subsequent to migration, mpcs proliferate. Most studies involving proliferation deal with the satellite cell population. Thus, in discussing further events, I will assume that presumptive myoblasts originate from satellite cells.

Extracellular matrix (ECM) components, growth factors and hormones

all play a role in the proliferation (and fusion) of mpcs *in vitro* and *in vivo* (Grounds, 1991). The **extracellular matrix** surrounding myofibers consists of a basement membrane (one component being the external lamina) and associated interstitial connective tissue. **Growth factors** are peptides which stimulate or inhibit cell division or affect cell differentiation (Allen & Rankin, 1990; Allen & Boxhorn, 1989): they are produced locally and often act in an autocrine or paracrine manner. Growth factors can either move cells from the quiescent G_0 state into G_1 (competence factors - bFGF, platelet derived growth factor-PDGF, macrophage derived growth factor-MDGF), act slightly later, moving cells through G_1 into DNA synthesis (progression factors - insulin-like growth factors-IGFs and epidermal-derived growth factor-EGF), or inhibit growth (negative factors - transforming growth factor beta-TGF-ß, interferon). **Hormones** are produced in distant sites and arrive via the circulatory system. Adrenocorticotrophic hormone, melanocyte stimulating hormone and glucocorticoids (dexamethasone) have been implicated in promotion of mpc proliferation. Growth hormone plays an important role in cell proliferation and myofiber growth in normal adult rats (Ullman & Oldfors, 1989). In regenerating muscle, growth hormone increases the growth and cell proliferation of regenerating muscle (Ullman et al., 1989), possibly by stimulating IGF production in the liver (Murphy et al., 1987). However, endogenous production of IGF-I in early stages of regeneration can occur independent from growth hormone (Sommerland et al., 1989). It is suggested that growth hormone dependence may be more pronounced in later stages of regeneration (Sommerland et al., 1989; Ullman et al., 1989). The functional and biochemical state of muscle is dependent upon thyroid hormone (section 2.8). The role of the above factors *in vitro* are summarized in the following table (from Grounds, 1991). In most cases *in vivo* roles are similar, or as of yet unknown.

Effects of various factors on muscle precursor cells (mpcs) *in vitro*.

	Proliferation	Differentiation and Fusion
Extracellular matrix (ECM) components		
Laminin	increase	-
Fibronectin	increase	decrease
Hyaluronic acid	-	decrease
Heparin	decrease	-
Heparin sulphate proteoglycans	decrease	-
Collagen	-	increase
Glycoproteins (high mannose type)	-	increase
Growth Factors (GF)		
Fibroblast GF (see section 2.6)	increase	decrease
Platelet derived GF	increase	decrease
Bischoff muscle GF	increase	-
Insulin GF	increase	increase
Dexamethasone	increase	-
Adrenocorticotrophin	increase	-
Prostaglandin	-	increase
Transforming GF-ß	decrease	decrease
Interferon	-	decrease

There is very little evidence available to indicate what factors might act either directly or indirectly in controlling the proliferation and fusion of mpc *in vivo*, because the situation is very complex. It is proposed that the quiescent state of muscle precursors in uninjured muscle could be due either to i) factors that actively repress cell replication, or to ii) the absence of factors which stimulate progression through the cell cycle. When trauma occurs, membrane and nerve damage occurs, macrophages and complement are activated, and angiogenic factors are produced. The mpcs must then be activated. Things which may activate mpcs (Grounds, 1991) include: i) proteases which might be mitogenic for mpcs, ii) general changes in the ECM, including a decrease in many of the components which may affect mpc shape and DNA synthesis (i.e. degradation

of heparin sulphate proteoglycans will release FGF), iii) increases in nonspecific competence growth factors mitogenic for mpc such as FGF, PDGF and MDGF, iv) increases in specific mpc mitogens such as Bischoff growth factor, ACTH and glucocorticoids, v) availability of receptors for FGF and other mitogens, vi) a damaged sarcolemma with abnormal electrical activity (Bischoff, 1990), and vii) the absence of inhibitory growth factors. Once the mpcs are activated, cells move through G_1 to DNA synthesis, and cell proliferation is maintained by elevated levels of growth factors, and perhaps hormones.

Mpcs undergo multiple divisions before fusing to form myotubes. Mpc replication is initiated anywhere from 30-48 hours after injury, depending on the severity of the injury (Roberts et al., 1989). There are two theories as to the number of cell divisions these initiated mpcs undergo. The first theory states that there are 2 discrete populations of mpcs, separated by a crucial cell cycle (quantal mitosis) which transforms replicating mpcs (potential myoblasts) into post-mitotic committed or terminally differentiated cells (myoblasts) ready for fusion (Quinn et al., 1984). Proponents of this theory propose that there is one myogenic lineage and once the stem cell becomes committed, it undergoes a specific number of symmetrical and obligate cell divisions to produce terminally differentiated myoblasts. In embryonic chick muscle *in vitro*, 4 determined symmetric divisions give rise to 16 terminally differentiated myoblasts (Quinn et al., 1984). The other theory proposes that there is one heterogeneous population of presumptive myoblasts and that there is no quantal cell cycle. Cells will continue to divide until they fuse. Grounds & McGeachie (1987) support this theory, and propose that at the onset of myogenesis in regenerating muscle *in vivo*, mpcs can divide as little as two times before fusing to form myotubes.

2.3.5 Fusion to form myotubes

Irrespective of the number of times a mpc divides or its origin, at some point during the early part of G_1, a mpc begins to differentiate and

becomes committed to fusion. Usually, myoblast numbers reach a peak 48-72 hours after mild injury in mice (McGeachie and Grounds, 1987). Afterwards, their population decreases, myotubes take their place (Grounds & McGeachie, 1987) and ultimately DNA synthesis virtually ceases (Roberts et al., 1989). Fusion is not a prerequisite for differentiation, but differentiation always follows fusion. Proliferation and fusion of mpcs are not dependent on the presence of infiltrating macrophages or other leukocytes (Robertson et al., 1992).

Fusion is a very complex process involving many biochemical and biophysical interactions. These interactions include the actions of glycoproteins, calcium, pH levels, adhesion-specific receptors, cell-surface proteins, cell recognition molecules, ECM, growth factors and prostaglandins. The effects of growth factors and ECM on fusion are summarized in Table A. The remainder will not be discussed here. Fusion can occur between 2 myoblasts, 2 myotubes, a myoblast and a myotube, a myotube and a sealed myofiber, and a myoblast and a sealed myofiber (Robertson et al., 1990). It has been suggested that a minimum density of mpcs must be attained before fusion can occur (Grounds, 1991).

In mice, fusion occurs in 3 stages, as seen by the electron microscope (Robertson et al., 1990). First, cells closely appose each other and internal junctions may be formed in myotubes. Recognition of cells intended for fusion depends upon certain cell adhesion molecules, one of which is NCAM (section 2.4). Second, vesicles are synthesized and move to areas of apposition. Vesicles fuse with the sarcolemma of each parent cell. Incorporation or insertion of lipid into the sarcolemma or secretion of some cell product destabilizes the cell membrane. Third, the modified cell membranes coalesce and fuse with each other, permitting cytoplasmic confluence and structural rearrangement of the myofiber syncytium. At no time during fusion is there a loss of integrity of the cell envelope around the sarcoplasm (Allbrook, 1981). Fusion reaches its maximum extent at 4-5 days after injury in mice (Robertson et al., 1990).

The original external lamina persists while the new myotubes are forming, and as they mature, new external lamina is deposited. For a while both external laminae co-exist, but typically, the old external lamina dissolves (Hansen-Smith & Carlson, 1979), although there are reports of duplicated layers around large regenerated fibers (Anderson et al., 1987).

2.3.6 Mature regenerated muscle

Following fusion, the expression of various genes changes from embryonic or juvenile isoforms to adult forms. Myofibrils become completely organized into cross-striated sarcomeres and most nuclei are pushed to the periphery by myofilaments. However, the persistence of centrally nucleated myofibers is common (a good diagnostic feature of regenerated muscle). The structure of the muscle closely resembles normal adult muscle except that regenerated muscle fibers are often smaller in diameter than normal, increased in number, split longitudinally (Ontell, 1986) and are surrounded by a thicker endomysium.

Muscle regeneration begins in the absence of nerve supply. However, the motor component of innervation is necessary for maintenance and voluntary activity of regenerating myofibers. The external lamina of the original myofiber is important as a cue for the localization of sprouting, regenerating nerve terminals and for presynaptic and postsynaptic differentiation of the nerve and muscle (Carlson & Faulkner, 1983). NCAM (section 2.4) is also involved in muscle-nerve interactions. Nerves often establish new synapses at sites of previous NMJs, proven by experiments involving the inhibition of myofiber regeneration (Carlson & Faulkner, 1983). These experiments show that nerve axons regenerate along their original pathways and terminate at the original endplate zone of the persisting external lamina.

After the motor end plates are established, the regenerating muscle fibers, which have homogeneously fast contractile properties up to this time, either differentiate into slow type fibers or continue to mature as fast fibers. Sensory and motor aspects of muscle spindles can regenerate

but they are often incompletely differentiated.

2.3.7 Crush injury and regeneration

There are many experimental models of muscle regeneration. Each model has specific merits and disadvantages, depending on which aspects of repair are under investigation. It is possible to study the regeneration of entire muscle by mincing muscle or by free nonvascular grafting. Localized injections of substances such as hot Ringers solution, a variety of commonly used local anesthetics and snake and spider venoms creates localized muscle degeneration and regeneration. Localized heat and cold have been applied in order to create muscle damage. Mechanical trauma such as crushing, transection, laceration, contusion and exercise have all been used and studied to varying degrees of success and comparison. Also, genetic models of muscle damage such as the muscular dystrophies give specific clues into muscle regeneration.

In this study, we have chosen to use the **crush injury** as the method for studying regeneration in a genetic mouse model of dystrophy (the *mdx* mouse). This is a mechanical injury in which the myofibers are directly crushed by some object, often artery forceps (Grounds and McGeachie, 1987). Longitudinal continuity of the muscle belly is maintained and the vascular supply is left relatively intact.

There are differences in muscle recovery from a crush injury between SLJ/J and BALB/c mice. Basically, SJL/J have increased and faster mononuclear cell infiltration, more efficient removal of necrotic muscle, plus a greater capacity for myotube formation, all resulting in more successful regeneration after injury (Mitchell et al., 1992). Mitchell et al. (1992) conclude that the migration of inflammatory cells and mpcs is greater/faster in SJL/J than in BALB/c.

One day after a 4mm wide by 2mm long crush injury of the tibialis anterior (TA), the center of the crush lesion consists of a large zone of necrotic myofibers, a few polys and some erythrocytes. This area is referred to as the central zone. In muscle adjacent to the direct crush

site (the adjacent zone), mononuclear cells are conspicuous in SJL/J mice. Replication of potential myoblasts is initiated at this time (30 hours after injury) (McGeachie and Grounds, 1987).

Two days after crush, SJL/J mice have many mononuclear cells in the adjacent zone and much less necrotic muscle in the lesion. There is a distinct alignment of fusiform mononuclear cells along the surviving external lamina. In both strains, 6-10% of nuclei are labelled by autoradiography.

Three days post-injury results in the disappearance of all necrotic material within the adjacent zone of SJL/J mice, and numerous macrophages appear at the borders of the central zone. Some immmature myotubes appear containing 2-11 nuclei at this time. Fusion of myoblasts into myotubes is consistently reported to occur abruptly between 60 and 72 hours after injury, regardless of how the injury is inflicted.

Four to five days after crush, the adjacent zone of SJL/J TA is completely filled with myotubes and numerous mononuclear cells are present in the necrotic central zone. BALB/c have fewer myotubes, more connective tissue deposition, persistent necrotic tissue and few mononuclear cells in the central zone. Significant mpc replication in the crush lesion is still occurring at this time (96 hours post-injury) (McGeachie & Grounds, 1987).

Six to ten days post-injury results in the central necrotic zone of SJL/J being completely removed and replaced by myotubes and a small amount of connective tissue. BALB/c show some necrotic muscle, myotubes restricted to the periphery of the central zone and conspicuous connective tissue with some calcification. Central nuclei are a consistent feature in many myofibers (Robertson et al., 1992).

2.4 NEURAL CELL ADHESION MOLECULE (NCAM) IN MUSCLE DEVELOPMENT AND REGENERATION

2.4.1 Structure, physiology and biological roles of NCAM

NCAM is the most widespread and abundant of the known cell-cell adhesion molecules and is involved in many cell membrane events (reviewed by Rutishauser, 1991). It is a large and complex integral membrane glycoprotein which exists in three major forms (180, 140 and 120kD in rodents) that are a result of alternative splicing of exons from a single gene. The relative abundance of the 3 forms varies during development. Some of the variation in NCAM form may arise at the mRNA level, in that NCAM RNA exist in multiple species which also vary in abundance during development (Andersson et al., 1993; Covault et al., 1986). The epitope HNK-1 (human natural killer cell-1) is present on NCAM carbohydrate sections.

It is hypothesized that NCAM participates in cell-cell adhesion via calcium independent homophilic interactions between NCAM molecules present on the surface of both interacting cells. These interactions occur either directly, through an interaction with a membrane bound heparin sulphate proteoglycan-like molecule, or with cytoskeletal components. The broad biological functions of NCAM are threefold: to act as an adhesive, to guide cell migration (i.e. of neurons) and to regulate other cellular processes that require physical contact or are triggered by signals directly generated by NCAM-mediated adhesion.

2.4.2 Distribution of NCAM in developing muscle

NCAM is distributed in many tissues during development, but its distribution in somites and skeletal muscle cells is of interest in this study. Very early in the embryonic development of the rat, the myotome exhibits positive NCAM staining, as do the spinal cord, ventral roots and spinal nerves (Lyons et al., 1992; Covault & Sanes, 1986; McIntosh & Anderson, unpublished observations). At this early time, however, the spinal nerves have not yet grown to the most ventral portions of the myotomes, hence NCAM is present in myotomes before they are contacted by

nerves. The observation that little NCAM is present in spaces surrounding myotomes suggests that NCAM might play a role in the segregation of myoblasts from other non-muscle structures and later in myoblast migration (Lyons et al., 1992; Covault & Sanes, 1986). Later in embryonic development, NCAM is associated with developing motor axons and NMJs, and it is suggested that NCAM could mediate some of the initial nerve-muscle interactions that lead to synapse formation (Covault & Sanes, 1986; Grumet et al., 1982).

Immunohistochemical staining of embryonic muscle *in vivo* and *in vitro* shows that NCAM is present on the surface of myoblasts, but not fibroblasts (Covault & Sanes, 1986; Moore & Walsh, 1985), and its antibody has been successfully used to purify myogenic cells from primary cultures (Jones et al., 1990; Webster et al., 1988a). NCAM is probably expressed before myosin (Covault & Sanes, 1986). Accordingly, NCAM likely participates in prefusion steps involving intracellular recognition and adhesion (Knudsen et al., 1990; Covault & Sanes, 1986). A 140kD form of NCAM and a 6.7kb NCAM mRNA are predominantly associated with myoblasts (Covault et al., 1986).

Antibodies directed against NCAM also localize to the surface of embryonic myotubes *in vivo* and *in vitro* (Covault & Sanes, 1986; Moore & Walsh, 1985). A change in NCAM forms occurs during myogenesis (to a 125kD form), and the extent of sialylation of muscle NCAM decreases *in vivo* (Covault et al., 1986). These changes correspond with myoblast fusion, but do not depend on it. The 125kD form and 5.2 and 2.9 kb RNAs are predominantly associated with newly formed myotubes and myofibers (Covault et al., 1986). Mouse myoblasts transfected to constitutively express the low molecular weight isoform of NCAM more readily fuse to form myotubes (Dickson et al., 1990), suggesting its role in the actual fusion of myoblasts. It appears that optimal action of NCAM requires the interaction of a calcium-dependent cell adhesion molecule, N-cadherin (Rutishauser, 1991; Knudsen et al., 1990).

NCAM distribution changes as embryonic myotubes mature. In rats, uniform distribution of NCAM is present on the entire surface of primary myotubes when they are the only myotubes present. However, as secondary myotubes form clusters around primary myotubes, NCAM becomes concentrated in the area of contact between adjacent myotubes, while the outer surface contains relatively little NCAM (Covault & Sanes, 1986). NCAM may regulate the recognition of embryonic myoblasts with primary myotubes, thus properly aligning secondary myotubes (Covault & Sanes, 1986). Also, since it is lost from the outer surface of myotubes, NCAM may limit the formation of new myotubes (Covault & Sanes, 1986). As myotubes separate and mature into myofibers, NCAM reappears over the entire muscle fiber surface, only to decline gradually over the first couple of postnatal weeks (Covault & Sanes, 1986) toward restriction to the NMJ.

2.4.3 Distribution of NCAM in adult muscle

NCAM is downregulated as myotubes mature, and is reduced to a very low level in young adult rat skeletal muscle (Thompson et al., 1987; Covault et al., 1986; Covault & Sanes, 1986). In adult muscle, NCAM has a complicated distribution at the NMJ (Moore & Walsh, 1985), and is also present on unmyelinated nerve fibers in intramuscular nerves and near blood vessels (Covault & Sanes, 1986). It is nearly undetectable in non-synaptic portions of the muscle, except in association with satellite cells (Thompson et al., 1987) and with a subpopulation of the mononucleated, fibroblast-like cells that occupy interstitial spaces between muscle fibers (Covault & Sanes, 1986). Covault & Sanes (1986) suggest that adhesion of satellite cells to myofibers in adult muscle may be mediated by NCAM. Alternatively, Moore & Walsh (1985) report that although activated satellite cells in culture express NCAM, there is no reactivity with cryostat sections of adult muscle (where 4% of the nuclei are satellite cells). This discrepancy is probably due to different antibody preparations and variations in the exposure of antigens in different tissue preparations.

In aged rat muscle (24 months), NCAM protein levels increase again and are clearly re-expressed, probably as a result of partial denervation of aging muscles (Andersson et al., 1993). Thus, membrane activity mediated by nerves appears to repress the expression of the NCAM gene (Thompson et al., 1987).

2.4.4 Distribution of NCAM in regenerating muscle

Following denervation, or during disease where there is muscle regeneration, NCAM is expressed on regenerating fibers (Moore & Walsh, 1985). This expression closely mimics the expression of NCAM on myoblasts and myotubes during development. It has been suggested that NCAM can be regarded as a specific marker for regenerating fibers (Moore & Walsh, 1985).

2.4.5 NCAM and perturbation by thyroid hormone

Innervation status may not be the only controlling factor in NCAM expression. Other factors such as hormones (Thompson et al., 1987) and growth factors (Lyles et al., 1993) may also be important. NCAM expression in rat skeletal muscle can be re-induced by hypothyroidism (Thompson et al., 1987). Thompson et al. (1987) report that thyroidectomized rats re-express NCAM mRNAs of 5.2 and 2.9kb, but not 6.7kb, suggesting that the NCAM is predominantly expressed in mature myofibers and not myoblasts in those muscles (Thompson et al., 1987). High levels of NCAM are also detected in the sarcolemma, and to some extent the myofiber cytoplasm (likely in transit to the membrane), by immunofluorescence (Thompson et al., 1987). Reversal of thyroid hormone deficiency by treatment with thyroxine reverses the changes in NCAM gene expression to that of normal adult (Thompson et al., 1987). It is possible that NCAM and MHC genes (section 2.8.2) are regulated similarly by thyroid hormone in adult muscles.

2.5 DUCHENNE MUSCULAR DYSTROPHY

Duchenne muscular dystrophy (DMD) is a primary myopathy which is characterized by persistent cycles of degeneration and regeneration with eventual failure to regenerate, leading to replacement of myofibers by adipose and fibrotic tissue.

2.5.1 Dystrophin

Dystrophin, first identified in 1987, is the gene product of the DMD locus (reviews by Partridge, 1993; Rojas & Hoffman, 1991; Bieber & Hoffman, 1990). The gene encoding dystrophin is located on the short arm of the X chromosome at band Xp21. It is the largest known gene, and it codes the large, highly conserved dystrophin protein (427kD). Dystrophin is a crucial component of the membrane cytoskeleton in all types of muscle cells, and in neurons (less well studied than muscle). Normally, it appears as a localized, continuous ring of fluorescence at the sarcolemma of each myofiber, and early observations localized it to the t-tubules. At the molecular level, the N-terminus of dystrophin is similar to α-actinin and likely binds actin (Fabbrizio et al., 1993). The C-terminus is strongly bound to a complex of proteins and glycoproteins (Ervasti & Campbell, 1991; Ohlendieck & Campbell, 1991) which span the membrane and interact with laminin in the external lamina.

Dystrophin is deficient in all tissues of the body in people affected with DMD, although reversion (possibly due to second site mutations) to truncated dystrophin-positive cells is possible (Hoffman et al., 1990). A mutation in the dystrophin gene occurs in 1 in 3500 male births. Sixty-five percent of DMD cases are a result of a deletion in the gene (some regions of the gene may be more prone to a deletion than others), 5% are a result of duplications that usually shift the reading frame, and the remaining 30% are due to point mutations. All affected relatives have the same mutations. The spontaneous mutation rate of the dystrophin gene is very high and accounts for about one third of all cases of DMD. The dystrophin-associated proteins, which are normally bound to

the C-terminus of dystrophin, are also reduced in dystrophin-deficient skeletal muscle (Ohlendieck & Campbell, 1991; Ervasti et al., 1990).

Although the primary structure of dystrophin has been determined, the precise functional role of dystrophin has not. It has been suggested that dystrophin provides mechanical reinforcement to the sarcolemma, thereby protecting it from the membrane stresses developed during muscle contraction (Petrof et al., 1993). Dystrophin-deficiency thereby leads to localized, transient, unregulated passage of material through the membrane (non-specific instability). An alternative view states that dystrophin anchors, localizes, or regulates integral membrane proteins, and that dystrophin-deficiency results in the dysfunction of these associated proteins (reviewed in Rojas & Hoffman, 1991; Ohlendieck & Campbell, 1991; Ervasti et al., 1990). This is supported by Matsumura et al. (1992b) who showed that the absence of one 50kD dystrophin-associated protein produced a DMD-like phenotype. The distinction between the two theories is subtle: does the defective membrane function arise from structurally identifiable rupture (Petrof et al., 1993) or from a smaller disturbance of surface structure at the molecular level?

All dystrophin-deficiency diseases involve early necrosis of muscle fiber segments. The earliest and most consistent evidence of dystrophin-deficiency is high serum levels of creatine kinase (CK) and other muscle enzymes (Bulfield et al., 1984), attributable to release of soluble cytoplasmic enzymes from skeletal muscle fibers. Since there is no extremely obvious evidence of myofiber pathology until about 10-15d postnatally in the *mdx* mouse (Karpati et al., 1988; Dangain & Vrbova, 1984) (section 2.6.2), and shortly after birth in the human, the elevated levels of CK present at birth must be due to chronic myofiber leakage. Dystrophin-deficient myofibers show an increased permeability in their membranes, possibly through transient rips and tears of the sarcolemma. At birth, the leakage is not enough to cause myofiber death. Abnormal calcium homeostasis may play a central role in the pathogenesis of DMD

(Rojas & Hoffman, 1991) and of *mdx* dystrophy (section 2.6). Influx of extracellular calcium (or increased $[Ca]_i$) would result from a leaky sarcolemma (Bakker et al., 1993; Turner et al., 1991), so it is probably safe to assume that dystrophin-deficiency results in calcium influx. *Mdx* gastrocnemius and heart muscle contains elevated levels of intracellular calcium compared to normal muscle (Turner et al., 1991; Dunn & Radda, 1991), but the amount of calcium does not correlate with the amount of necrosis occurring (Dunn & Radda, 1991). It is believed that when the calcium influx overwhelms the calcium-regulatory capacity of the cell, segmental necrosis ensues. Perhaps, once necrosis begins, it is an "all or none" phenomenon.

2.5.2 Clinical Presentation of DMD

Brooke et al. (1989) performed a study, following 283 boys with DMD for up to 10 years, and defined a series of milestones in the progression of the disease. At birth, most affected children appear physically normal. However, in one-third of the cases, some mental retardation is evident. At 3-4 years of age, boys experience difficulty rising from a sitting position on the floor and climbing stairs. Hypertrophy of the calf muscles is evident as degenerating muscle is replaced by fat and connective tissue. Atrophy of all muscle soon follows.

At about 6 years, ambulation becomes difficult and the upper extremities become weak. Physical therapy becomes necessary. Walking is only possible with assistance, or independently with long leg braces. Scoliosis is a major problem in the clinical management of DMD, and after 11 years of age, 74% of patients develop scoliosis which often requires back surgery. Eventually children may stand with leg braces, but cannot walk, and at this time (usually 12 years of age), a wheelchair becomes necessary. Patients also lose useful function of the hands. Death usually occurs in the late teens to early twenties from respiratory (often brought on by pneumonia), or cardiac failure.

2.5.3 Histopathology

Histopathologically, DMD is evident shortly after birth when necrosis of short segments of myofibers occurs in focal groups, accompanied by regeneration. This regeneration results in true hypertrophy of the muscle in the very early stages of DMD. However, the regeneration becomes progressively ineffective as the muscle structure is distorted by dense connective tissue and fatty tissue within, and between, muscle fascicles. The fibrofatty component becomes more prominent (fibrosis), and muscle more sparse (atrophy) (reviewed in Partridge, 1993). Very high levels of soluble muscle enzymes (creatine kinase and aldolase) are also found in the serum of boys with DMD from birth onwards.

Each muscle is affected at a different time in the progression of DMD, with some muscles more susceptible to damage (see Liu et al., 1993). This differential response of the muscles to dystrophin-deficiency could by due to the fiber size (smaller fibers do not seem to suffer as much) (Karpati & Carpenter, 1986), the fiber types (faster fibers are the first to degenerate and regenerate) (Webster et al., 1988b), the type of contraction (eccentric contractions are more damaging) (Edwards et al., 1984), or the contractile speed force (strain) vs surface area to volume (Petrof et al., 1993).

The following schematic from Partridge (1993) is a hypothetical representation of the pathogenesis of the dystrophin-deficiency diseases. The balance between myogenesis and fibrosis is the critical point in the progression of the disease, as fibrosis takes over in place of successful regeneration in DMD. In the *mdx* mouse model of dystrophy (section 2.6), muscle hypertrophy is accentuated instead of fibrosis. The right hand branch of the final pathway depicts an end-stage dystrophy, in which accumulation of fibrous scar tissue acts to exacerbate the disease process.

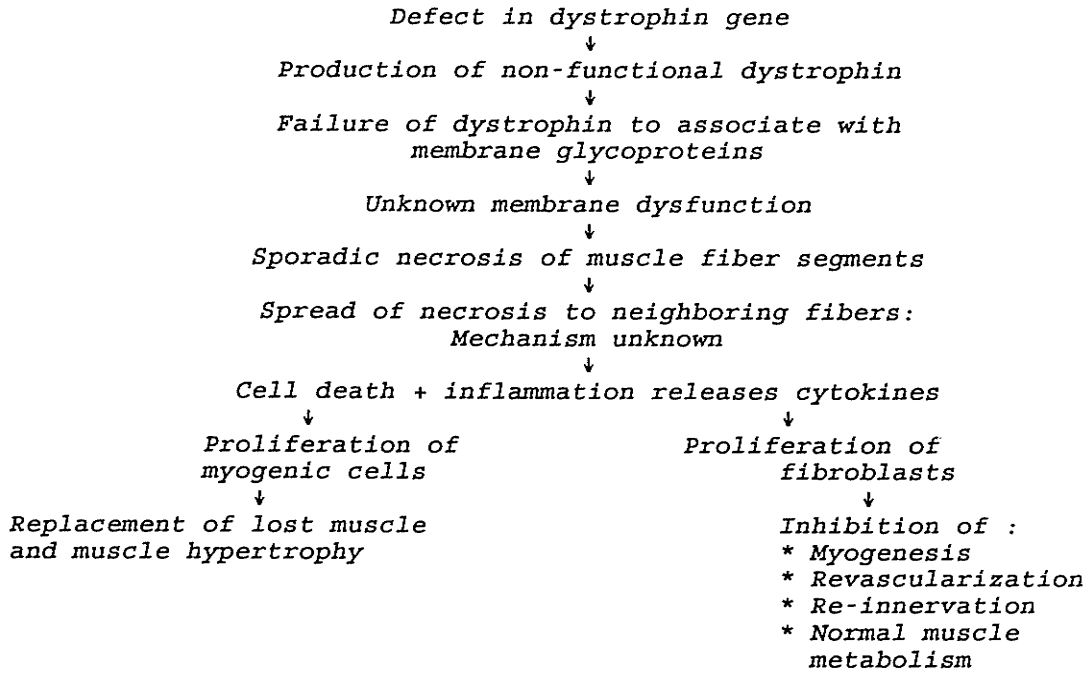

The grouped focal necrosis of myofibers in DMD is probably a direct result of the lack of dystrophin (Partridge, 1993), but how does this translate to death of several contiguous fibers? It is suggested that a progressive component of DMD, not solely due to dystrophin- deficiency, results in a gradual reaction of the tissue to chronic myofiber damage, resulting in extensive fibrosis (Bieber & Hoffman, 1990). If fibrosis is secondary to dystrophin-deficiency and assumes a dominant role later in the disease process, it is important to identify the disease and begin treatment before the secondary effects predominate. The lesions then, perhaps, could be limited to the single fibers in which they originated, greatly reducing the severity of the disease.

2.5.4 Therapies

Potential DMD therapies are focused on two goals: to replace dystrophin in muscle, and to slow the progression of the disease so that it is more similar to the progression of dystrophy in the *mdx* mouse (section 2.6). Gene transfer and myoblast transplantation are methods for attempted replacement of dystrophin. Steroid treatments attempt to slow

the progression of the disease.

The concept of myoblast transplantation takes advantage of the facts that muscle fibers are multinucleated and that myoblast fusion occurs during muscle regeneration. Large populations of normal cultured myoblasts (which are injected into muscle) form hybrid muscle cells containing nuclei with the dystrophic gene and nuclei with the normal gene (Huard et al., 1992; Partridge et al., 1989). Various researchers (Gussoni et al., 1992; Huard et al., 1992) have found that injection of normal myoblasts into a few sites of human DMD muscle results in the formation of some dystrophin-positive fibers. However, this occurs only in a minority of cases (3 of 8 in Gussoni et al., 1992) and is more effective when done at an early age. The technique, as yet, is not feasible for full-scale treatment of the disease. The migratory capacities of mpcs are restricted to a few millimeters (Partridge et al., 1989) and cells would have to be injected in millions of sites in order to be effective. Also, cardiac muscles and the diaphragm are affected by dystrophin-deficiency, and direct injection here would be difficult (Stratford-Perricaudet et al., 1992), although a recent study reports that direct gene transfer into the diaphragm of the *mdx* mouse is possible with minimal damage (Davies & Jasmin, 1993). Neumeyer et al. (1992) suggest that intra-arterial delivery of myoblasts may target myoblasts to heart and diaphragm. However, immunological problems would certainly be encountered. Long-term effects of myoblast transplantation have not been studied in humans.

Somatic gene therapy (gene transfer) includes the introduction of normal alleles of a gene into cells which are missing it. If long-term expression of the transferred gene results in the production of the missing protein, the target cell could acquire a normal phenotype. Striated muscle is the only tissue presently capable of taking up and expressing reporter genes transferred in the form of plasmid DNA, but the present results are insufficient and too variable to use this therapy in humans. Only 1-2% of adult *mdx* fibers of the muscles injected with cDNA in

plasmid vectors have been reported to express dystrophin (Karpati & Acsadi, 1993). Davies et al. (1993) improved the variability somewhat by using a pre-incubation procedure.

Adenovirus-mediated direct *in vivo* gene transfer via intravenous may also be a possibility for treatment of DMD (Stratford-Perricaudet et al., 1992), and has a better efficiency when injected into young *mdx* muscle (Karpati & Acsadi, 1993). Direct gene injection thus may be equally efficient, but simpler and safer than myoblast transplantation in the delivery of proteins to muscle.

The above studies prove that dystrophin can be successfully incorporated into the genome. However, before cell or gene implantation can be considered as means of therapy for DMD, it is important to establish whether the introduction of dystrophin into myofibers by the above means actually will prevent their subsequent necrosis. In order to study this, transgenic *mdx* mice have been recently created that express full-length dystrophin in the sarcolemma of muscle cells (Cox et al., 1993; Lee et al., 1993). Cox et al. (1993) report that the expression of dystrophin in muscles of transgenic *mdx* mice completely corrected the dystrophic pathology in the transgenic animals. Necrosis, large variation in fiber size, increased degeneration and regeneration with centrally nucleated fibers, and progressive degeneration and fibrosis of diaphragm muscle, are all absent from these transgenic *mdx* mice. Overexpression of dystrophin does not cause deleterious side-effects (Cox et al., 1993). They also find an increase in the dystrophin-associated proteins to normal levels (Cox et al., 1993). Lee et al. (1993) report variability in the amount of dystrophin expressed in the muscles of their *mdx* transgenics, and believe that dystrophin was relatively absent in the diaphragm. However, in the fibers expressing dystrophin, they report an improvement in muscle pathology, as indicated by the increased number of myofibers with peripheral nuclei.

Many problems need to be worked out before we can seriously consider

myoblast transplantation and direct gene transplantation as therapies for DMD. In the meantime, physical therapy and steroid treatment seem to be the only alternatives. Treatment of DMD with prednisone significantly slows the progression of weakness and loss of function for up to 2 years (reviewed by Khan, 1993; Fenichel et al., 1991). The mechanism by which prednisone enhances muscle strength is not known. However, its use over extended periods results in various side-effects. Deflazacort is a newly developed steroid which has fewer side- effects than prednisone, and a small preliminary clinical trial shows that it significantly increases muscle strength in DMD boys (Mesa et al., 1991). Multi-center long term trials of deflazacort are presently ongoing, including a center in Winnipeg. Results should prove exciting.

Early detection of DMD is imperative for successful treatment. There are many methods of detecting DMD (see Bieber & Hoffman, 1990) pre- and postnatally. Between January 1986 and August 1990 in Manitoba (Manitoba Pilot Neonatal Screening Programme for DMD and BMD), 43,513 newborn males have been screened for DMD and Becker muscular dystrophy by analysis of CK (creatine kinase) measurements in blood spots. Eight asymptomatic infant boys have been identified to date with elevated CK levels and were subsequently diagnosed as having DMD (Greenberg et al., 1991). This early diagnosis allows for early treatment and management of the disease, as well as genetic counselling for family planning of that family and extended family members (siblings and aunts).

2.6 THE *MDX* MOUSE

The murine equivalent to Duchenne muscular dystrophy is the *mdx* mouse. It is homologous to DMD at the genetic and biochemical levels. However, the clinical and pathological characteristics of the disease differ from DMD.

2.6.1 Animal models of Duchenne muscular dystrophy

In order to be a true model of DMD, the disease must present a dystrophin-deficiency and be inherited as an X-linked recessive trait. To date, 3 true animal models of DMD have been identified (reviewed by Hoffman, 1991): a dog (*xmd*), a cat, and a mutant mouse (*mdx*) derived spontaneously from the C57Bl/10ScSn mouse strain (characterized by Bulfield et al., 1984). In the *mdx* mouse, the mutation has been characterized as a premature stop codon produced by a single base substitution in the DMD gene resulting in the absence of dystrophin (Sicinski et al., 1989). Among the excluded disorders for use as animal models of DMD are dystrophic chickens, dystrophic mice (*dy/dy*), cardiomyopathic hamsters and muscular dysgenic mice (*mdg/mdg*), which are all carried on autosomal chromosomes.

Within each species showing dystrophin-deficiency, the disease appears relatively uniform, but many pathological and clinical differences exist between the species. Similarities between species appear early in the necrotic phase of the disease, while dissimilarities mainly occur consequent to the progressive aspects (eg-fibrosis) of the disease (Partridge, 1993) (section 2.5.3). Dystrophin-deficiency in the dog closely parallels human DMD (section 2.5), except that it progresses at a more rapid rate. Muscle wasting occurs in both the dog and human. In contrast, the cat and *mdx* mouse appear clinically unaffected by dystrophin-deficiency, and hypertrophy of muscles occurs, instead of wasting. Muscle regeneration remains successful in the mouse and cat. However, although in DMD and dog dystrophy regeneration does occur initially, giving rise to fiber centronucleation, some process frustrates

repair and ultimately muscle is replaced by fibrous connective tissue and adipose tissue.

The *mdx* mouse model is examined in the present studies. Direct comparison of *mdx* mice to DMD is often not possible, because of the different outcome of their dystrophin-deficiency. Some investigators suggest that the *mdx* mouse cannot be used for investigating therapies aimed to slow the progression of human DMD because it does not share the progressive characteristics of weakness. However, dystrophy does occur (increased centronucleation with increased age), so therapies which change that sequence can be examined (Hoffman, 1991). As well, the longevity and overall fitness of the dystrophin-deficient *mdx* mouse is encouraging when trying to devise a treatment to attenuate the progression of DMD. If we could only stop the progressive aspects, the DMD muscle would probably fare quite well.

Despite questions of usefulness in studying treatments, the *mdx* mouse should be an excellent model to study therapies aimed at understanding the primary mechanisms of the disease originating with dystrophin-deficiency. It fully manifests dystrophin-deficiency, dystrophin-replacement can be accurately monitored by immunoblotting and immunofluorescence, and the effects of dystrophin replacement therapy are not masked by any progressive secondary effects. The *mdx* model is also invaluable for studying regeneration dynamics. Precise characterization of muscular dystrophy in the *mdx* mouse will definitely clarify the process in humans, and will highlight elements imperative for successful regeneration in the diseased state.

2.6.2 Progression of muscular dystrophy in the limb muscles of the young *mdx* mouse

In the *mdx* mouse, muscle degeneration begins shortly after birth. It is reported that during the first 10-15d of life most *mdx* fibers appear normal (Dangain & Vrbova, 1984; Bulfield et al., 1984). It could be that these young fibers are protected from necrosis because they are small (Karpati et al., 1988; Karpati & Carpenter, 1986), or because they are not

subjected to adult levels of cell activation and muscle strain (Petrof et al., 1993). It is suggested that a larger surface area to volume ratio in small diameter myofibers allows strain to be better distributed over the myofiber surface, thus somewhat sparing the fibers (Karpati et al., 1988). It could also be that small diameter myofibers have an advantage in the discharge of harmful molecules that may be accumulated as a result of dystrophin-deficiency (Karpati et al., 1988).

Mdx muscle degeneration is most active 3-5wks after birth (Tanabe et al., 1986; Dangain & Vrbova, 1984; Bulfield et al., 1984). At this time, extensive grouped necrosis occurs, where as many as 100 fibers can be seen undergoing synchronous degeneration or regeneration (Anderson et al., 1987; Tanabe et al., 1986). Very few intact myofibers can be found in large foci, but many phagocytic inflammatory cells are present. The inflammation and degeneration are segmental, involving only part of the fiber length (Anderson et al., 1987). Degeneration affects contiguous fibers (Carnwath & Shotton, 1987). Groups of regenerated myofibers are evident by their small caliber, basophilic cytoplasm and centralized large myonuclei (which remain central) (Karpati et al., 1988).

Focal myocardial necrosis and inflammation are seen in the *mdx* mouse at this time (Anderson et al., 1991; Bridges, 1986). Necrotic myocytes have swollen and fragmented sarcoplasm devoid of striations and nuclei (Bridges, 1986). Inflammation consists of numerous macrophages located between bundles of cardiomyocytes (Bridges, 1986). However, cardiac muscle does not regenerate and fibrosis may be seen in older animals, as in DMD muscle (Anderson et al., 1994; Bridges, 1986).

Young *mdx* limb muscles exhibit a wide distribution of myofiber sizes compared to control muscles (Anderson et al., 1987; Bulfield et al., 1984) because of many small regenerating myofibers. Autoradiograms from 4wk-old mice (injected with tritiated thymidine) show an increased proportion of labelled sublaminal nuclei at 24 to 48 hours after injection compared to controls (Anderson et al., 1987). Thus, the regeneration at this time is

very active. In *mdx* mice, MyoD and myogenin mRNA levels increase and peak from 21d to 40d, paralleling the most active stages of degeneration and regeneration (Beilharz et al., 1992). Levels remain high up to 420d of age. Between the second and fifth week of life, *mdx* muscle shows contractile weakness (Muntoni et al., 1993; Anderson et al., 1987; Dangain & Vrbova, 1984).

It appears that muscle necrosis and mononuclear cell infiltration decreases in intensity after 9 weeks of age (Anderson et al., 1987; Tanabe et al., 1986). At the end of this vigorous stage of regeneration, there are reports of 80% centronucleation (at 9wk, Karpati et al., 1988), 75% centronucleation (at 13wk, Zacharias & Anderson, 1991), more than 50% centronucleation (at 9wk, Tanabe et al., 1986), and close to 100% centronucleation (at 10wk, DiMario et al., 1991) (at 26wk, Carnwath & Shotton, 1987). Since almost all fibers are centrally nucleated, at least one necrotic episode must have occurred in all fibers at these times (Tanabe et al., 1986). As such, centronucleation has been used as a marker of accumulated dystrophic injury and subsequent regeneration, although it can not be ascertained from centronucleation the exact number of times one fiber has undergone degeneration and regeneration.

2.6.3 Adult morphology of the *mdx* mouse

In the adult *mdx* mouse, the majority of limb muscle fibers exhibit normal ultrastructure, albeit with central nuclei. There is no replacement of previously lost muscle by fat or connective tissue (fibrosis), and there is no apparent fiber loss (Carnwath & Shotton, 1987; Anderson et al., 1987; Tanabe et al., 1986). In the soleus, fiber number is unchanged, while in the EDL, the fiber number is slightly higher than normal, possibly due to fiber branching during regeneration (Anderson et al., 1987). One report (Marshall et al., 1989) shows an accumulation of collagen in the endomysium and perimysium of *mdx* muscles compared with age-matched controls, but this is not enough to produce functional weakness or atrophy.

Frequency distributions of fiber cross-sectional areas of *mdx* mice at 32 weeks show a wider range than in their control counterparts (Anderson et al., 1987). The mean cross-sectional area of limb myofibers increase at a constant rate between 15d and 360d (Karpati et al., 1988). Most studies find that when the weights of males and females are separated, *mdx* mice weigh significantly more than controls, due to hypertrophy of the limb and heart muscles (Anderson et al., 1994; Zacharias & Anderson, 1991; Anderson et al., 1987). In older mice, labelling of replicating *mdx* muscle is greater than controls, but is reduced compared to labelling in younger *mdx* mice (Zacharias & Anderson, 1991; Anderson et al., 1987). Thus muscle regeneration is more active and more effective in young than old *mdx* mice (Zacharias & Anderson, 1991). Overall, contractile properties of *mdx* adult mice are similar to control mice (Dangain & Vrbova, 1984; Tanabe et al., 1986). The progressive weakness of DMD is not seen in *mdx* dystrophy.

There are conflicting studies regarding the extent of recovery from necrosis in aging *mdx* mice - is it transient (DiMario et al., 1991; Dangain & Vrbova, 1984) or does it continue throughout life (Karpati et al., 1988; Anderson et al., 1987; Carnwath & Shotton, 1987; Bridges, 1986)? Dangain & Vrbova (1984) believe that *mdx* mice suffer from an acute episode of muscle degeneration at an early age, and by adulthood, when contractile properties of *mdx* mice and control mice are similar, full recovery has been achieved. Further to this, DiMario et al. (1991) believe that the benign phenotype of adult *mdx* mice is due to the fact that once fibers regenerate, some mechanism saves them from another round of degeneration and regeneration. In contrast, Anderson et al. (1987) conclude that degeneration does decrease in intensity after 8wks, but does not stop completely, since they show centrally nucleated fibers that are degenerating. Their findings of greater than normal muscle weight in the absence of fatty infiltration or fibrosis, continuous appearance of small and immature centrally nucleated fibers, normal or above normal numbers of

fibers by 32wks, and larger increases in the distributed range of myofiber size in muscles at 4 and 32wks back-up their claim. Also, a low baseline labelling of muscle nuclei is noted in *adult mdx* mice (Zacharias & Anderson, 1991), and high levels of MyoD and myogenin mRNA expression exist in adult *mdx* compared to control mice (Beilharz et al., 1992). These mRNAs are expressed in the early regeneration of myoblasts and myotubes (section 2.3.3). Karpati et al. (1988) viewed necrosis at 1 year in *mdx* mice, proving that it indeed still occurs into adulthood, such that full recovery is not achieved, or that dystrophy is a continuous, albeit declining, disease process.

The difficulty of the above discrepancy is the use of a centronucleation index (CNI) to detect accumulated dystrophy. Since satellite cell nuclei are always peripheral, there is an upper limit (around 80%, Karpati et al., 1988) at which the CN index plateaus. After that proportion of regenerated fibers is reached, no further necrosis is detected despite continued expression of MRFs (Beilharz et al., 1992) and fetal MHCs (DiMario, 1991; Anderson et al., unpublished).

Mdx hindlimb muscles are differentially affected by dystrophin-deficiency. There is earlier and more diffuse involvement of the slow-twitch SOL than the fast-twitch EDL in degeneration, infiltration, and regeneration at 4wk (Anderson et al., 1987; Carnwath & Shotton, 1987). Ultimately, the EDL (32wks) exhibits more centronucleation (and thus more regenerated fibers as a percentage of total fiber number) than the SOL (Anderson et al., 1987). Anderson et al. (1988) report no significant changes in fiber-type proportions in *mdx* SOL, apart from normal age-related increase in type 1 fibers, and that the *mdx* EDL maintains its fast-twitch character after recovery. Alternatively, Carnwath & Shotton (1987) show a progressive increase in the proportion of slow type 1 fibers in *mdx* SOL (58% are type 1 compared to 27% in control mice at 26wks). In any case, there is a higher potential for regenerative capacity in slow-twitch skeletal muscle (Anderson et al., 1988).

The process of regeneration from injury is not precisely the same as that in response to dystrophy (Zacharias & Anderson, 1991). Grounds & McGeachie (1992) found that control and *mdx* mice do not differ in their regenerative capacity after a crush injury. Based on similar distribution of myofiber cross-sectional areas and the percentage centronucleation, Zacharias & Anderson (1991) also found that older control and *mdx* do not differ in their regenerative capacity after devascularization and denervation, although younger *mdx* mice were reported to recover better than control (Anderson et al., 1991).

2.6.4 Progression of muscular dystrophy in the diaphragm of the *mdx* mouse

Recently, it was discovered that dystrophin-deficiency affects the diaphragm of the *mdx* mouse differently than *mdx* limb muscles. A pattern of degeneration, fibrosis and severe functional deficit are seen in the diaphragm which is more comparable to DMD than *mdx* limb muscle (Dupont-Versteegden & McCarter, 1992; Stedman et al., 1991). However, adult *mdx* mice show no overt respiratory impairment.

It has been reported that histopathological changes of the diaphragm do not precede that seen in the limb muscles and, at 4 weeks, foci of myofiber degeneration and regeneration are comparable in amount to the limb (Stedman et al., 1991). However, considering the early development of the diaphragm and its functional requirement at birth, dystrophy probably affects it earlier than limb muscles.

Progressive degeneration is seen in the diaphragm, and at 6 months there is wide variation in myofiber size and architecture, continued necrosis and connective tissue proliferation (Stedman et al., 1991). As well, there is much more re-injury of centrally nucleated fibers than in limb muscles (Penner & Anderson, unpublished). By 16 months, the entire *mdx* diaphragm is grossly pale, owing to fiber loss, fibrosis and adipose tissue accumulation (Stedman et al., 1991). The collagen density rises to at least 7 times that of control diaphragm and 10 times that of *mdx* hindlimb muscle (Stedman et al., 1991). Attempted regeneration does

persist in the *mdx* diaphragm even at 16 months. Similar changes to those described above occur in the accessory muscles of respiration at 1 and 1.5 years of age (Stedman et al., 1991). Contractile properties of the *mdx* diaphragm demonstrate muscle weakness compared to *mdx* hindlimb or control muscles (Petrof et al., 1993; Dupont-Versteegden & McCarter, 1992; Stedman et al., 1991).

Electron microscopic immunolabelling for bFGF (section 2.7) shows that the *mdx* diaphragm has lower bFGF content than the control diaphragm (Penner & Anderson, unpublished). Also, the *mdx* soleus has higher bFGF localization than either control soleus or *mdx* diaphragm. These results suggest that the amount of bFGF sequestered in muscle tissue may correlate with the capability of different muscles to compensate for dystrophic insult in the *mdx* mouse (Penner & Anderson, unpublished).

2.6.5 Why does *mdx* muscle regenerate so successfully?

Why is it that *mdx* muscle has such an amazing capability to regenerate and withstand dystrophin-deficiency? Many suggestions have been put forth. However, the answer remains a mystery.

An increased population of satellite cells in *mdx* muscles compared to control muscles (Zacharias & Anderson, 1991; Anderson et al., 1988; 1987) could allow regeneration, instead of letting degeneration progress to the end stage of fibrosis. *In vitro* the total cell yield is routinely much greater from *mdx* than control muscles (DiMario & Strohman, 1988). Presumably, increased yield would include satellite cells. The increased number of satellite cells could be due to the increased weight of *mdx* compared to control mice. Brown & Stickland (1993) report that there is a significant increase in satellite cell density in larger compared with smaller mice, but that this is not accompanied by an alteration in myofiber nuclear density.

Alternatively, satellite cells in normal numbers could have a higher mitotic index than controls (Anderson et al., 1987). This would explain why *mdx* satellite cells in culture respond to lower amounts of bFGF

(section 2.7.4) than control cultures (DiMario & Strohman, 1988). Both mechanisms may co-exist, each possible also in conjunction with slow connective tissue proliferative capacity. A third possibility is offered by Blau et al. (1983); the early senescence of DMD myoblasts *in vitro* may not be present in *mdx* mpc populations, thus suggesting a basic defect in undifferentiated satellite cells from individuals with DMD.

Another possible explanation of the successful regeneration of muscle in the *mdx* mouse and not in DMD, is that regenerated fibers may compensate by producing dystrophin analogues that provide for sufficient function and myofiber stability (Matsumura et al., 1992a; DiMario et al., 1991). Alternatively, once-regenerated myofibers may acquire functions not present in initial myofiber populations (DiMario et al., 1991). The recent identification of a dystrophin-related protein (DRP, utrophin) (Matsumura et al., 1992a), an autosomal homologue of dystrophin, may play a role in sparing *mdx* muscle from the progressive deterioration found in DMD. Utrophin is found in the sarcolemma of small-caliber skeletal muscle and cardiac muscle of the adult *mdx* mouse (Matsumura et al., 1992a), and may explain why these muscles are not affected as much by the dystrophin-deficiency (Karpati et al., 1988). However, utrophin is absent in the sarcolemma of large caliber limb muscles, and these muscles still cope with dystrophin-deficiency successfully, particularly in the very large regenerated fibers. Also, recently it was found that DMD muscles do express utrophin, although this expression may decrease with age and thus may be partly related to the progression of the disease (Mizuno et al., 1993). In any case, utrophin cannot be the only factor protecting fibers in the *mdx* mouse from dystrophy.

It is possible that the deterioration of the *mdx* mouse is not as severe as DMD in its progression because the weight-bearing requirements of mouse hindlimb muscles are less demanding than human DMD muscles (Dick & Vrbova, 1993). Functionally, overloaded *mdx* limb muscles progressively deteriorate with age (Dick & Vrbova, 1993). The *mdx* diaphragm, which is

exposed to continuous use, shows both histological and functional similarities to the progressive component of DMD (Stedman et al., 1991). This fact could partly account for the distinct pattern of dystrophic change seen in muscle fibers bearing the greatest workload. However, the magnitude of the difference between DMD and *mdx* dystrophies may not be explained by this fact alone.

Higher amounts of bFGF found in *mdx* muscle *in vivo* may possibly contribute to explaining its continued successful regeneration (section 2.7). Also, the production of greater than normal amounts of phospholipids (an *in vitro* study) by *mdx* muscle, could foster membrane fusion (Anderson, 1991), and result in faster myotube formation. In any case, to date it has not been successfully resolved as to why *mdx* muscle regenerates so well, and does not progress to the fibrosis seen in DMD. It could be that the above mechanisms work together or as of yet unidentified mechanisms exist.

2.7 BASIC FIBROBLAST GROWTH FACTOR (bFGF) AND MUSCLE REGENERATION IN NORMAL AND *MDX* MOUSE

2.7.1 Structure, physiology and biology of bFGF

Basic fibroblast growth factor (bFGF or FGF-2) is the best characterized member of a family of at least 7 structurally related polypeptides (Baird & Klagsbrun, 1991). It is a single chain peptide composed of 146 or 131 (truncated) amino acids. It is highly distributed among species and has been well conserved throughout evolution (reviewed by Schweigerer, 1990; Gospodarowicz et al., 1987). Low (16-19 kDa) and high (over 20 kDa) molecular weight forms of bFGF have been characterized (Kardami et al., 1991). Basic FGF is released from an unknown source (cells? or ECM?) by simple damage of tissue and cells. It is probably stored in the ECM bound to heparin-like compounds (Baird & Klagsbrun, 1991). Its biological effects are mediated via binding to specific cell surface receptors. The molecular mechanism of action and the mode of secretion of bFGF are unknown.

Of all the known growth factors, bFGF probably has the widest tissue distribution and the broadest spectrum of biological activites. It has been identified in a large number of tissues, tumors and cells of mesoderm or neuroectoderm origin, including skeletal muscle (Gospodarowicz et al., 1987). *In vitro* and *in vivo* functions of bFGF have been characterized (Schweigerer, 1990; Gospodarowicz et al., 1987). *In vitro* functions include: maintenance of vital cellular functions, modulation of proliferation of many cells, modulation of cellular differentiation, stabilization of cellular phenotype, inhibition of cell senescence, stimulation of various different cellular functions and promotion of tissue organization. *In vivo* functions of bFGF include: induction of angiogenesis (thus endothelial cells are positive for bFGF), stimulation of tissue regeneration and wound healing, promotion of maintenance and survival of certain tissues (Baird & Klagsbrun, 1991), tumor progression and roles in early embryonic development.

Thus, bFGF mainly controls proliferation and differentiation of

tissues and cells, possibly in an autocrine, paracrine or intracrine manner. It is readily detected in proliferating, but not quiescent cells, and is scarce in adult tissue (Schweigerer, 1990). Discussion of bFGF will be limited to one of its major roles *in vivo*, namely its role in muscle regeneration (and to some extent muscle development).

2.7.2 bFGF localization in normal limb muscle

Basic FGF has been localized (by immunocytochemical methods using bFGF purified for its [1-24] residues) and studied in humans, dogs and rodents. In normal adult human and dog muscle, little or no staining is seen in the myofiber periphery or the sarcoplasm (Anderson et al., 1993). Perinuclear sarcoplasmic staining varies from weak to moderate. Fetal human muscle shows more sarcoplasmic and perinuclear staining than the adult (Anderson et al., 1993). Fetal dog muscle exhibits moderately stained positive myotube nuclei (Anderson et al., 1993).

In normal intact rat muscle, bFGF mRNA transcripts (localized by *in situ* hybridization) are detected in the cytoplasm of myotubes, but not satellite cells (Guthridge et al., 1992), suggesting that myotubes may be a source of bFGF. In the C57Bl/ScSn mouse, bFGF is immuno-localized to the myofiber periphery, likely the external lamina (Anderson et al., 1993, 1991; DiMario et al., 1989). This suggests an association of bFGF with myofibrils or with ECM components such as heparin (Anderson et al., 1991; DiMario et al., 1989; Kardami et al., 1988). It is also localized to muscle and non-muscle nuclei and to single, dystrophin-positive cells in close association with the myofiber (probably myosatellite cells) (Anderson et al., 1993, 1991). A mosaic pattern of bFGF is evident and this suggests that small, slow fibers are more intensely labelled for bFGF than larger fast fibers (Anderson et al., 1991). There is fivefold more immunoreactive bFGF in slow- than in fast-twitch muscle extracts (Anderson et al., 1991). BALB/c mice show less staining than C57Bl/ScSn (Anderson et al., 1993), as does normal cat muscle (Anderson et al., unpublished data).

There is close correspondence to the tissue levels of bFGF and the intensity of staining by immuno-fluorescence (Anderson et al., 1993, 1991). Thus, we see a continuum in labelling intensity in the above species: C57Bl/ScSn > BALB/c mice > normal dog > human. The bFGF that is bound to the myofiber periphery of normal non-regenerating cells could be required for the continued low-level replication of satellite cells during growth and maintenance of muscles (DiMario et al., 1989).

2.7.3 bFGF expression in limb muscle regeneration

Basic FGF promotes proliferation and inhibits differentiation of myoblasts ***in vitro*** (Allen & Boxhorn, 1989; Clegg et al., 1987). The bFGF receptor is present in myoblasts in culture, but not in differentiated myotubes (Olwin & Hauschka, 1988). In primary cell cultures bFGF mRNA is detected close to the nucleus of myoblasts prior to fusion and in myotubes (Guthridge et al., 1992). Guthridge et al. (1992) suggest that the differentiation of myoblasts just prior to fusion is accompanied by elevated mRNA levels of bFGF and that myotubes are the major source of bFGF in muscle. This source of bFGF then serves to activate quiescent satellite cells and stimulate their proliferation (Guthridge et al., 1992).

Apart from the angiogenic role of bFGF which promotes revascularization of regenerating muscle, bFGF plays important roles in cell proliferation and differentiation ***in vivo***. In injured rat muscle *in vivo*, bFGF mRNA is observed in degenerating and regenerated myotubes and in mononucleated cells that are probably myoblasts aligned in preparation for fusion (Guthridge et al., 1992). Thus it is suggested (Guthridge et al., 1992), that bFGF is released following damage to myotubes and that this primes satellite cells and myoblasts for cell proliferation and inhibits differentiation. Likewise, the release of bFGF from immature myotubes would activate more mpcs cells to proliferate. In regenerating BALB/c muscles, strong bFGF staining is seen in the sarcoplasm of myotubes and some in the perinuclear areas (Anderson et al., 1993). The same is

true for SJL/J myotubes (Anderson et al., in preparation).

2.7.4 bFGF localization in the limb of X-linked dystrophic species

Human dystrophic muscle (DMD) exhibits little staining of interstitial areas, but some staining of the myofiber periphery (Anderson et al., 1993). There is also strong staining in the sarcoplasm of some degenerating myofibers, large centrally nucleated myofibers and smaller newly formed myotubes (Anderson et al., 1993). Nuclear labelling is present in occasional mononuclear cells. Dystrophic dog muscle has a similar staining pattern, with discontinuous or little staining of the myofiber periphery of intact fibers.

A unique characteristic of *mdx* skeletal muscle is that it contains twice as much total extracted bFGF than control counterparts (Anderson et al., 1991). This probably is due to increased amounts of bFGF in the myofiber periphery (DiMario et al., 1989), or to release of bFGF from damaged fibers (Clarke et al., 1993; Anderson et al., 1991). Even at 2 weeks of age, before regeneration and degeneration is very active, higher levels of bFGF are found in *mdx* muscle (DiMario et al., 1989). Intense bFGF labelling distinguishes degenerating areas and recently regenerated areas from adjacent normal-looking areas (Anderson et al., 1993, 1991). Staining in small recently regenerated fibers localizes exactly with the central nucleus (Anderson et al., 1991). DiMario et al. (1989) did not see distinct degenerating and regenerating localization of bFGF because they used a different antibody preparation. There is some nuclear and heterogeneous cytoplasmic bFGF labelling of intact *mdx* fibers, but it does not differ from control areas in intensity of bFGF labelling (Anderson et al., 1991). However, slow-twitch muscles exhibit greater immunoreactive bFGF than the fast-twitch *mdx* muscles (Anderson et al., 1991), and this corresponds to differences in regenerative capacity between these tissues (Anderson et al., 1988, 1987).

2.7.5 bFGF localization in the heart muscle

Basic FGF is found pericellularly, in association with the

intercalated discs and Z-lines. It is also seen in muscle and non-muscle nuclei in the ventricles and the atria of the heart of the rat, mouse and bovine (Anderson et al., 1991; Kardami et al., 1990; Kardami & Fandrich, 1989). Mammalian cardiac muscle exhibits limited regenerative potential. Thus, the control of cardiomyocyte growth and differentiation may be exercised in part by the expression of bFGF (Kardami et al., 1991; Kardami & Fandrich, 1989). It is also interesting to note that the atrial muscle, which has a greater potential for regeneration, exhibits more immunoreactive bFGF than the ventricles (Kardami & Fandrich, 1989). Basic FGF may play a role in cardiac repair processes (Kardami et al., 1991). Recently a cardio-protective role for bFGF has been investigated (Davey & Kardami, 1993, unpublished).

In the heart of the *mdx* mouse, actively degenerating areas stain strongly for bFGF, as do areas of intact myocytes that are adjacent to necrotic tissue (Anderson et al., 1991). *Mdx* cardiac muscles also exhibit more immunoreactive bFGF compared to controls, and both *mdx* and control cardiac extracts show more bFGF than fast-twitch limb muscles from the same animal (Anderson et al., 1991). Basic FGF probably plays a positive role (Anderson et al., 1991) in the *mdx* heart.

2.7.6 Possible roles of bFGF in the *mdx* mouse

As in normal muscles (section 2.7.2), a continuum of the levels of bFGF are seen in dystrophin-deficient species: *mdx* limb muscles > *mdx* heart > *mdx* diaphragm > dystrophic dog muscles > DMD muscles. This continuum corresponds to the regenerative capacity of each muscle and it is proposed that there is a correlation between the local concentration of bFGF and the regenerative processes of skeletal muscle (Anderson et al., 1993, 1991). Abundance of bFGF in the myofiber periphery of the *mdx* mouse may be related to an increase in both satellite cell and regenerative activity (DiMario et al., 1989) and might ultimately increase the mpcs within the damaged tissue long enough to fully compensate for fiber loss (Anderson et al., 1993, 1991). Also, since *mdx* myoblasts may be more

sensitive to bFGF *in vitro* than control myoblasts while the fibroblasts remain unresponsive longer (DiMario & Strohman, 1988), high rates of new fiber formation *in vivo* may be possible without a proliferation of fibroblasts (DiMario & Strohman, 1988).

Since bFGF is associated with heparin in the myofiber periphery (Kardami et al., 1988) and heparin inhibits proliferation *in vitro* (Kardami et al., 1988; DiMario & Strohman, 1988), disruption of this association during active dystrophy or injury could result in the positive response seen in the dystrophin-deficient *mdx* mouse (DiMario et al., 1989, DiMario & Strohman, 1988). The absence of dystrophin in *mdx* sarcolemma may lead to alterations in the external lamina. This would result in enhanced bFGF deposition or altered bFGF-heparin interactions, which would ultimately activate nearby satellite cells to divide (DiMario et al., 1989). Alternatively, Anderson et al. (1993) suggest that the general pattern of bFGF immunofluorescence within myofibers is very similar among species, and relates primarily to the processes of regeneration and degeneration rather than to dystrophin-deficiency (Anderson et al., 1993).

Anderson and colleagues (1991) hypothesize that bFGF may promote tissue repair at 3 levels: as a chemotactic agent released after injury to attract responsive cells, by providing contact guidance to cells converging to the most recent dystrophic injury, and by stimulating the proliferation and/or differentiation of migratory cells at the site of the injury.

2.7.7 bFGF and perturbation of thyroid hormone

Recent findings indicate that bFGF expression (and muscle phenotype) is changed by metabolic disturbances (hyper- and hypothyroidism) (Anderson et al., 1994; Liu et al., 1993). Hyperthyroidism in control and *mdx* limb muscles creates no change in the localization of bFGF, but there is a general reduction of immunostaining for bFGF in skeletal muscle of hyperthyroid mice (Anderson et al., 1994).

In the heart of hyperthyroid control mice, the intensity of bFGF is

reduced (Anderson et al., 1994), but more low molecular weight bFGF compared to euthyroid controls is present (Liu et al., 1993). In the *mdx* hyperthyroid heart, more frequent and larger areas of intense intracellular staining for bFGF are seen, indicating an increase in recent fiber damage (also seen with H&E staining) (Anderson et al., 1994).

Elevated levels of a high molecular weight form of bFGF are found in extracts from hypothyroid adult rat ventricles, atria and skeletal muscle compared to those from euthyroid controls (Liu et al., 1993). This accumulation is similar to that seen in the immature heart (Liu et al., 1993).

A correspondence is observed between high molecular weight bFGF and the immature cardiac phenotype on one hand, and low molecular weight bFGF and the adult, differentiated phenotype on the other (Liu et al., 1993). It is suggested that this difference may be to the size of myocytes (Liu et al., 1993). Thyroid hormone may directly or indirectly down-regulate accumulation of a high molecular weight form of bFGF in the heart. Liu and colleagues (1993) suggest a complex, tissue-specific effect of thyroid hormone on the accumulation of different bFGF species, suggestive of distinct physiological functions. Hypothyroid ventricles display more intense bFGF immunolocalization compared to euthyroid or hyperthyroid hearts (Liu et al., 1993). So while thyroid hormone is known to play a role in differentiation and in bFGF regulation, it is not known how low thyroid hormone level influences muscle regeneration.

2.8 THYROID HORMONE PERTURBATION OF MUSCLE DEVELOPMENT & GROWTH, MUSCLE REGENERATION AND MUSCULAR DYSTROPHY

The thyroid gland synthesizes triiodothyronine (T3) and thyroxine (T4), generally referred to as thyroid hormones, which stimulate the rate of metabolism. The major regulator of the anatomic and functional state of the thyroid gland is thyroid stimulating hormone (TSH), derived from the anterior pituitary gland. TSH stimulates the synthesis and secretion of the hormones produced by the thyroid gland. Secretion of TSH is controlled by a regulating factor produced by the hypothalamus called thyrotropin releasing factor (TRF). The release of TRF depends on the serum levels of T4 and T3 and the body's metabolic rate (among other factors), and operates according to a negative feedback system. When considering muscle, thyroid hormone plays important roles in its development, growth and maturation, regeneration, and in the phenotype of muscular dystrophy.

2.8.1 Thyroid hormone and muscle development

The thyroid gland becomes functional in producing thyroid hormone in mouse fetuses between 15 (van Heyningen, 1961) and 17 days of gestation (d'Albis et al., 1987a). At birth, thyroxine levels show that the neonatal rat is essentially hypothyroid (Gambke et al., 1983), but serum thyroid hormone levels increase shortly after birth in mammals (d'Albis et al., 1987a; Dubois & Dussault, 1977). At approximately day 16 postpartum (mouse) (d'Albis et al., 1987a) and day 35 (rat) (Gambke et al., 1983), thyroid hormone levels begin to approach adult values.

Thyroid hormones and growth hormones act together during development of skeletal muscle. For example, the impaired muscle growth evident in hypothyroid neonatal mice is not only due to thyroid hormone deficiency, but also growth hormone deficiency, possibly via IGF-1 which stimulates fiber growth of skeletal muscle (Murphy et al., 1987). The following effects of thyroid hormone appear to be independent of growth hormone (Simonides & Hardeveld, 1989; Gambke et al., 1983).

Fiber type and isomyosin transitions: Various researchers report a correlation between increased serum concentration of thyroid hormone and

a change in both the fast fiber type proportion and the type of myosin in developing rat (d'Albis et al., 1990; Butler-Browne et al., 1984; Gambke et al., 1983) and mouse muscles (d'Albis et al., 1987a). The transition from neonatal type I and IIC fibers into adult type IIA and IIB fibers, and from embryonic to neonatal to adult isoforms of MHCs corresponds with the gradual increase in serum thyroid hormone levels in the first few weeks of postnatal life (d'Albis et al., 1987a).

Hypothyroidism in neonatal mice (d'Albis et al., 1987a) or rats (d'Albis et al., 1990; Butler-Browne et al., 1984; Gambke et al., 1983) induces an inhibition or delay in muscle differentiation of fast muscles, in that the myofibrillar profile does not mature and there is a large delay in the synthesis of fast adult isomyosins (d'Albis et al., 1987a; Gambke et al., 1983). However, hypothyroidism does not ultimately prevent isomyosin transitions in fast muscle, indicating that thyroid hormone is not an absolute requirement for the transition, but definitely modulates it (d'Albis et al., 1990). Hyperthyroidism significantly accelerates the transition to the adult fast muscle phenotype (d'Albis et al; 1990, 1987a; Gambke et al., 1983). By comparison, hypothyroidism has no effect (d'Albis et al., 1990) or a small effect (Gambke et al., 1983) on slow isomyosin synthesis in slow muscles, whereas hyperthyroidism is inhibitory to the maturation process in slow muscles (d'Albis et al., 1990).

In general, the above reports suggest that thyroid hormone directly regulates the appearance of adult fast myosins and fibers, and either directly or indirectly modulates the disappearance of neonatal types. Innervation does not appear to intervene (d'Albis et al., 1990; Gambke et al., 1983), although there is some uncertainty about this (Nwoye et al., 1982). Various muscles do not display the same sensitivity to thyroid hormone, but appear to be regulated by it in a similar way (d'Albis et al., 1990).

Development of the sarcoplasmic reticulum (SR): In rodents, the SR develops to maturity during the first 4-10 weeks after birth, during which

time the maximal calcium uptake activity increases nearly 10-fold (Simonides and Hardeveld, 1989). This development is absent in hypothyroid rats in which the calcium uptake activity remains constant at 10% of the normal adult values (Simonides & Hardeveld, 1989).

Other effects of thyroid hormone in development: In the development of cardiac muscle, it is suggested that an interaction of T3 and bFGF may modulate neonatal myocardial cell proliferation (Liu et al., 1993; Kardami et al., 1991). This is due to the fact that bFGF is downregulated in hyperthyroid neonatal rat hearts and upregulated in hypothyroid rats (Liu et al., 1993).

2.8.2 Thyroid hormone in adult muscle

Effects on muscle and fiber growth: Thyroid hormone has important effects on muscle and fiber growth. Hypothyroidism induced by thyroidectomy in adult rats, either decreases (Nwoye et al., 1982) or does not affect (Matoba et al., 1982) body weight. Also, myofiber diameters either decrease (Butler-Browne et al., 1984), or show an overall trend to increase in thyroidectomized animals (Matoba et al., 1982). Kaminsky et al. (1991) found that the ratio of muscle to body weight increases with hypothyroidism (0.5 g/l propylthiouracil-PTU in water for 2, 4 or 6wks) in adult male rats.

Hyperthyroidism results in lower body weights of adult male rats (3mg T4 + 1mg T3/kg in food for 6 wks) (Widner et al., 1975), or increased body weights (injection of 2μg/g body weight T3 per day for 2wks in 8wk old mice) (Anderson et al., 1994). Larger myofibers in comparison to body weight are reported by d'Albis et al. (1987a) (injection of 3μg T3/10g for 8-14d postpartum). However, Anderson et al. (1994) report that T3 treatment produces atrophy in all skeletal muscle fibers (injected at 3wks or 8wks of age), and in agreement to this the muscle weights (normalized to body weight) are decreased by T3 treatment. The above discrepancies must be due to differences in the age of the animals or to differing surgeries and/or treatments. Cardiac hypertrophy results from

hyperthyroidism (Anderson et al., 1994; Widner et al., 1975) and is seen as increased cardiac myofiber diameters, likely due to increased metabolic demands on the heart in hyperthyroidism (Anderson et al., 1994).

Fiber type and isomyosin transitions: Fast- (and intermediate-) to slow-changes in fiber types (ie. decreased proportions of type II fibers) (McAllister et al., 1991; Salviati et al., 1985) and the reappearance of embryonic and neonatal myosins (Izumo et al., 1986) are two hallmarks of hypothyroidism in rats. The main changes seen in hyperthyroidism are changes from slow- to fast-fibers (Salviati et al., 1985; Nwoye et al., 1982), and thus more rapid isometric twitches by slow muscles (Dulhunty et al., 1986).

All MHC genes respond to thyroid hormone, but the same MHC gene can by regulated by thyroid hormone in highly different modes in a muscle-specific manner (Fitzsimons et al., 1990; Izumo et al., 1986). Overall, fast MHC (IIA) genes are up-regulated by thyroid hormone in slow-twitch muscles but down-regulated, with different degrees of sensitivity, in fast-twitch muscles (Izumo et al., 1986). Fast (IIB) MHC genes are responsive to thyroid hormone in some muscles (SOL, diaphragm, masseter), but not in others (Izumo et al., 1986). Nwoye and colleagues (1982) favor a direct action of thyroid hormone on myofibers over a neurally mediated mechanism.

Effects of thyroid hormone on MRFs: Recently it has been suggested that thyroid hormone controls the accumulation of MyoD and myogenin mRNAs in fast and slow adult skeletal muscle (Hughes et al., 1993). Muscles with different fiber type compositions demonstrate differential MyoD and myogenin mRNA accumulation, with predominantly slow muscles showing high levels of myogenin and fast muscles showing mainly MyoD mRNA (Hughes et al., 1993). As we saw in the previous section, hyperthyroidism alters the fast/slow fiber type distribution, with activation of fast MHC gene expression in the SOL (Izumo et al., 1986). This alteration also corresponds with changes in the MyoD/myogenin mRNA expression pattern (ie.

an increase in MyoD mRNA in hyperthyroid SOL) (Hughes et al., 1993). It is not known whether the change in MyoD expression precedes or simply parallels the changes in MHC expression.

Other effects of thyroid hormone on muscle: Thyroid hormones have been shown to have many other effects on mature skeletal muscle, which include the regulation of: **i)** ATPase activities (decreased in hypothyroidism) (Nwoye et al., 1982), **ii)** myosin light chain amounts (decreased in hypothyroidism) (Nwoye et al., 1982), **iii)** calcium uptake by the SR (decreased in hypothyroidism, increased in hyperthyroidism) (Salviati et al., 1985; Nwoye et al., 1982), **iv)** the number of mitochondria and thus the amount of aerobic metabolism (decreased in hypothyroidism, increased in hyperthyroidism) (Nwoye et al., 1982; Widner & Holloszy, 1977; Widner et al., 1975), and the mitochondrial enzyme amounts (decreased in hypothyroidism, increased in hyperthyroidism) (Widner & Holloszy, 1977; Widner et al., 1975), **v)** muscle capillarity (enhanced in hypothyroidism) (McAllister et al., 1991), **vi)** Na^+-K^+ pump concentration (hypophysectomy decreases the concentration of Na^+-K^+ pumps in skeletal muscle, independent of growth hormone status) (Everts et al., 1990), **vii)** muscle bioenergetics (using phosphorus magnetic resonance spectroscopy, Kaminsky et al. (1991) found that hypothyroid muscle exhibits abnormal muscle bioenergetics), **viii)** lipid composition and membrane fluidity of the sarcolemma (in hyperthyroidism there is a decrease in the cholesterol to phospholipid ratio, and membrane fluidity increases) (Pilarska et al., 1991), and **ix)** the amount of t-tubule system (increased in hyperthyroidism) (Dulhunty et al., 1986).

2.8.3 Thyroid hormone and muscle regeneration

Limited studies have been performed on the roles of thyroid hormone in muscle regeneration. However, it is expected that the roles of thyroid hormone in muscle development will, to some extent, be recapitulated in regeneration.

Early in the regeneration of fast-twitch muscles (after injection of

a snake venom cardiotoxin), neonatal and adult myosins are synthesized in euthyroid rats (d'Albis et al., 1987b), and the neonatal myosins disappear 10 days after the initial insult as adult isoforms appear. In hyperthyroid rats, regenerating muscles exhibit only adult myosins at 7 days after injury, while in hypothyroid rats, neonatal myosins are still present up to 21 days after injury in combination with adult isoforms (d'Albis et al., 1987b).

2.8.4 Thyroid hormone and muscular dystrophy

It is suggested that any change in the balance of thyroid hormone will change a muscle's response to dystrophy. Anderson and colleagues (1994) have completed an extensive study of the effects of hyperthyroidism (by injection of 2μg/g T3 for 2wks) on muscular dystrophy of the *mdx* mouse and their results follow.

Young (5wk old) treated *mdx* mice have a significantly increased body weight gain compared to both control and untreated *mdx* mice. This increase in weight in treated animals includes an increased heart weight, but atrophied limb muscles. In older mice (10wk old) the weight gain of treated *mdx* animals does not differ from untreated *mdx* mice, likely as the mice are adults at 10 weeks. However, cardiac hypertrophy and limb muscle atrophy are still present in the older treated mice. Fiber diameter in *mdx* heart muscle is increased by T3 treatment in both 5- and 10-week old mice, while the fiber diameter of skeletal muscle is decreased by the treatment.

By studying the extent of inflammatory lesions and fiber centronucleation in dystrophic muscle, Anderson et al. (1994) concluded that dystrophy is worsened in slow-twitch muscles (heart and SOL) by treatment of *mdx* mice with T3. In contrast, damage to the fast-twitch muscles (EDL and TA) is not increased by hyperthyroidism, and in fact appears to be decreased (Pernitsky & Anderson, unpublished results). In the heart, there is a dramatic increase in the number and size of dystrophic lesions in *mdx* T3-treated mice. Also, there is a significant increase in the area of centronucleated fibers in young *mdx* mice in the SOL (an area of active

damage). Probably increased fiber damage, rather than inhibition of repair, is the main effect of T3 treatment in *mdx* mice (Anderson et al., 1994). The effect of excess thyroid hormone on dystrophy is probably related to increased fast MHC expression in slow muscles, increased mechanical strain on slow skeletal and cardiac muscles, or possibly decreased bFGF staining in hyperthyroidism (Anderson et al., 1994).

From this review of the literature, it is obvious that there are many questions to be answered about muscle development and regeneration. The *mdx* mouse is a very useful model for studying regeneration dynamics, as well as for understanding the implications of dystrophin-deficiency. Since the effects of hypothyroidism on muscular dystrophy have not been examined, the purpose of my study was to characterize the effects of hypothyroidism on dystrophic damage in the *mdx* mouse. In addition, the effect of hypothyroidism on muscle regeneration (created by a crush injury) in *mdx* and control mice was studied.

3. PROJECT HYPOTHESES AND OBJECTIVES

Hypothesis:

It was hypothesized that *mdx* mice would regenerate better from a crush injury than control mice. We also hypothesized that hypothyroidism would decrease the level of effective muscle regeneration in control and *mdx* mice, and would worsen dystrophy in the *mdx* mouse. Finally, it was proposed that the localization of neural cell adhesion molecule (NCAM) and basic fibroblast growth factor (bFGF), morphometric studies of tissue sections, and autoradiographic studies of muscle cell proliferation would give clues as to the mechanism of action of thyroid hormone on dystrophy and muscle regeneration.

Specific Objectives:

1. To describe the events in muscle regeneration of control and *mdx* mice by examining the tibialis anterior (TA) muscle at different times during repair from a crush injury.
2. To study the effect of a lowered metabolic rate (by treatment with propylthiouracil) on the myogenesis and muscle regeneration (created by a crush injury and by *mdx* dystrophy) in the TA muscle of *mdx* and control mice by using morphometric techniques.
3. To characterize the pattern of immunostaining for NCAM in *mdx* and control mice, and to determine whether it is a specific and sensitive marker for myoblasts.
4. To use antibodies against NCAM and bFGF in an attempt to locate muscle precursor cells (mpcs) in the TA of both mouse strains, and to determine if hypothyroidism has any effect on this localization by the 2 antibodies. The original idea was that: i) cells that colocalized both NCAM and bFGF would be early muscle precursors, ii) cells that stained with NCAM-only would be myoblasts preparing for fusion, and iii) cells that stained with bFGF-only would be other mononuclear cells (ie inflammatory cells and

fibroblasts).

5. To use autoradiographic studies to determine if a hypothyroid state affects the number and proportion of mpcs undergoing division in muscle repair and muscular dystrophy.

4. METHODS

4.1 EXPERIMENTAL ANIMALS

In this study, the dystrophic *mdx* mouse and its normal control (C57Bl/10ScSn) were used to study dystrophy and muscle regeneration in a hypothyroid state. The mice were bred and housed in the Central Animal Care Facility at the University of Manitoba and were descendants of the original breeding pairs of *mdx* mice (Bulfield et al., 1984). Animals were cared for according to the Council on Animal Ethics.

4.2 TREATMENT

Hypothyroidism was created in *mdx* mice and their controls (C57Bl10/ScSn) by treatment with 0.05% propylthiouracil (PTU) (D'Albis et al., 1987a) *ad libitum* in drinking water. The mice were treated for eight weeks after the onset of dystrophy at three weeks of age (Bridges, 1986). Age-matched littermate *mdx* and control mice were left untreated for the same period. Mice were checked daily for side effects of the treatment. The experiment was run 5 times in order to provide samples for a variety of studies.

4.2.1 Measures of metabolic and growth parameters

To ensure that a hypothyroid state was achieved, various metabolic and growth parameters were measured. Mice were weighed weekly and the percentage of weight increase over the treatment period was calculated. Weekly percent weight increase was plotted. Water consumption was measured daily for each cage and calculated as a per mouse amount. Also, the respiratory rate at the end of the treatment period was estimated, in a double blind fashion, by counting the number of breaths of each mouse over three 30 second intervals. This was done five minutes after anesthetic was administered. At the time of death, blood was drawn from the heart for TSH assay (Cadham Provincial Labs, Winnipeg). Blood was allowed to clot overnight in the fridge and was taken to the lab the next morning. The

soleus and gastrocnemius muscles were dissected from the limbs, weighed, and reported as absolute values and as proportions to body weight. Behavior and body movements of the mice were also monitored during the treatment period.

4.3 SURGERY

After the eight week PTU treatment period, mice were anesthetized (1:1 ketamine:rompin, 0.01cc/10g body weight) in random coded order and the respiratory rate was measured for each mouse. The mice were then subjected to a crush injury of the right, or both, TA muscles (Grounds & McGeachie, 1989). Skin and fascia were antiseptically cut, and the TA was gently separated from underlying muscle and bone. A serrated hemostat was placed around the muscle belly of the TA and was closed (to one notch) and held for five seconds. The same hemostat was used by the same researcher to minimize the variation of the crush size. Muscle continuity was not disrupted. The skin and fascia were quickly closed with 3 or 4 silk sutures (5-0).

After the respective recovery time, mice were anesthetized and blood was drawn from the right atrium for TSH assay. The TA muscles were quickly removed and bisected longitudinally with a razor blade (through the center of the crush). The left and right muscles were frozen in pairs in OCT compound (Tissue-Tek), for cryosectioning (8μm), by immersing molds containing OCT and tissue sample block in isopentane cooled to below -50°C on dry ice. The other half of each muscle was quickly frozen on dry ice and kept at -70°C in sealed eppendorf tubes for electrophoresis and Western Blotting.

4.3.1 Protocol 1: Preliminary time course study

Both right and left TA muscles were crush-injured after 8 weeks of PTU treatment, and mice were left to recover for 0 (2 hours), 2, 4, 11 or 15 days (1 control untreated, 21 control treated, 1 *mdx* untreated and 1 *mdx* treated mouse per each time period).

4.3.2 Protocol 2: 4 day recovery

A total number of 7 control untreated (5 males, 2 females), 7 control treated (5 males, 2 females), 7 *mdx* untreated (5 males, 2 females) and 6 *mdx* treated mice (4 males, 2 females) were subjected to a crush injury of the right TA after 8 weeks of treatment. This protocol was performed twice and the results were pooled. The left TA was uncrushed so that this TA served as a control for the right (crushed) TA. Mice were allowed to recover for 4 days, were anesthetized, blood was drawn and TA specimens were collected as before. The diaphragm was also removed and the costal (anterior right) portion was frozen in OCT. The soleus and the gastrocnemius muscles were removed and weighed. Morphometric, immunohistochemical, autoradiographic and blotting analyses were performed as described below.

4.3.3 Protocol 3: 4 week treatment

To determine whether the changes in dystrophy observed with PTU were different with a shorter period of treatment, 7 *mdx* mice (5 males, 2 females) were treated (0.05% PTU) for 4 weeks. Seven age-matched littermate *mdx* mice (5 males, 2 females) were untreated for the same 4 weeks. The mice were subjected to a crush injury of the right TA muscle and left to recover for 4 days. Histological and morphometric analysis of the TA muscles were done as per the 8 weeks treatment (see below).

4.3.4 Protocol 4: Restoration of euthyroid state

As a further small study, one mouse in each treatment group was removed from the PTU-treatment after 8 weeks of treatment (untreated mice were used as controls once again) and left untreated for 2 further weeks. This was done in order to test whether restoring normal thyroid state would be accompanied by restoration of any changes in muscle repair. The crush injury was performed on both legs after the 2 weeks of non-treatment. Mice were allowed to recover for 4 days and muscles were prepared as above for sectioning.

4.4 HISTOLOGY

Frozen TA or diaphragm muscle blocks were longitudinally sectioned (8μm thick) with a cryostat. The orientation of the muscle block for a longitudinal alignment of myofibers was carefully made on initial sections using phase contrast optics and adjustment of block positioning during sectioning. It is the architecture of the TA muscle, pennate, with a central tendon, which dictates that when fibers on one half of a proximal-distal section of the muscle are longitudinal, those fibers on the opposite side of the central tendon will be oblique or cross-sectioned. This was taken into consideration when examining each muscle.

Alternate serial sections were stained with Hemotoxylin and Eosin (H&E) for examination under the light microscope. These were examined in a double-blind fashion (coded slides) and observations were recorded. An Olympus BHT-2 microscope was used to observe specimens and to photograph selected fields. Also, some sections were stained with a basic fuchsin, methylene blue and Azure II stain (Ontell, 1974) and photographed.

4.5 MORPHOMETRY

4.5.1 Unoperated TA

The morphometric analyses were made only on the muscles allowed to recover for 4 days. On coded H&E sections, various measures were used to assess the extent of regeneration and dystrophy in defined longitudinal zones of the TA, prior to decoding the sections.

Parameters analyzed: 1. Dystrophic areas: In the *mdx* unoperated (left) TA, the total area of active dystrophy (defined as all degenerating and inflammatory areas in a TA as a proportion of the total muscle area) and the number of dystrophic foci (the number of degenerating and inflammatory areas as a proportion of the total muscle area) were measured. The Sigma Scan program (Jandel Scientific, CA) and a calibrated computerized graphics tablet were used to measure the areas. 2. Nucleation: In the muscles of the left leg of *mdx* mice, the

centronucleation index (CNI, defined as the number of cells with central nuclei as a proportion of the total number of fibers) was determined, as a measure of accumulated fiber injury and regeneration during dystrophy. Also, the total number of central and peripheral nuclei, and the ratio of central-to-peripheral nuclei (CN:PN) in 2 areas of the unoperated TA were determined.

4.5.2 Operated TA

Zonal analysis: In the operated (right) TA, zones of crush site, adjacent muscle, and surviving muscle were analyzed in a systematic manner (after Mitchell et al.,1992) at 200X by measurement of set distances from the centre of the necrotic crush zone which was acellular at 4 days post-injury (Fig. 1). The parameters analyzed are detailed below. Two fields were assessed within the crush area in each operated muscle, four in the adjacent area (3 proximal, 1 distal), and three fields in the region of distant surviving muscle (2 proximal, 1 distal). The adjacent and surviving zones were determined by their pre-set distance from the crush, and not according to the cells prevalent in those regions. If there were more than five surviving fibers in a field of "adjacent zone", as defined, that field was not counted. For statistical analysis, the four fields adjacent to the crush were pooled, as there was no difference between proximal and distal fields in that zone. However, the distal and proximal fields in the surviving muscle were analyzed separately.

Care was taken to ensure that the morphometric study was always carried out on the longitudinal aspect of the muscle and not on the oblique or cross-sectioned fiber areas. As explained above, the architecture of the TA muscle may make parts of the muscle cross-sectional instead of longitudinal.

Parameters analyzed: 1. Nucleation: The numbers of central and peripheral muscle nuclei were counted in each zone (Fig. 1) of the operated TA, and the ratio of central-to-peripheral nuclei was determined (CN:PN) within the same fields. 2. Myotubes: The number of small myotubes

in each of the above areas was also counted. 3. Crush area: Using the Sigma Scan program in conjunction with a camera lucida at 100X magnification, the area of the necrotic acellular crush zone was outlined and measured. 4. Fiber diameter: Fiber diameter was measured from the unoperated TA and from the distal surviving zone of operated TA in both control and *mdx* mice, again using the calibrated graphics tablet and a camera lucida at 100X. At least one hundred fibers were sampled from each muscle section, along cords perpendicular to the longitudinal axis of each muscle as previously reported for fiber area (Anderson et al, 1987). Measurements at the smallest diameter of each fiber were recorded.

4.5.3 Statistical Analysis

Data (mean ± SEM) for each muscle ($n \geq 6$-7) was determined and the means from the 4 groups were analyzed using a 2-way ANOVA to detect strain (control vs *mdx*), treatment (PTU) and interactions (strain and treatment). Individual groups were compared using Duncan's multiple range test *post hoc* where appropriate. The distribution of fiber diameter in the different groups was compared using Chi-square statistics. In addition, the distribution of fiber diameter was plotted. Repeated measures ANOVA was used to compare fiber diameter and CNI between unoperated (left) and operated (right) TA in the 4 groups. The mice treated for 4 weeks were analyzed with unpaired t-tests, and 2-way ANOVAs were used to compare 4 week and 8 week groups. In all cases, a probability of $p<0.05$ was used to reject the null hypothesis.

4.6 IMMUNOHISTOCHEMISTRY

4.6.1 Staining Procedure

NCAM has been found to be specific to mpcs (Jones et al., 1990; Covault & Sanes, 1986; Moore & Walsh, 1985) (section 2.4). Also, bFGF localizes to probable mpcs and to inflammatory cells, and has been found to be more abundant in *mdx* than control muscles (Anderson et al., 1993; 1991). Thus, it was of interest to see if the 2 antibodies stained for the

same cell population.

Alternate serial sections were double-immunostained for fluorescent localization of the [1-24] residues of bFGF (Anderson et al., 1991) and for NCAM antibody (monoclonal anti-HNK-1/N-CAM (Sigma) - mouse IgMμ isotype), according to the protocol detailed below. The anti-bFGF antibody has been well characterized (Kardami & Fandrich, 1989; Anderson et al., 1991; Penner & Anderson, unpublished results) as specific and sensitive. The anti-NCAM monoclonal antibody localizes the 145 and 170 high molecular weight, integral membrane forms of NCAM. It also recognizes myelin-associated glycoprotein in some species, and a high molecular weight chondroitin sulphate proteoglycan.

Tissue sections of both unoperated and operated TA muscles were dried at room temperature for one hour and then blocked for one hour with PBS containing 10% horse serum (HS) and 1% bovine serum albumin (BSA). The primary antibodies used were anti-bFGF raised in rabbit (see Anderson et al., 1993) and anti-NCAM raised in mouse (Sigma clone). Anti-bFGF and anti-NCAM were used respectively at 1:1500 and 1:2000 dilutions. Both antibodies were added to the blocking solution of 10% HS, 1% BSA in PBS containing 0.01 ml sodium azide. After incubation overnight at 4°C, sections were thoroughly rinsed with PBS, again blocked for 1 hour, and rinsed in PBS. Combined incubation with secondary antibodies (diluted in PBS containing 1% BSA) for two hours occurred at room temperature. Fluorescein-conjugated anti-rabbit immunoglobulin raised in donkey (Amersham) was used at 1:200 to detect rabbit anti-bFGF. Biotinylated anti-mouse immunoglobulin (against IgMμ) raised in goat was used at 1:250 to detect mouse anti-NCAM. After extensive rinsing, sections were incubated with Texas Red - streptavidin (from *streptomyces avidinii*) (Amersham) at 1:250 dilution in 1% BSA in PBS for 20 minutes to detect the biotinylated antibody. Sections were rinsed in PBS, fixed in cold ethanol, rinsed in PBS again and mounted (Immumount). Negative control slides (omission of primary antibodies) accompanied the immunostaining procedures

in each case. In addition presorption of anti-bFGF with human recombinant bFGF (Sigma) was used as a control. Brain sections were a positive control for anti-NCAM.

In addition to the double-staining procedure described above, some sections were stained singly either for NCAM or for bFGF, and observations were recorded. In this case, the secondary antibodies were linked to horse-radish peroxidase. Visualization was achieved by a DAB (diaminobenzadine) kit (Dimension Labs) which resulted in a more permanent brown-black precipitate of NiCl. Endogenous peroxidase activity exhibited by some cells (red blood cells, macrophages) was quenched by incubating sections in hydrogen peroxide (0.3% in water) for 1 hour prior to incubation with the respective primary antibody. Dilutions of antibodies and rinsing steps were followed as described for double-staining.

4.6.2 Indirect fluorescence microscopy

An Olympus microscope equipped with epifluorescence and phase contrast optics was used for specimen observation and to photograph selected fields. The anti-bFGF positive cells fluoresced green (FITC) under ultra violet light while the anti-NCAM positive cells fluoresced red (Texas Red). Sections of at least 5 muscles per group were closely examined.

4.6.3 Analysis

The adjacent zone of the operated TA was carefully examined. A blink-comparator method was used as follows. Photographs of the fluorescent fields were made at the 2 different emission wavelengths. One wavelength was used to visualize the anti-bFGF (FITC) and the second visualized the anti-NCAM (Texas Red), as described above. A third photograph of the same field was taken using phase contrast optics. This allowed the histology of the exact area of the fluorescence photograph to be identified. The film was developed and the negatives were mounted as slides for viewing with a slide projector.

The slides were coded as to the treatment group and strain and

placed in pairs (matching anti-bFGF and anti-NCAM fields) into a slide carousel. They were then projected onto white paper covered with a sheet of transparent acetate mounted on a nearby small screen. Each positively-stained cell or nucleus was marked with a felt marker. First the slide of the anti-bFGF-stained field was projected, and any positive cells or nuclei were marked in green. Then the slide of the anti-NCAM-stained cells from the same field was projected onto the same paper and aligned to precisely match the previous anti-bFGF field. The anti-NCAM-positive cells or nuclei were marked in red. In this way the nuclei and cells could be identified which showed colocalization of anti-bFGF *and* anti-NCAM staining, as well as those which showed localization of anti-bFGF *only* or of anti-NCAM *only*.

Each pair of slides (n=5-7 per treatment group) was analyzed separately. The numbers of positive cells/nuclei were counted for each matched pair of fields under three categories: anti-bFGF and anti-NCAM positive; anti-bFGF positive only; anti-NCAM positive only. The slides were then decoded and statistics were performed on the data. The proportion of positive cells in each category (mean ± SE) was calculated, although it was not used for statistical analysis. The distribution of positively stained cells in the three different categories was compared using Chi-square statistics. The Chi-square test was then partitioned in order to compare individual groups. In all cases, a probability of $p<0.05$ was used to reject the null hypothesis. A histogram was prepared of the distributions, shown as percent of total for each category (mean ± SE for each group).

4.7 AUTORADIOGRAPHY

4.7.1 Procedure

An additional 9 *mdx* and 11 control mice were treated (5 *mdx*, 5 control) or untreated (4 *mdx*, 6 control) for 8 weeks (see section 4.2) and operated on (detailed in section 4.3). Twenty-four hours before death

(death occurred 4 days post-operation), animals were injected (ip) with tritiated thymidine (2μCi/g body weight, 1 mCi/ml, Amersham) to label cells in which DNA synthesis was occurring. The TA was collected and frozen for sectioning as previously outlined. Samples of intestine were also taken to monitor the uptake of tritiated thymidine into the blood stream.

In addition, mice which recovered for 2 days (from protocol 1, preliminary time course study) were injected with tritiated thymidine 24 hours before death, TA samples were collected, and 2 muscles per each group were analyzed (outlined below).

After drying the slides overnight, sections were fixed in formalin for 10 minutes, rinsed with water, individually dipped in warmed photographic emulsion (Ilford KD5, diluted 2:1), and dried in complete darkness in an oven for 2 hours. Slides were then placed in black light-tight boxes and were exposed at 4°C for 7 weeks. The exposure time was determined using an additional set of identical slides developed at regular intervals prior to 7 wks (Anderson et al., 1987).

The slides were developed after the 7 weeks. In darkness, slides were developed in D-19 developer (diluted 1:9, 5 mins), rinsed in water (1 min), fixed (5 mins), washed in water (15 mins), dehydrated, counter-stained with hematoxylin and eosin (for autoradiography) and mounted with coverslips.

4.7.2 Assessment of autoradiograms

Slides were examined under the light microscope. The radiolabelled cells had silver grains above the level of the tissue. Cells which had 3 or more grains on top of the nucleus were considered positively labelled for DNA synthesis during the 24 hours prior to animal death.

A scheme similar to the examination of tissue morphometry was used for counting positively labelled cells (Fig. 1). In the operated TA, positive cells were counted in adjacent areas. Twelve fields at 400X were assessed (6 proximal, 6 distal). Three categories of positive cells were

examined: i) polys as a proportion of total polys, ii) positive myotube nuclei as a proportion of total myotube nuclei, and iii) total positive cells as a proportion of total cells in the field.

Proportions for each category of cell type (see above) were determined for each field (not pooled) and analyzed using 2-way ANOVAs. As well, distal and proximal areas were analyzed separately. Individual groups were compared using Duncan's multiple range test *post hoc* where appropriate. In all cases, a probability of $p<0.05$ was used to reject the null hypothesis.

Gel electrophoresis and Western blotting were performed using TA muscle samples. These methods and results are presented in appendix A.

5. RESULTS

5.1 MEASURES OF METABOLIC AND GROWTH PARAMETERS

In order to confirm hypothyroid status, a number of metabolic and growth parameters were measured: body weight gain, water intake, respiratory rate, TSH level, muscle weight and muscle to body weight ratio (Table 1). These parameters indicated that hypothyroidism was achieved by treatment with 0.05% PTU for 8 weeks. However, it was inconclusive as to whether a hypothyroid state was created by the 4 week treatment period, since the commercial TSH assay changed between experiments.

The age-related increase in body weight (Fig. 2) was decreased (compared to normal) in *mdx* mice treated for 8 weeks (significant interaction by ANOVA, $p<0.05$). Control body weight was not significantly affected by PTU treatment. In agreement with previous reports (Anderson et al., 1987; 1988), *mdx* mice weighed significantly ($p<0.02$) more than their age-matched controls. However, the weight of *mdx* mice treated for 4 weeks was unchanged compared to those untreated for the same period.

Neither the absolute muscle weight nor the ratio of muscle to body weight of the soleus and gastrocnemius was affected by 4 or 8 weeks of PTU treatment. *Mdx* soleus and gastrocnemius muscles were heavier ($p<0.05$) than in control mice. Lower water intake ($p<0.001$), lower respiratory rate ($p<0.01$) and increased TSH levels ($p<0.01$) were noted in all groups of mice treated with PTU for 8 weeks. Lower water intake ($p<0.001$) was also noted in *mdx* mice treated for 4 weeks.

After decoding observations made at the time of tissue preparation, it was noted that the crushed areas of operated TA from untreated and treated control mice were clearly more hemorrhagic than crush sites from *mdx* untreated TA. Also, crush sites of PTU-treated *mdx* TA appeared very similar to the TA of either treated or untreated control mice.

5.1.2 Observations when handling mice

Throughout the treatment period, all mice appeared outwardly

healthy. However, during handling the treated mice were noted to be less excitable and less active than the untreated *mdx* or control mice. Treated *mdx* mice did not demonstrate extension (dorsiflexion) of the hindlimb toes during suspension above the cage floor, typical of untreated control and *mdx* mice. This suggested some clinical signs of muscle weakness were present during PTU treatment of *mdx* mice. Also, the *mdx* untreated mice appeared to be less active than control untreated mice, probably due to their larger size, in addition to their ongoing dystrophy.

5.2 HISTOLOGY: PROTOCOL 1: Preliminary time course study

TA muscles from untreated and PTU-treated control and *mdx* mice were examined at 0 days, 2 days, 4 days, 11 days and 15 days (1 control untreated, 1 control treated, 1 *mdx* untreated, 1 *mdx* treated per each time period) after a crush injury in order to survey the events in muscle regeneration and to obtain a general idea of the effects of hypothyroidism on regeneration. The events were very similar in sequence to those described by Mitchell et al. (1992) and will be briefly outlined below.

At **0 days** (2 hours after crush) (Fig. 3A), no measurable necrotic crush area was present, since the myofibers were just beginning to lose their integrity. No inflammatory cells were present in the damaged area.

Two days after a crush injury (Fig. 3B), a large necrotic zone with many degenerating fibers was present at the mid-belly of each TA muscle. Adjacent to the necrotic zone (both proximally and distally), there was a small area of mononucleated cells. Some of these cells were inflammatory cells (such as macrophages and neutrophils), involved in removing debris in advance of the growth of new blood vessels in the area. Presumably, there were mpcs in the same population of mononucleated cells, but they could not be positively identified by the light microscope. Few myotubes were present in the area adjacent to the crushed zone at 2d. In order for a cell to be considered a myotube, it had to have greater than 2 centrally placed nuclei and exhibit a light pink to purple cytoplasm stained by H&E.

Next to the adjacent areas were areas of surviving muscle that were mainly unaffected by the crush. In *mdx* muscles, most of the surviving areas exhibited centrally-nucleated myofibers, due to the continuing dystrophic process. Some areas of active dystrophy were observed independent of the crushed area.

Differences between treatment groups 2 days after injury were as follows. The control untreated TA exhibited a crush area that was smaller (2.0×10^{-4} μm^2) than the control treated necrotic crush area (2.1×10^{-4} μm^2), and the treated *mdx* TA exhibited a larger necrotic zone (1.7×10^{-4} μm^2) than the untreated *mdx* (1.3×10^{-4} μm^2). *Mdx* TA exhibited more mononucleated cells and myotubes in the adjacent area than controls.

Operated control and *mdx* muscle, **4 days** after muscle injury showed zones (Fig. 1) typical of crushed muscle (McGeachie and Grounds, 1987; Mitchell et al., 1992). Areas of necrotic tissue at the crush site, the adjacent region of inflammatory and mononuclear cells plus small regenerating myotubes, and the distant area of surviving muscle fibers were obvious (see Figs. 4 & 5). At 4 days after injury, the necrotic degenerating zone was considerably smaller than at 2 days and the adjacent zones were larger and more active (Fig. 3B vs 4C-F). Many myotubes were present in the adjacent area in all TA muscles. The untreated *mdx* TA appeared to have more myotubes extending further into the crush zone and a smaller crush site (Fig. 4D) than the PTU-treated *mdx* TA (Fig. 4F). Histologically, no large differences were seen between control groups (Fig. 4C vs 4E).

Myotube formation in the crushed TA of control untreated mice was typical of earlier reports of crush injured muscle (McGeachie and Grounds, 1987; Grounds and McGeachie, 1989; Mitchell et al., 1992). Short chains of 5-7 nuclei in longitudinal section were found within control myotubes located in the zone adjacent to the crush site (Fig. 5A&C). In untreated *mdx* TA, myotubes appeared longer and contained many more nuclei (Fig. 5B) than in control TA. The presence of long myotubes in the adjacent zone

close to the crush site of untreated *mdx* TA appeared to be reduced in PTU-treated *mdx* TA (Fig. 5D). As well, the number of control fibers in the distal surviving zone which contained central nuclei in both untreated and PTU-treated (Fig. 5E) mice appeared to be greater than in the unoperated control TA, an observation confirmed by CN:PN data (see below, and Tables 2 and 3). In *mdx* TA from untreated and treated (Fig. 5F) groups, there also appeared to be more fibers containing central nuclei in both the proximal and distal surviving zones than in the unoperated *mdx* TA.

No measurable necrotic area was present **11 days** after crush injury (Fig. 3C). The central mid-belly area was instead filled with new small myotubes and centrally nucleated myofibers. The area of new small myotubes appeared smaller in *mdx* untreated than control untreated TA.

At **15 days** after crush (Fig. 3D), it was difficult to see the area where the injury had been inflicted, especially in *mdx* muscles. Myotubes and myofibers had filled in the crush area.

In conclusion, muscles regenerating from a crush injury underwent massive degeneration, beginning sometime in the first day after injury. Many phagocytes migrated into the area, and the formation of some myotubes began at 2 days post-injury. This regenerative response continued to 4 days after injury, when many myotubes and mononuclear cells were observed in zones adjacent to the crush injury. After this time, myotube formation did not appear to be quite as active (at 11 and 15 days). By 15 days after the injury, little evidence of the crush remained.

Therefore, 4 days of recovery after the crush injury was determined to be the best stage in which to pursue further studies on the effects of hypothyroidism on muscle regeneration and dystrophy. This stage of very rapid myotube formation and active regeneration might be affected by PTU-treatment.

5.3 HISTOLOGY AND MORPHOMETRY: PROTOCOL 2: 4 day recovery

The experiment was repeated with PTU treatment for 8 weeks, with larger groups, and the mice recovered for 4 days after the surgery.

Detailed histological and morphometric analyses were performed. These results are now reported (McIntosh et al., 1994).

5.3.1 Histology

Unoperated TA: Unoperated control and *mdx* muscle histology was characteristic of previous reports (for example see Anderson et al., 1987; Coulton et al., 1988; Dangain & Vrbova, 1984). Control muscle fibers with peripherally located nuclei (Fig. 4A), exhibited characteristic organization in fascicles. *Mdx* muscle presented foci of active dystrophy, and many areas of myofibers with central nuclei (regenerated fibers), as well as intact fibers with peripheral nuclei (Fig. 4B). No large differences were observed between unoperated muscles of PTU-treated and untreated *mdx* or control mice, such that groups of coded slides were not separable by observations made in a double blind manner.

Operated TA: The histology of the operated TA was similar to that described in section 5.2.1. Double blind observations by two observers were unable to find differences between slides from untreated and treated control animals. In contrast, the same type of observation was able to clearly detect two different groups of muscle sections among the *mdx* group. After decoding, it was determined that the untreated *mdx* group had consistently more myotubes extending further into the crush zone and a smaller crush site than the PTU-treated *mdx* TA.

Sections that were stained with basic fuchsin, methylene blue and Azure II (Ontell, 1974) were examined. Some histological features were more prominent with this stain than with H&E. Small vesicles and spikes of cytoplasm could often be seen near the blunt end of sealed myofibers (Fig. 9C). Also, myotubes were clearly seen fusing with myofibers, and some branched myotubes were obvious (Fig. 9D).

5.3.2 Morphometry

Unoperated TA (Table 2): The general character of regeneration from dystrophy appeared to be worsened by the PTU treatment. The area of active dystrophy in treated *mdx* TA was significantly greater ($p<0.05$) than in

untreated *mdx* TA. However, no change in the number of foci of active injury was noted between treated and untreated *mdx* TA.

The centronucleation index was not changed by PTU treatment. The ratio of central to peripheral nuclei (CN:PN) was much larger in *mdx* TA ($p<0.001$) than in age-matched control TA due to the dystrophy in *mdx* mice, but no effect of PTU treatment on this ratio in unoperated *mdx* or control TA was noted. Interestingly, there was a significant correlation ($r=0.725$, $p=0.005$, $df=11$) between body weight and centronucleation index in untreated *mdx* mice. This correlation was not changed by PTU treatment. The total number of nuclei per field of unoperated muscle was larger in *mdx* than control TA.

Mean fiber diameter in unoperated TA was significantly smaller ($p<0.01$) in PTU-treated *mdx* muscle than in untreated *mdx* TA. The *mdx* TA also had a larger mean fiber diameter than control TA ($p<0.01$). PTU treatment did not affect mean fiber diameter or distribution (Fig. 6) in control unoperated muscle. However, *mdx* unoperated fiber diameter distribution was significantly left-shifted with PTU treatment, indicating greater numbers of small myotubes had regenerated from dystrophic injury during the treatment period.

Operated TA (Table 3): Regeneration from a crush injury appeared to be decreased by PTU-treatment, especially in *mdx* mice. The size of the necrotic crush zone was not different between control and *mdx* TA. However, the crush zone in *mdx* PTU-treated TA was greater in area than in untreated *mdx* TA, while treatment did not change the area of the crush zone in control TA (significant interaction by ANOVA, $p<0.05$). More myotubes (ANOVA, $p<0.001$) were observed in *mdx* crush-injured TA than in control TA, regardless of treatment or zone, 4 days after injury. In general, PTU treatment seemed to reduce the number of myotubes in *mdx* TA, although statistical significance was noted only in the surviving zone (significant interaction by ANOVA, $p<0.02$), likely due to variability within groups.

The ratio of central to peripheral nuclei (CN:PN) in all zones

(except for the distal surviving zone) of operated *mdx* muscles was significantly higher ($p<0.001$) than in control operated TA. This was especially noted in the adjacent zone, in agreement with the observation of longer myotubes with more central nuclei extending into the adjacent zone in injured *mdx* muscles. As well the CN:PN ratio was higher in the distal surviving zones of crushed muscles than in the contralateral unoperated TA for all groups ($p<0.001$), suggesting that the crush injury had an effect on nuclear position in distant fiber segments 4 days after the injury. The CN:PN in distal surviving muscle was also greater ($p<0.001$) than in the zone of fibers surviving proximal to the crush. PTU-treated *mdx* operated muscles generally had higher CN:PN ratio (and greater variability) in all three zones, although the ratio was not significantly different from that in untreated *mdx* TA zones.

In the operated TA, the mean diameter of surviving fibers in untreated mice was smaller in *mdx* than in control TA ($p<0.01$). After PTU treatment, the diameter of the surviving fibers in operated *mdx* TA was greater ($p<0.01$) than in the surviving fibers in untreated *mdx* TA. In untreated *mdx* mice, the diameter of surviving fibers distal to the crush was also lower ($p<0.01$) than fibers in the contralateral unoperated TA.

The distribution of fiber diameters (Fig. 6) was unaffected by treatment in the surviving fibers of control crushed TA. In comparison, the distribution of surviving fiber diameters in the treated *mdx* TA was shifted toward the right (larger fiber diameter) ($p<0.01$).

5.4 HISTOLOGY AND MORPHOMETRY: PROTOCOL 3: 4 week treatment

To determine whether the changes in dystrophy observed with PTU were different with a shorter period of treatment, mdx mice were PTU-treated or untreated for 4 weeks. Treatment began at 3 weeks of age, since dystrophy begins in *mdx* mice at this time. Interestingly, 3 treated mice and 1 untreated mouse died during the surgery or immediately afterwards.

5.4.1 Histology

The **unoperated TA** in the younger *mdx* mice (treated or untreated for 4 weeks) exhibited areas of degeneration and regeneration as per older *mdx* mice (treated or untreated for 8 weeks). However, less centrally nucleated fibers were present because of the shorter time span of dystrophy. In the **operated TA**, the zones (Fig. 1), and cells prevalent in those zones, were similar to those described for older *mdx* mice (section 5.3.1). Histological differences between *mdx* treated and untreated TA were not apparent after 4 weeks of treatment.

5.4.2 Morphometry

This study was performed in order to determine whether the large centronucleation index in the unoperated TA of older untreated *mdx* mice had obscured a change in the CNI after PTU treatment. However, all morphometry data after 4 weeks (treated or untreated) closely mimicked that after 8 weeks (treated or untreated).

Unoperated TA (Table 2, last 2 columns): The proportionate area of active dystrophy was significantly increased by 4 weeks of treatment with PTU ($p<0.05$), similar to the change after 8 weeks of treatment. There was also an increase ($p<0.02$) in the number of peripheral nuclei (satellite cells plus myonuclei) with PTU treatment of *mdx* unoperated muscles, although the CNI was unchanged.

Differences between older (treated or untreated for 8 week) and younger (treated or untreated for 4 weeks) were determined (age effect, Table 2), and were similar to previous reports (Zacharias & Anderson, 1991; Karpati et al., 1988; Anderson et al., 1987). Basically, the dystrophy in the younger *mdx* mice was more active than in the older *mdx* mice, as reflected in the greater number of dystrophic foci ($p<0.001$). As expected, the number of centrally placed nuclei was significantly less ($p<0.001$) in the younger *mdx* mice, due to the shorter duration of dystrophy.

Operated TA (Table 3, last 2 columns): The only significant change

with PTU treatment for 4 weeks was an increase in the myotube density in the surviving zone of the TA ($p<0.02$). This was in contrast to a decrease in the myotube density in the surviving zone of *mdx* mice treated with PTU for 8 weeks compared to *mdx* untreated for the same period.

Once again, differences between older (treated or untreated for 8 weeks) and younger (treated or untreated for 4 weeks) *mdx* TA were evident. The crush was not significantly different between the *mdx* mice injured after 4 or 8 weeks. The CN:PN ratio was significantly decreased in adjacent ($p<0.05$) and proximal ($p<0.001$) surviving zones of the young *mdx* mice. As well, the crush zone ($p<0.05$) and the surviving zone ($p<0.01$) exhibited fewer myotubes in younger than older mice. However, the adjacent zone in younger mice showed as many myotubes as in older mice.

5.5 PROTOCOL 4: Restoration of euthyroid state

In order to test whether restoring a normal thyroid state would be accompanied by restoration of any changes in muscle repair, one mouse per treatment group was left untreated for 2 weeks following 8 weeks of treatment. Since only one mouse per group was treated in this manner, no morphometrical analyses were performed. However, by observations when handling the mice, it appeared that the mice gradually regained the movements demonstrated by the untreated mice. As the 2 weeks progressed, the mice moved more freely when held by the tail and extension of the hindlimb toes was observed, suggesting thyroid status was closer to normal than in treated mice.

It was difficult to tell the TA of untreated mice apart from the TA of mice that were treated and then untreated. The crush zones of all mice appeared very similar in size. This observation, albeit subjective and crude, suggests the possibility that restoration of normal thyroid state restored at least the most obvious marker of muscle regeneration. Gel electrophoresis and Western blotting were performed using these TA muscles. Results are reported in appendix A.

5.6 HISTOLOGICAL OBSERVATIONS OF THE DIAPHRAGM

Recent reports have shown that the diaphragm of *mdx* mice undergo much more degeneration and regeneration than the limb muscles of the *mdx* mouse (Penner & Anderson, unpublished; Dupont-Versteegden & McCarter, 1992; Stedman et al., 1991) (section 2.6.4). Thus, a cursory study of the diaphragm of control and *mdx* (treated and untreated) mice was carried out.

Control diaphragm exhibited mostly peripherally nucleated fibers, but some centrally-nucleated fibers were present (Fig. 7A). The myofibers present in the diaphragm were much smaller in caliber than limb muscle myofibers. *Mdx* diaphragm exhibited many centrally-nucleated fibers, as well as many areas of active dystrophy with new small myotubes forming (Fig. 7B-D). When compared to limb muscles, the diaphragm of *mdx* mice had more areas of active dystrophy, more fibrous connective tissue, and some adipose tissue located between degenerating fibers (Fig. 7B). Control treated (n=5) and untreated (n=6) diaphragms were hard to tell apart. *Mdx* treated (n=5) and untreated (n=4) diaphragms also looked very similar, with one exception; *mdx* untreated diaphragms showed areas of calcification in the muscle (Fig. 7C) while *mdx* treated diaphragms did not.

5.7 IMMUNOHISTOCHEMISTRY

Sections were stained (separately and together) for the NCAM and bFGF antibodies by immunohistochemical techniques. All immunohistochemistry staining runs included slides in which the primary antibody was omitted, which resulted in no staining for bFGF on muscle sections (not shown). However, sections in which the NCAM antibody was omitted (Fig. 8A) resulted in moderate amounts of background staining, especially in the crush and degenerating areas. This was considered non-specific staining and could be partially due to recognition of the secondary antibody (which was made in mouse) to degenerating mouse antigens, and not specifically to NCAM antigens. Mpcs, myotubes, peripheral nuclei and satellite cells were not stained when the primary (NCAM) antibody was omitted.

First, the staining pattern of NCAM and bFGF will be described separately, as observed using both the HRP and FITC methods of visualization. Subsequently, the colocalization results will be presented.

5.7.1 NCAM and bFGF localization in the unoperated TA

NCAM: In unoperated control TA and in unaffected areas of *mdx* TA, NCAM was localized only to NMJs (Fig. 8B), muscle spindles, and very lightly to the periphery of some myofibers. Degenerating cells in the *mdx* TA exhibited dark anti-NCAM staining (non-specific), while some small mononuclear cells and myotubes were considered to be positive in regenerating areas. Due to the staining in the dystrophic areas, *mdx* muscle showed more NCAM positive cells than control muscle. It was difficult to see any changes in the amount or intensity of NCAM between treated and untreated groups.

bFGF: The pattern of bFGF staining in unoperated control and *mdx* TA muscles was similar to previous reports (Anderson et al., 1993; 1991) (section 2.7). Staining of the myofiber periphery, as previously reported (Anderson et al., 1991) was not always evident, possibly due to a different antibody preparation (Anderson et al., 1993). Overall, the *mdx* TA showed more staining than control muscles. Differences between PTU-treated and untreated muscles were less obvious. There appeared to be more positive cells in the active dystrophic areas in *mdx* untreated compared to *mdx* treated animals.

5.7.2 NCAM and bFGF localization in the operated TA

NCAM (Fig. 10&11): Overall, the crush and adjacent areas were darkly stained in all TA muscles, so it was difficult to pick out individual positive cells. However, there was a population of mononucleated cells (inflammatory cells and mpcs) that stained darker than the background in the adjacent area, and these cells were considered to be positive (Fig. 8C). Some of these positive cells were myoblasts lining up, ready for fusion. Myotube cytoplasm stained positively (Fig. 8D). NCAM-positive

cells were often located near the surviving ends of damaged and retracted fibers (Fig. 9A). Surviving muscle in the crushed TA appeared similar to muscle in the uncrushed TA, except that there appeared to be more NCAM in the surviving zone of the crushed TA than in the uncrushed TA, indicating that the distant zones might be affected by the crush.

Overall, *mdx* muscles seemed to have more staining for NCAM than control muscles. On gross observation, anti-NCAM antibody (linked to HRP) stained the section darker in *mdx* untreated than *mdx* treated muscle. Also, on microscopic observation anti-NCAM staining appeared to be more intense in the *mdx* untreated than treated mice. It was difficult to tell the control treated and untreated muscles apart by examining HRP-linked anti-NCAM staining.

bFGF (Fig. 10&11): Basic FGF was localized to some cells in the crush area of operated animals. These cells included polys, macrophages and mpcs. The retracted end of fibers was stained with bFGF-positive cells, which were often distributed between a fan-like array of projections from the sealed end of the old fiber (Fig. 9B). As reported previously (Anderson et al., 1991), *mdx* TA showed cytoplasmic staining in areas of degeneration. Surviving muscles in the operated leg stained similar to fibers in the unoperated leg.

There appeared to be more staining in the crush area of *mdx* than control muscles. Basic FGF immunostaining appeared more intense in *mdx* treated than in *mdx* untreated TA in the crushed leg.

5.7.3 Colocalization results

As described in the methods (section 4.6), it was possible to colocalize bFGF and NCAM by double immunofluorescence staining of the muscle sections. In this manner, it was possible to obtain the proportions of fluorescent mononuclear cells that were immunostained with NCAM-only, with bFGF-only and with both antibodies (ie cells which colocalized bFGF & NCAM).

Upon close observation, it was apparent that some of both the dually

stained and NCAM-only cells were obviously polys. Thus, the significance of the hypothesized staining pattern (section 3) was less certain, since the NCAM antibody did not discriminate between inflammatory cells and mpcs (see discussion). The proportions (Fig. 12) and statistics of the distribution of cell staining (bFGF & NCAM, bFGF- only, NCAM-only) are presented below. However, it was difficult to interpret these results, therefore autoradiography was performed in an attempt to obtain a clearer estimate of the effect of thyroid hormone on mpc numbers during regeneration.

Chi-square statistics were performed on the distributions of positive cells obtained by double-staining. There was a significant difference (chi-square=127.2; p=0.001) between the distribution of the 3 staining patterns (ie colocalized, NCAM-only and bFGF-only) in the 4 groups of mice. The Chi-square test was then partitioned in order to compare individual groups. The distribution (see Fig. 12) of proportions of cells stained in control untreated TA versus *mdx* untreated TA was significantly different (chi-square=73.2; p=0.001). The three major contributing factors to this significance were i) an increase in NCAM-only positive cells in *mdx* untreated mice (chi-square=34.4), ii) a decrease in bFGF-only positive cells in *mdx* untreated mice (chi-square=6.2) and iii) a decrease in NCAM-only positive cells in control untreated mice (chi-square=25.1). *Mdx* and control treated groups also exhibited a significantly different cell-staining distribution (chi-square=13.8, p=0.001). However, no single factor contributed solely to this significant effect.

Apart from differences in the distribution of positive cells between *mdx* and control muscles, there were differences due to treatment. *Mdx* untreated and treated groups were significantly different from one another (chi-square=70.4; p=0.001). There were four main contributing factors to this significance: i) increased NCAM-only positive cells in *mdx* untreated mice (chi-square=21.4), ii) decreased double-stained cells in *mdx*

untreated mice (chi-square=13.5), iii) decreased NCAM-only cells in *mdx* treated mice (chi-square=21.6) and iv) increased double-stained cells in *mdx* treated mice (chi-square=13.6). Control untreated and treated groups exhibited no changes in the staining distribution.

Figures 10 and 11 show double-staining of control untreated (Fig. 10A&B), control treated (Fig. 10C&D), *mdx* untreated (Fig. 11A&B) and *mdx* treated (Fig. 11C&D) operated TA muscle. It is obvious that NCAM and bFGF stain for some of the same cells, but also stain for separate populations of cells.

5.8 AUTORADIOGRAPHY

To label cells in which DNA synthesis was occurring, mice were injected with tritiated thymidine 24 hours before death. General observations were made of both unoperated and operated TA (4d recovery), and the adjacent zone was thereafter carefully analyzed (both 2d and 4d recovery) (section 4.7, methods).

5.8.1 Histology

Tritiated thymidine labelling was evident on epithelial cells of the intestine (Fig. 13B), as evidence that the uptake of tritiated thymidine had occurred. In the unoperated control TA (Fig. 13A), very little nuclear labelling was evident, except for endothelial cell nuclei. Rarely, peripherally located nuclei in myofibers (satellite cells) were labelled in control muscles. Many labelled nuclei were noted in areas of active dystrophy in *mdx* mice (Fig. 13C). It was assumed that some of these labelled nuclei belonged to mpcs, while others were within myotubes, fibroblasts, polys, or macrophages. Also, in the *mdx* muscles, satellite cell nuclei (Fig. 14B) were labelled more often than in control muscles.

Similar labelling to that of the active dystrophic areas was observed in areas adjacent to the crushed region of TA in control (Fig. 13D) and *mdx* mice. Many, but not all, myotube nuclei were labelled (Fig. 14C&D). The proportion of labelled myotube nuclei appeared to be decreased

in the PTU-treated (Fig. 14C&D) compared to untreated TA. It was often possible to view three or more large, round nuclei in a row (Fig. 14C), and these nuclei probably belonged to myoblasts preparing to fuse into myotubes. The surviving areas near to adjacent zones of the operated TA often had labelled nuclei (Fig. 14A). It appeared that more satellite cells were replicating in these surviving areas than in the contralateral unoperated leg.

5.8.2 Two day recovery (Table 4)

Proximal and distal proportions of labelled nuclei from muscles left to recover for 2 days were considered separately, since proportions of labelled polys ($p<0.001$) and total labelled nuclei ($p<0.001$) differed from one another in the different areas.

Total labelled cells: There was a significant interaction between strain and treatment in the proportion of total labelled nuclei in the proximal area (significant interaction by ANOVA, $p<0.02$). This was seen as a lower proportion of total labelled nuclei in *mdx* untreated compared to control untreated (Duncan's, $p<0.05$).

Polys and myotube nuclei: In the proximal area, the proportion of poly nuclei that were labelled was more with PTU-treatment ($p<0.002$) than without. This effect was not seen in the distal area. Treatment did not affect the proportion of labelled myotube nuclei. However, since there were very few myotubes at 2 days after injury, this low labelling of myotubes was expected.

5.8.3 Four day recovery (Table 4)

Proximal and distal adjacent zones were considered separately in statistical analyses, since their proportions were slightly different.

Total labelled cells: When the total proportion of labelled nuclei was considered, it was evident that treatment did indeed have an effect. In proximal areas, PTU-treatment was accompanied by an increase in the proportion of total labelled nuclei in *mdx* mice (Duncan's, $p<0.01$), but treatment did not affect the proportion of total labelled nuclei in

control mice (significant interaction by ANOVA, $p<0.001$). Also, *mdx* treated TA showed more nuclear labelling than control treated TA (Duncan's, $p<0.01$). In distal areas, the proportion of total labelled nuclei was decreased with treatment in controls (Duncan's, $p<0.01$), but remained unchanged by treatment in *mdx* TA (significant interaction by ANOVA, $p<0.002$). Also, in distal areas, there was a greater proportion of total labelled nuclei in control untreated than *mdx* untreated muscles (Duncan's, $p<0.01$).

Polys and myotube nuclei: The number of polys that were labelled in distal and proximal areas was minimal. However, the proportion of labelled polys in the distal adjacent area was smaller in both control and *mdx* PTU-treated TA ($p<0.05$) than in untreated TA. Also, the proportion of labelled myotube nuclei in the distal adjacent area was less in PTU-treated animals than in untreated animals ($p<0.05$).

6. DISCUSSION

6.1 OVERVIEW OF RESULTS

Measurements of growth (Fig. 2), water intake, respiratory rate, TSH level (Table 1) and daily activity confirm that *mdx* mice and their age-matched controls were rendered hypothyroid by treatment with 0.05% PTU for 8 weeks. *Mdx* mice treated with PTU for 4 weeks drank less water and exhibited decreased daily activity compared to untreated *mdx*, but their body weights were not different from untreated mice, nor were TSH levels measured.

Histological and morphometric analyses after 8 weeks of PTU-treatment show that *mdx* dystrophy is worsened by PTU treatment, as evidenced by the increased proportionate area of active dystrophy and decreased fiber diameter in the PTU-treated *mdx* TA compared to untreated *mdx* TA (Table 2). Also, muscle regeneration after a crush injury is delayed in hypothyroid *mdx* mice, but is ultimately successful, since at 15 days post-injury, treated *mdx* TA was fully regenerated. A larger necrotic crush area and decreased number of myotubes (4d after injury) in *mdx* PTU-treated TA compared to untreated *mdx* were the main evidences of delayed regeneration (Table 3). In contrast, control muscles did not appear to be as affected by hypothyroidism. Similar results were obtained in *mdx* mice treated with PTU for 4 weeks. In agreement with previous studies (Anderson et al., 1987; Zacharias & Anderson, 1991) muscles of younger *mdx* mice had more active dystrophy than those in older *mdx* mice.

Double-immunohistochemical studies using anti-NCAM and anti-bFGF antibodies were performed in an attempt to positively identify mpcs. However, these studies were inconclusive, since it was discovered that our anti-NCAM antibody localized to a glycoprotein on human natural killer cells (HNK-1), and many other inflammatory and non-inflammatory cell types. Therefore, it is not specific to muscle and not an accurate marker for mpcs in damaged tissue *in vivo*. Keeping in mind that our anti-NCAM

antibody was not specific for mpcs, we compared the proportions of cells that were double-labelled with anti-NCAM and anti-bFGF, labelled with anti-NCAM-only or labelled with anti-bFGF-only (Fig. 12). The important findings were that the proportion of cells labelled with anti-NCAM-only were increased in *mdx* untreated mice compared to control untreated mice. Also, treatment of *mdx* mice resulted in a smaller proportion of total mononuclear cells being labelled with anti-NCAM-only compared to untreated *mdx* mice.

Autoradiographic studies on crushed muscle allowed to recover for 2 days (lower Table 4) showed that the proportion of poly nuclei in active DNA synthesis (or recently produced) was increased with PTU treatment compared to untreated muscles (proximal). This was the only effect seen with treatment. There were more labelled polys (proximal) and fewer total labelled cells (proximal), as a proportion of total cells, in *mdx* untreated compared to control untreated TA. Hardly any labelled myotube nuclei were seen at 2 days, since myo2tube formation is only beginning at this time. These results demonstrate that phagocytic clean-up is still occurring, and regeneration is just beginning at 2 days post-injury.

Autoradiographic studies on muscle allowed to recover for 4 days (upper Table 4) showed that the proportion of total labelled nuclei in *mdx* was increased with PTU treatment (proximally). The labelled proportions of poly nuclei (distal) and myotube nuclei (distal) were decreased compared to untreated muscles. Thus, lack of thyroid hormone probably affects myoblast proliferation and myotube fusion in *mdx* TA, but these changes are seen to a lesser extent in controls (see discussion below). Differences between labelling of control and *mdx* mononuclear cells were as follows: i) proximally, the numbers of total labelled nuclei were increased in *mdx* treated TA compared to control treated TA. ii) distally, the total labelled nuclei were less in *mdx* untreated TA compared to control untreated TA.

6.2 METABOLIC AND GROWTH PARAMETERS (Table 1)

Previous studies have shown that *mdx* mice are euthyroid (Anderson et al., 1994). In this study, it appears that PTU interfered with the synthesis of sufficient amounts of thyroid hormone required to maintain normal homeostasis. Measurements of metabolic (respiratory rate, water consumption and TSH levels) and growth parameters (% weight gain) strongly support this. An elevated TSH level in PTU-treated mice was the major indicator that hypothyroidism was created. TSH level is a good indicator of thyroid function because its synthesis operates according to a negative feedback system. When thyroid hormone levels are low, the pituitary responds by increasing TSH synthesis with the aim of stimulating the thyroid gland to produce more thyroid hormone.

TSH levels were not measured in the *mdx* mice treated for 4 weeks because of a change in the commercial TSH assay. It would have been ideal to do a T4 assay as well as TSH but, clinically, TSH is used as the indicator of hypothyroidism, not T4. Also, technical problems by the researcher did not permit T4 assay, as clotted blood was left too long and hemolyzed prior to separation. An attempt could have been made to measure O_2 consumption to confirm hypothyroidism, but this has been shown to be quite difficult (Grounds, personal communication). An estimation of the respiratory rate was performed instead. Only data from one run of the experiment are included in the statistics on respiratory rate because a large variability was encountered in the counts of breaths between trials in the second run.

In humans, when thyroid hormone insufficiency is present during childhood, cretinism results; and in adulthood, hypothyroidism creates myxedema. Cretinism results in short stature, among other things. Myxedema results in lethargy and slowing of movement. Symptoms of decreased hindlimb movement and decreased body weight of *mdx* mice were observed with PTU treatment, and correlate with mild clinical symptoms of hypothyroidism in humans. Also, the weight data agrees with previous research using PTU

to induce hypothyroidism in mice (d'Albis et al., 1990), in that growth was decreased in treated *mdx* compared to euthyroid *mdx*. Treatment did not affect the weight gain of control mice. Weights of the soleus and gastrocnemius muscles were not significantly decreased by hypothyroidism. Body weights of *mdx* mice treated for 4 weeks were not decreased compared to *mdx* untreated possibly because treatment was not long enough, or some seasonal influences on growth were different for that experiment. As well, the mix of male and female mice may have been sufficiently different to obscure changes.

Less active movement by hindlimbs of *mdx* untreated mice was observed compared to controls. This is the first evidence of overt clinical signs of dystrophy in the *mdx* mouse. However, this lethargy could be at least partly due to increased body weight of *mdx* untreated mice.

In order to see if hypothyroidism was reversible, as reported by other researchers (Simonides & van Hardeveld, 1989; Thompson et al., 1987), 1 *mdx* and 1 control mouse was allowed to regain thyroid function for 2 weeks after being PTU-treated for 8 weeks. Because only 1 mouse per group (both hindlimb TA crushed) was studied, the results were inconclusive. However, during the 2 weeks of non-treatment, mice were observed to gradually regain movement of their hindlimbs as per untreated mice of the same age. They also appeared to have crush sites similar in size to untreated mice, indicating some recovery of muscle regenerative capacity. Densitometry plots of Western blots were compared in this group of mice (which were allowed to recover thyroid function for 2 weeks after 8 weeks of treatment). NCAM protein amount in treated crush injured muscle appeared to convert back to euthyroid levels, while bFGF protein amount did not appear to be totally recovered in treated TA (see Appendix A). The TSH level, respiratory rate and body weight were overlooked, but ideally should have been measured.

From the above discussion, it is quite certain that an actual hypothyroid state was reached, and that the drug (PTU) itself did not

produce the effects observed, since the muscle regeneration apparently was restored after PTU treatment was stopped.

6.3 PRELIMINARY TIME COURSE STUDY

Even though the timing of muscle regeneration has been carefully studied after a crush injury (Robertson et al., 1992), this part of the study was of value to the investigator in that it allowed familiarization with the process of muscle regeneration. Also, it was performed in order to generally view the effect of 0.05% PTU on control and *mdx* mice, and to find the best recovery time in which to do further studies (0, 2, 4, 11 or 15 days) (Fig. 3). It was decided that 4 days of recovery after a crush injury was a good representative time for further studies, since necrosis, mononuclear cells and myotubes are all present in regenerating muscle at this time.

Since there was only one mouse (both hindlimb TA crushed) per time period in each of the treatment/nontreatment groups, morphometric analyses were not performed. The areas of the necrotic crush reported at 2 days are not statistically valid as they represent only 2 muscles (1 mouse) per group. However, they serve as a guide in determining the effect of hypothyroidism on regeneration after a crush injury and point to a decreased regenerative capacity in treated mice. The ultimate end-point in treated mice is the same as in untreated mice, in that successful regeneration eventually occurred (by 15 days post-crush).

6.4 FOUR DAY RECOVERY RESULTS

6.4.1 Hypothyroidism and its affect on dystrophy (Table 2)

The distribution of fiber diameter is an indicator of the profile of muscle regeneration in that regenerating fibers often fail to achieve normal size (Ontell, 1986). The activity of dystrophy in stimulating new fiber production can also be monitored by the distribution of fiber size (Anderson et al., 1987; 1988; Zacharias & Anderson, 1991). Hyperthyroidism

shifts the profile toward smaller fibers (Anderson et al., 1994). Hypothyroidism also shifted the diameter distribution toward smaller fibers in unoperated *mdx* muscle compared to untreated *mdx* muscle (Fig. 6). This shift indicates that more new small myotubes are present in *mdx* treated muscle compared to *mdx* untreated muscle of the same age. Taken together with the finding that the proportionate area of active dystrophy (but not the number of dystrophic foci) in PTU-treated *mdx* was increased, we conclude that dystrophy is worsened in *mdx* mice by PTU-treatment.

The question arises as to whether PTU-treatment i) increases degeneration or, ii) slows regeneration. Both possibilities would increase the amount of active dystrophy. In the first case, more active dystrophy would be present because more fiber damage was occurring. Anderson et al. (1994) suggest that hyperthyroidism (induced by T3) in *mdx* mice increases fiber damage, rather than or in addition to inhibiting repair, since hyperthyroidism makes muscle faster, and faster muscle is more affected by dystrophy (Webster et al., 1988b; Anderson et al., 1987; 1988). However, hypothyroidism makes muscle slower (McAllister et al., 1991), which could slightly protect fibers from dystrophy. In this study, the number of dystrophic foci, per unit muscle area, was not significantly different with PTU treatment. It appears then, that the amount of degeneration is not increased with treatment.

In the second case, more active dystrophy would be present because regeneration was slower, and thus dystrophic lesions at slightly different phases of degeneration and regeneration would be seen. The same basal level of degeneration could be occurring, but slowed regeneration would give the appearance of more area of active dystrophy as a proportion of total muscle area. Since control unoperated muscles were not affected by hypothyroidism and the proportionate area of active dystrophy was increased with treatment, I propose that hypothyroidism primarily alters muscle repair, rather than changing the amount of active fiber degeneration.

CN:PN ratio and CNI did not change with treatment, possibly because maximal centronucleation is reached in *mdx* mice at 11 weeks-of-age (treated for 8 weeks) (see section 6.5 for further discussion on CNI).

Body weight was found to be correlated to CNI and this could explain why active dystrophy increases and then plateaus, since body weight increases and plateaus. Thus, active dystrophy could be related to work-induced injury from weight bearing.

6.4.2 Hypothyroidism and its effect on muscle regeneration

The use of crush injury during a systemic treatment permitted a focused study of the effects of hypothyroidism on the timing of muscle regeneration. The influence of hypothyroidism on muscle repair following crush injury was apparent in five types of double-blind observations: the gross appearance of muscles, general histopathology, morphometry, immunocytochemistry and autoradiography. These observations suggest that muscle regeneration is decreased in PTU-treated *mdx* mice. However, control mice did not appear to be as affected by hypothyroidism, possibly because they have to deal with only one insult (hypothyroidism), not two (hypothyroidism and dystrophy), as in *mdx* mice. It is also possible that the endocrine feedback loop for thyroid hormone-TSH in *mdx* mice is less adjustable in response than control endocrine setpoint. This is also evidenced by a higher pituitary growth hormone in *mdx* than control mice (Anderson, unpublished).

Gross appearance: There was more hemorrhagic damage visible at the crush site of PTU-treated *mdx*, PTU-treated control and untreated control compared to untreated *mdx* TA. Increased hemorrhagic damage points to a more severe reaction and less effective regeneration to injury in these animals after 8 weeks of hypothyroidism. Also, since control TAs are more hemorrhagic than *mdx* untreated TA, it appears regeneration in *mdx* is better than in control TA.

General histopathology: In crush injured *mdx* mice there was a clear separation between treated and untreated groups, on the basis of the size of necrotic crush area and the number of myotubes in the adjacent zone (Figs. 4&5).

Morphometry: (Table 3): The increased area of the necrotic crush and the decreased density of myotubes are the main indicators that PTU decreases regeneration in the *mdx* TA. Myotube density was consistently, but not significantly, lower in all zones of *mdx* treated compared to untreated TA. This suggests that the effect of hypothyroidism on muscle regeneration occurs during early formation of myotubes, possibly during the fusion of mpcs. The observation of myotubes in treated TA which appeared shorter and contained fewer nuclei than those in untreated TA is in agreement with the idea that there may be a delay in fusion related processes induced by hypothyroidism. The actual length of myotubes was not measured, nor was myotube diameter, but this would have served as a positive indicator that fusion related processes were delayed. The reduced number of myotubes in the surviving zone (significant) in PTU-treated compared to untreated *mdx* TA, indicates that: i) the crush affects areas at some distance, ii) that hypothyroidism changes that affect and, iii) that hypothyroidism interferes with ongoing regeneration due to dystrophy in these areas.

The density of myotubes in operated *mdx* TA was consistently and significantly larger than in control operated TA, in agreement with a previous study that found young *mdx* mice able to recover better than controls (Anderson et al., 1991). However, Grounds & McGeachie (1992) concluded that dystrophic *mdx* muscle does not have any exceptional capacity for muscle regeneration, possibly due to the small number of myotubes studied in that report which measured the number of myotube nuclei synthesizing DNA.

The CN:PN ratio did not show differences due to treatment in *mdx* or control mice. However, centronucleation of control fibers in the distal

surviving zone was present (Fig. 5E), and quite different from the amount of centronucleation in unoperated controls (Fig. 4A) or in surviving proximal areas. This again indicates that there is a response to injury by muscle fiber segments quite distant from the site of injury. It has been suggested that the movement of myonuclei from their peripheral position is a rapid response to myofiber damage (Robertson et al., 1992). Therefore, centronucleation in control surviving distal zones is probably not a result of myofiber regeneration, since these distant areas are not directly affected by damage. Rather, the internalization of nuclei in apparently normal muscle fibers is more likely to result from transmission of some signal along the fiber from the injury. It is also possible that the proximal origin of the TA blood supply has a role in the proximo-distal feature of the fiber response to injury, and that distal areas are more affected because of some probable disruption in blood supply due to the more proximal injury.

The fiber diameter distribution (Fig. 6) in *mdx* operated TA was measured in surviving areas, and it was increased with PTU-treatment compared to untreated muscle. It is difficult to explain these results, although some edema may account for the increased dimension. It is not known, however, whether the length of distant fiber segments changed after crush injury, since that may have also contributed to increased diameter of remnant fibers.

Immunocytochemistry: NCAM is supposedly specific to myoblasts (Jones et al., 1990; Webster et al., 1988a) and myotubes (Covault & Sanes, 1986), and one report suggests that it is expressed before myosin (Covault & Sanes, 1986). Moore & Walsh (1985) believe that NCAM can be regarded as a specific marker for regenerating cells. Basic FGF is a mitogen for mpcs (Clegg et al., 1987), and localizes to mononuclear cells in areas of dystrophy in *mdx* mice (Anderson et al., 1994; 1993; 1991). Thus, it was of interest to characterize the staining pattern of NCAM and bFGF (Figs. 10 & 11), and to hopefully identify a population of cells that co-expressed

the 2 proteins. So, the initial hypothesis was that cells expressing both NCAM and bFGF would be early mpcs (replicating), cells expressing NCAM-only would be myoblasts preparing for fusion and fused myotubes (differentiated), and cells expressing bFGF-only would be inflammatory cells. This entire hypothesis broke down on the finding that this antibody against the HNK-1 moiety of NCAM additionally labelled polys (Fig. 8C), and hence is non-specific to muscle. Also, reports of bFGF being down-regulated during differentiation do not appear to be as accurate as once thought, since bFGF (protein) and myogenin (mRNA) appear to colocalize in differentiating myoblasts and myotubes (Garrett, personal communication). Thus, non-specific staining with both anti-NCAM and anti-bFGF antibodies precluded the positive identification of mpcs by the light microscope.

Despite this, some useful information was gained. The information derived from the colocalization study can be of some benefit in understanding muscle regeneration. It is recognized that these results are in the form of a distribution (Fig. 12), and that when the staining with one antibody goes up, the other antibody staining patterns are affected accordingly. Results from pooled chi-square tests show that cells stained for NCAM-only plays the largest role in the significance; they constitute more cells in *mdx* than control mice, and more in untreated *mdx* than in treated *mdx*. The increased amount of NCAM-only positive cells could play a role in the increased regenerative capacity of the mice exhibiting more of it.

It has been reported that NCAM expression by adult non-regenerating muscle is reinduced by hypothyroidism (Thompson et al., 1987). Since NCAM staining in the unoperated TA was not quantified (blots using uncrushed TA were not examined), it is uncertain whether NCAM was re-expressed in treated animals in this study. The crush injury masked any results purely due to hypothyroidism in the operated TA. It is suggested that NCAM and MHC genes are regulated similarly by thyroid hormone in adult muscle (Thompson et al., 1987).

Autoradiography: (Table 4): Since double-immunostaining did not identify mpcs, autoradiography was performed in an additional repeat of protocol 2 (4 day recovery) in order to estimate the number of mpcs in the crush area. Autoradiography on muscles already collected from protocol 1 (2 day recovery only) was also performed. These animals were injected with tritiated thymidine 24 hours before death (3 or 1 day after crush). Tritiated thymidine is available for about 1 hour after injection, therefore only cells synthesizing DNA during this interval are labelled (Grounds & McGeachie, 1992). Thus, myotube nuclei labelled upon tissue examination would have been mpcs replicating at the time of injection that subsequently fused (Roberts et al., 1989). In the same regard, mononuclear cells that are labelled upon observation under the microscope represent daughter cells of mpcs, inflammatory cells, endothelial cells, or fibroblasts which were replicating at the time of injection.

Guthridge et al. (1992) report that the main mononuclear cell population in injured muscle is probably myoblasts. To make myoblast identification easier, the number of labelled poly nuclei (as a proportion of total polys) and the number of labelled myotube nuclei (as a proportion of total myotube nuclei) were counted, and thus eliminated from the unidentified mpc population. Then, when the total labelled nuclei were counted, it was more certain that changes seen were due to mpc population changes, and not changes among other mononuclear cells. In further discussion, reference to total labelled cells will imply mainly mpcs (minus the polys and myotube nuclei).

Distal and proximal areas were separated when comparing autoradiography counts because differences were evident upon examination. However, the message derived from both proximal and distal areas indicate that treatment has the same effect, only at a slightly delayed rate in distal areas likely due to slower revascularization. There may be a larger likelihood of sparing from ischemia for satellite and mpcs in the area

proximal to the crush, while the more distal segments of TA fibers would be subject to greater or more prolonged ischemia, and therefore a more marked or delayed response to injury.

2 days recovery: Distal: It is recognized that there are only 2 crushed muscles per group in the 2 day recovery portion of this study. However, at least 12 fields were counted per muscle, and statistics were performed on unaveraged counts. There were no changes in labelling between untreated and treated muscles, or between control and mdx muscles at 2 days after injury. Previous reports indicate that replication of mpcs occurs at about 30 hours after crush injury (McGeachie & Grounds, 1987). Injection of tritiated thymidine at 24 hours after injury in this study, suggested that this initial early response phase in distal regions is not affected by hypothyroidism.

Proximal: A few small changes in labelling occurred in the proximal area at 2 days after a crush. This supports the idea that regeneration in proximal areas is enhanced because of an increased efficiency in revascularization. Labelled poly nuclei were more abundant in treated than untreated TA. This could be due to a slightly decreased ability of polys to act in hypothyroid muscle, seen as an increased demand for their function at this phase 1-2 days post-injury.

Some differences in labelling were obvious in control vs *mdx* TA. There were more labelled polys and fewer total labelled cells in *mdx* untreated compared to control untreated TA. This would correspond to fewer labelled mpcs in *mdx* untreated TA than in control, if non-myotube, non-poly labelled mononuclear cells are primarily mpcs.

4 days recovery: Distal: Fewer labelled myotube nuclei (Figs. 14C&D) in treated TA compared to untreated TA means that fewer mpcs were dividing at the time of injection into treated animals. There was no difference in total labelled nuclei per field between *mdx* untreated and treated TA, but fewer labelled poly and myotube nuclei were present in *mdx* treated TA. This would mean that there are more labelled mpcs, which must be due to

more mpcs in untreated animals undergoing cell division between the time of injection and death. Thus, something keeps the mpcs proliferating, and inhibits differentiation (ie. fusion). This is in agreement with the morphometry data on myotube number, which shows that there is lower myotube density in fields of treated *mdx* compared to untreated *mdx* TA. Control treated TA had fewer total labelled cells than control untreated TA, which means that approximately the same number of mpcs are present in control treated and untreated. This is in agreement with the minor histological and morphometric changes in control muscle with PTU treatment.

Differences between control and *mdx* labelling in distal regions indicate that mpcs replicate more in control than in *mdx*. However, the number of labelled myotube nuclei are the same. This could mean that myotubes are shorter in controls, or that more myotubes are already present in *mdx* TA before the injection of the tritium. Both these possibilities agree with the morphometric finding that the total number of myotubes is less in control than *mdx*.

Proximal: Since, in the proximal areas, the number of labelled poly and myotube nuclei were not affected by treatment, we assume that the etiology of what is creating any significant effect on total labelled cells lies in the number of labelled mpcs. Thus, as in distal areas, more divisions by mpcs probably occurred between injection and death in *mdx* treated than untreated TA. However, labelling of myotube nuclei was not affected by treatment. So, more myotubes must have been formed in untreated TA before injection, and *mdx* treated TA are stimulated to compensate for the effects of hypothyroidism by increasing replication rates and/or prevalence. No differences in the number of mpcs were seen in control treated vs untreated TA.

Differences between control and *mdx* mice in the proximal area include an increase in the mpc population in *mdx* treated compared to control treated TA. This effect is difficult to explain unless one

considers the response of *mdx* treated TA at the same time (4d) post-injury is really somewhat earlier (ie. delayed from normal) in regeneration such that mpc proliferation is faster and there are more mpcs simply because fewer myotubes have formed by their fusion.

It is interesting to note that many cells were labelled in the autoradiograms in surviving areas (more so than in the contralateral unoperated muscle of the same strain or treatment). It is possible that activated satellite cells migrate into the damaged area from these regions. Two possibilities exist: i) satellite cells could come from the ischemic core, but migrate out to the periphery upon injury, and then later, migrate into and repopulate the injured area (Schultz et al., 1988), or ii) satellite cells could be activated in remote uninjured muscle (in a response transmitted along the fiber) and later migrate into the area of injury (Grounds et al., 1992a).

6.5 **FOUR WEEK TREATMENT RESULTS** (Tables 2 & 3)

By 11 weeks-of-age (8 wks of treatment), maximal centronucleation is probably attained, thus a further experiment was performed in order to determine whether there would be a difference between treated and un-treated *mdx* CNI after only 4 weeks of treatment (7 wks-of-age). However, this was not the case; CNI was not changed by PTU-treatment for 4 weeks. Since we found a change in the active dystrophy with treatment, this suggests that CNI is not a very precise measure of the amount of dystrophy that has previously occurred, as suggested by Karpati et al. (1988), and masks subtle changes in dystrophy which may be due to treatment. This discrepancy could be attributed to the fact that once a fiber undergoes one round of degeneration and regeneration, it becomes centrally nucleated. This precludes any evidence of the occurrence a second or third round of degeneration and regeneration, since CNI would not change to reflect this second population of repaired fibers, and thus would underestimate the amount of accumulated dystrophy. It is possible that

some fibers, such as those under the greatest mechanical strain in a muscle (Petrof et al., 1993), may be more prone to undergo multiple degeneration-regeneration cycles, while others may be saved (or relatively spared after a single cycle) throughout the life of the mouse. For this same reason, CN:PN was not found to be useful in assessing the tissue level of dystrophy during thyroid hormone perturbation.

The relatively small or absent effect of PTU on younger *mdx* TA regeneration may be partly age related, in that the effects of PTU treatment on fusion and debris clearance, necessitated by ongoing dystrophy, would be anticipated to be less over 4 than 8 weeks of treatment. Thus, there would be a smaller difference between untreated and treated muscles in the number of mpcs, satellite cells and resident polys and macrophages after 4 than 8 weeks of treatment. In *mdx* muscles, the effect of treatment on younger mice may also be obscured by a larger variation between muscles and animals during the peak rate of dystrophic injury.

There was an increase in the myotube density (significant) in the surviving zone in the *mdx* treated compared to untreated TA. It is possible that the distant response to injury has been large enough to provide enough mpcs between surviving fibers that they can fuse and form new myotubes there. It also suggests that mpcs don't migrate as well in treated as in untreated muscle.

6.6 SPECULATION AS TO THE ACTION OF THYROID HORMONE IN MUSCLE REGENERATION

Regeneration of muscle within 4 days after a crush injury is dependent on the rapid production and fusion of mpcs. Hypothyroidism could interfere with many aspects of this process, including: i) resealing of viable from nonviable portions of the myofiber, ii) efficiency and removal of necrotic tissue by phagocytes, iii) activation or number of mpcs, iv) proliferation of mpcs, v) migration of mpcs, or vi) fusion into myotubes.

i) The separation of the viable portion from the injured portion of

a myofiber (Papadimitriou et al., 1990) may be less effective in hypothyroidism. This would explain why there was a larger necrotic crush zone (and larger proportionate area of active dystrophy) in treated TA in this study. Resealing is not dependent on infiltrating leukocytes (Papadimitriou et al., 1990), hence the effect of hypothyroidism may be seen even before phagocytosis and revascularization occurs, and may involve interference with vesicle fusion (Fig. 9C) into new sarcolemma.

ii) Mitchell et al. (1992) conclude that muscle regeneration is more successful when the migration of inflammatory cells is fast or the population of these cells is increased in number. Decreased infiltration of phagocytes makes it harder for myoblasts to fuse, due to interference by cellular debris. This would explain differences between proximal and distal areas, and between 2 days recovery vs 4 days recovery. However, it is more likely that interference with phagocytosis plays a minimal part in the effects of hypothyroidism, since autoradiographic studies showed overall that the number of labelled (and clearly identified) polys was not decreased by treatment.

iii) Mpcs are derived from satellite cells, and it is possible that hypothyroidism affects the responsiveness or the number of activated satellite cells. Insufficient evidence is present in this study to either agree or disagree with this possibility. However, it has been suggested that myoid cells in the thymus could be a reserve population of mpcs that enter the circulation in response to muscle degeneration (Grounds et al., 1992b; Garrett, personal communication). Similar myoid cells are found in the anterior pituitary and might actually be a hormone responsive cell population that could signal to thymic or muscle mpcs. Since thyroid hormone synthesis level is regulated by the anterior pituitary, it could be that hypothyroidism affects these populations of possible mpcs, thus lowering the amount of effective regeneration in *mdx* TA muscle.

iv) Hypothyroidism could interfere with the proliferation of mpcs. It is suggested that a minimum density of mpcs must be reached before

fusion can occur (Grounds, 1991). It seems that more proliferation of mpcs occurs during the 24 hours between tritiated thymidine injection and death in treated animals. The density of mpcs required for fusion in treated TA may be increased compared to untreated TA. Also, smaller numbers of proliferating mpcs are probably seen in untreated TA because more nuclei are already fused into myotubes. Thus, it is possible that lack of thyroid hormone decreases mpc proliferation between 2 and 3 days post-injury, and results in more mpcs at 4 days after injury which are trying compensate for earlier delays in myotube formation. Alternatively, the mpc might be able to compensate for decreased myotube density by communicating with the regenerating myotube population, possibly through the extensions on the stumps of myofibers and the processes between myoblasts and new myotubes (Fig. 9). Mpcs might actually detect when compensatory divisions are needed to increase myotube number.

v) The migration of mpcs cells may be impeded by hypothyroidism, as explained above (4 week treatment results).

vi) The myotube number was decreased in treated *mdx* TA compared to untreated *mdx* TA, and less labelled myotube nuclei (distal) were seen in treated *mdx*. These results point to a problem in myotube fusion. Previous work (Anderson, 1991) has shown that *mdx* myotubes may synthesize greater concentrations of phospholipids which permit membrane fluidity and could help in membrane fusion; thyroid hormone may interact with this aspect and thus decrease the efficiency of fusion (Anderson et al., 1994). The decreased amount of NCAM in treated *mdx* TA may decrease the co-recognition between myoblasts, thus inhibiting fusion.

Thus, these results suggest that hypothyroidism mainly interferes with muscle regeneration by acting to decrease mpc proliferation and to inhibit fusion.

6.7 GENERAL COMMENTS ON THE CAUSE OF MUSCULAR DYSTROPHY IN *MDX* MICE AND IN HUMAN DMD

This work informs us about muscle regeneration and what factors

might inhibit the process. Circumstances that demand muscle repair, such as surgery and dystrophy, should consider the metabolic situation during treatments. Myoblast transfer and occupational and physical therapy treatments of DMD patients will be maximally effective when a normal thyroid hormone level is present. Also, it is imperative that the culture media of purified myoblasts (for transplant) have the correct amount of thyroid hormone and other serum factors. This and other studies in the lab suggest that optimal metabolic support of muscle regeneration appears to be crucial to the outcome of treatment.

Degeneration is probably a direct result of lack of dystrophin (Partridge, 1993). Regeneration is initially vigorous in DMD, but eventually, it cannot keep up with degeneration due to infiltration of the area with fibrosis and adipose tissue, thus decreasing muscle mass. This is not seen in the hindlimbs of *mdx* mice where muscle mass and fiber number (Anderson et al., 1987) are maintained. Adipocytes and mpcs both derive from mesodermally derived stem cells. It could be that some signal in the development of boys with DMD, such as those involved in MRFs, is altered and that the mesoderm stem cells become more committed to adipocytes than to mpcs. Alternatively, later on when degeneration is occurring, a gene may switch mpcs into adipose cells just as fibroblasts can be transfected to form muscle cells *in vitro*. If there was some way we could induce those mesodermal cells to remain or to become mpcs instead of adipose cells, some of the problems with persistent muscle repair in DMD could be alleviated. It is possible that there is an adipocyte regulatory gene that should be studied in a similar fashion to muscle regulatory genes.

6.8 FUTURE STUDIES

1.) In this study, examination of the diaphragm was very cursory (Fig. 7). It appeared that hypothyroidism slightly spared the muscle from degeneration due to dystrophy, judging by the fact that there were no areas of calcification in treated diaphragms, a sign of severe

degeneration. This could be due to less use of the diaphragm in hypothyroidism. The lowered respiratory rate of mdx treated mice supports this theory.

Judging from previous reports and our own observations on the diaphragm of the *mdx* mouse (that indicate it exhibits degeneration and regeneration similar to human DMD) (Stedman et al., 1991; Penner & Anderson, unpublished), the focus of further studies should concentrate on this muscle. Even though dystrophy is much worse in the *mdx* diaphragm than limb muscle, probably due to their different embryonic origins and the greater continuous work-load, the *mdx* mouse does not die from respiratory failure. So, what allows the *mdx* diaphragm to function successfully despite the insult, whilst in human DMD, respiratory failure is a very common cause of death? What could we give this muscle that might spare it from dystrophy? Studies of plasmid injection into control diaphragm have recently been performed (Davies & Jasmin, 1993) and indicate that direct injection of possible regulatory constructs into the *mdx* or human diaphragm is possible and may be safe. It is possible that DMD therapy may one day be targeted at the diaphragm.

Thus, a careful morphometric and autoradiographic analysis of the *mdx* diaphragm would be very beneficial in determining the mechanisms of dystrophy in this muscle.

2.) It is felt that functional testing would be make this study more complete. Physiologic studies and Nuclear Magnetic Resonance Spectroscopy may be performed on hypothyroid and normal *mdx* and control muscles.

3.) There have been no studies that identify the number of satellite cells in *mdx* mice compared to control mice or to DMD muscle. It is quite possible that the differences in regenerative capacity between *mdx* and DMD muscles are due to differences in satellite cell number, activity, or sensitivity to various factors and stimuli. In the context of this study, it is possible that hypothyroidism interferes somehow with the satellite cell's response to damage. This would explain why mpc cell replication

peaks at a later time in PTU-treated mice.

Thus an interesting study would be to identify and compare the satellite cell numbers in *mdx*, control, normal human and human DMD muscle using electron microscopy techniques. This could prove to be a definitive way of predicting regenerative capacity. Snow (1977) reports that repeated trauma increases the number of satellite cells at the trauma location, and as a result, regeneration occurs faster. *Mdx* mice definitely undergo repeated trauma, and this could partly explain why their muscles regenerate better than control. However, DMD muscle also undergoes repeated trauma and does not regenerate well.

It would be very interesting if the satellite cell number in DMD was the same as in *mdx* dystrophy. If so, the atrophy and degeneration of muscle seen in DMD might be entirely due to fibrosis and adipose tissue deposition, and not at all due to mpc number (although mpc activity could still be a problem).

4.) It would have been very helpful to have been able to positively identify mpcs and myoblasts in this study. Myogenin and MyoD antibodies could be the solution to this dilemma, since *in situ* hybridization has identified expression of these genes as early markers for mpcs (Ground et al., 1992a). Also, M-cadherin (Moore & Walsh, 1993) and N-cadherin (Mege et al., 1992), calcium dependent cell adhesion molecules, may be more specific to muscle than the NCAM molecule our antibody was raised against.

6.9 SUMMARY AND CONCLUSIONS

This study identifies a factor, namely thyroid hormone, which inhibits, or at least delays, muscle regeneration in *mdx* mice. The specific conclusions derived from the study are as follows.

1. It was confirmed that 0.05% PTU induced a hypothyroid state in *mdx* and control mice.

2. The events in muscle regeneration after a crush injury were described in treated and untreated *mdx* and control mice.

3. Morphometric techniques confirmed the hypothesis that *mdx* mice

regenerate better from a crush injury compared to control mice. Also, the phenotype of *mdx* dystrophy in hypothyroidism was shifted toward that of DMD, since the dystrophic changes during treatment were more severe than in untreated *mdx* littermates. In addition, the extent of *mdx* muscle regeneration after crush injury appeared to be delayed by hypothyroidism, probably due to decreased myotube fusion.

4. NCAM was found to be non-specific to regenerating muscle *in vivo*, thus double-immunocytochemistry for NCAM and bFGF was unsuccessful in identifying mpcs.

5. Autoradiographic studies point toward a decreased proliferative capacity of mpcs and delayed fusion of myotubes in treated *mdx* and control TA. In all cases, control mice did not appear to be as affected by treatment compared to *mdx* treated mice.

7. FIGURES AND TABLES

FIGURE 1:

A: This diagram indicates the zones and fields of a typical longitudinal section of the tibialis anterior muscle, taken between proximal origin (top) and distal tendon (bottom). The fields were assessed during morphometric study of myotubes and nucleation. The center of the crushed area (necrotic and acellular) was established under the microscope at 100X, and two 200X fields were located, one field apart and horizontally, in the crush zone. Fields in the adjacent zone (3 proximal, 1 distal) were sampled at a distance of one field diameter from the crush fields. Two fields of fibers in the surviving zone were sampled one field away from the proximal adjacent zone. One additional field was sampled 1½ field diameters away from the distal adjacent zone. These criteria were strictly adhered to, such that zones were determined by the distance from the crush, not by particular cells types prevalent in the region. A similar scheme was also used in autoradiography counts, where fields in the adjacent zones were examined. Six fields were examined in both the proximal and distal adjacent zones. In this case, examination occurred at 400X under the microscope, and fields were one field diameter away from each other.

B: This photo is representative of a crushed tibialis anterior muscle (X45; bar=200μm). It corresponds to the diagram in A. The crushed necrotic zone is in the center of the photo, and is mostly acellular. This area was exactly outlined and measured in all muscle sections, using the Sigma Scan program in conjunction with a camera lucida at 100X magnification. The proximal (top) and distal (bottom) adjacent zones exhibit many inflammatory cells, other mononuclear cells and myotubes. Surviving zones show intact myofibers.

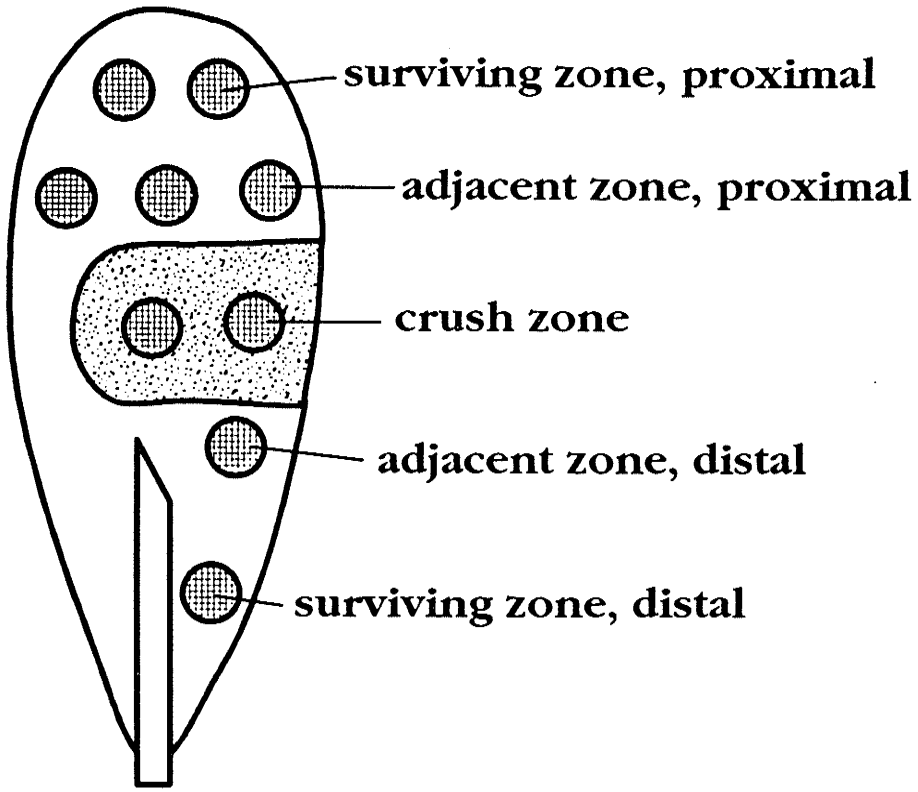
surviving zone, proximal
adjacent zone, proximal
crush zone
adjacent zone, distal
surviving zone, distal


B

FIGURE 2:

This graph depicts the age-related body weight gain (mean %) by untreated and PTU-treated *mdx* and control mice. It is obvious that *mdx* untreated mice weigh significantly more than age-matched controls or *mdx* treated mice. This difference becomes quite pronounced at treatment week 2, and continues until week 7. No differences in weight are apparent between control treated and untreated mice.

% WEIGHT GAIN

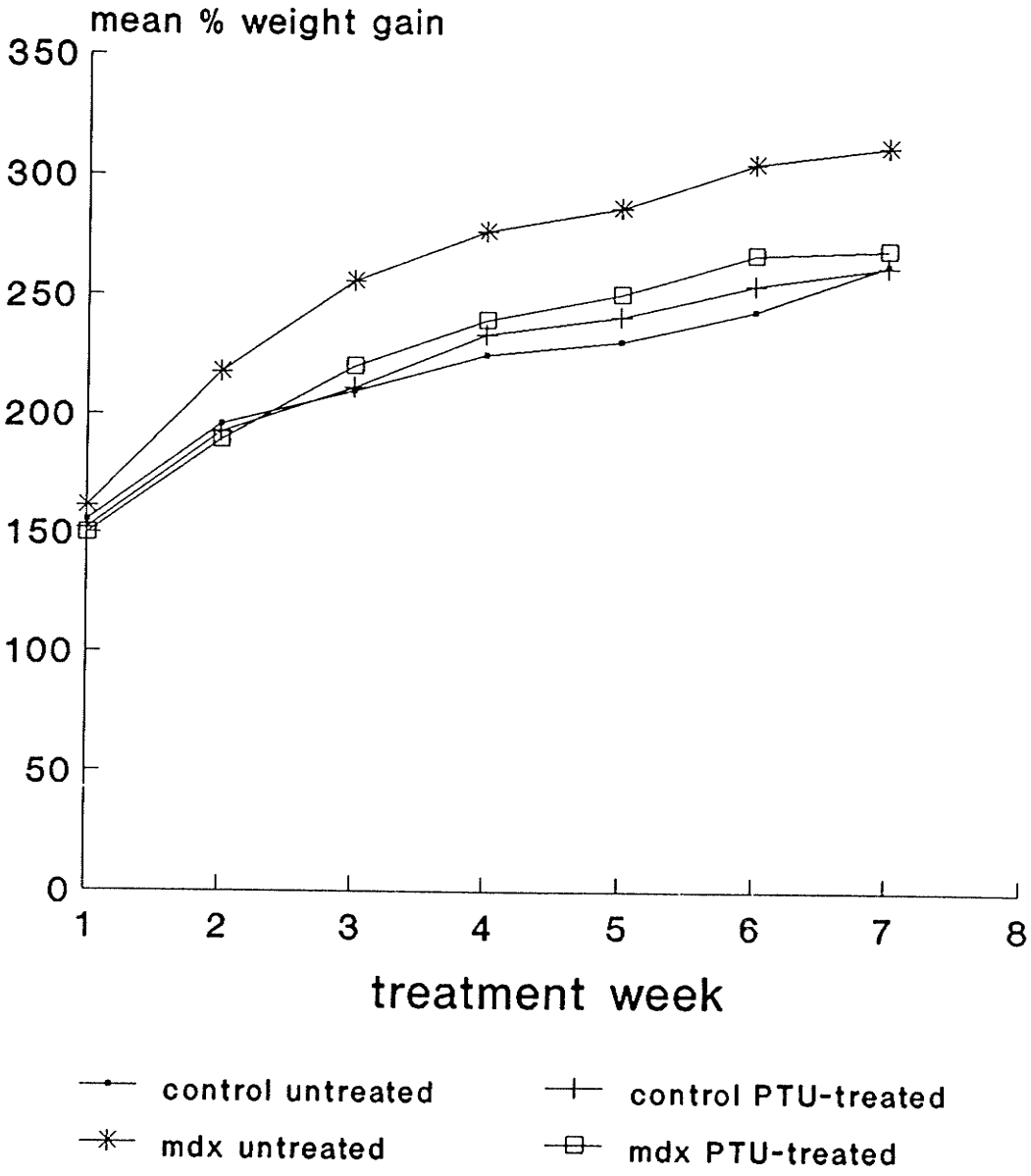
mean % weight gain
350
300
250
200
150
100
50
0
1
2
3
4
5
6
7
8
treatment week
control untreated
control PTU-treated
mdx untreated
mdx PTU-treated

FIGURE 3:
Micrographs of sections of *mdx* PTU-treated TA after various recovery times after crush injury (A: X240; B-D: X50; bar=100μm).

A: *Mdx* treated TA, 2 hours after crush injury. Myofibers are just beginning to lose their integrity. No inflammatory cells or necrotic zone is present.

B: *Mdx* treated TA, 2 days after crush injury. The necrotic crush zone (c) is quite large. A few myotubes (arrows) can be seen in the adjacent (a) zone, but it is mainly filled with mononuclear cells. Centrally nucleated surviving muscle is present on the left edge of the photo.

C: *Mdx* treated TA, 11 days after crush injury. Longitudinal regenerated myotubes (arrows) have almost filled in the crushed area. A small area of mononuclear cells (star) is present, but no necrotic tissue is evident. Most of the myofibers are centrally nucleated.

D: *Mdx* treated TA, 15 days after crush injury. In this cross-sectional view, the muscle appears completely regenerated with many myotubes and centrally nucleated myofibers.

A
B
C
D

FIGURE 4:
Low power micrographs of longitudinal sections of control (A,C,E) and *mdx* (B,D,F) TA in untreated (A-D) and PTU-treated (E,F) mice (X50; bar=200μm). While sections may not appear completely longitudinal due to the pennate architecture of the TA (see Methods), all myotubes and nucleation counts were made only on the side of the tendon where fibers were in longitudinal section.

A: Unoperated, untreated control TA (normal uninjured muscle).

B: Unoperated, untreated *mdx* TA with centrally nucleated fibers, an area of active dystrophy (asterisk), and an area of recent regeneration containing small myotubes (arrows).

In panels C-F, areas of necrosis in the crush site (c), the adjacent zone (a) containing myotubes (arrows) and inflammatory and mononuclear cells, and distant surviving areas (s) are indicated in the operated TA.

C: Control untreated TA contains a typical necrotic area and short myotubes lining up in the adjacent zone.

D: *Mdx* untreated TA with no obvious necrotic crush area. Many long myotubes are lined up in the adjacent zone.

E: Control PTU-treated TA has a large crush site.

F: *Mdx* PTU-treated TA shows a larger area of necrosis in the crush zone than in panel D, and an area of calcification (arrowhead) is present. Fewer myotubes extend into the adjacent zone than in untreated *mdx* operated TA (panel D).

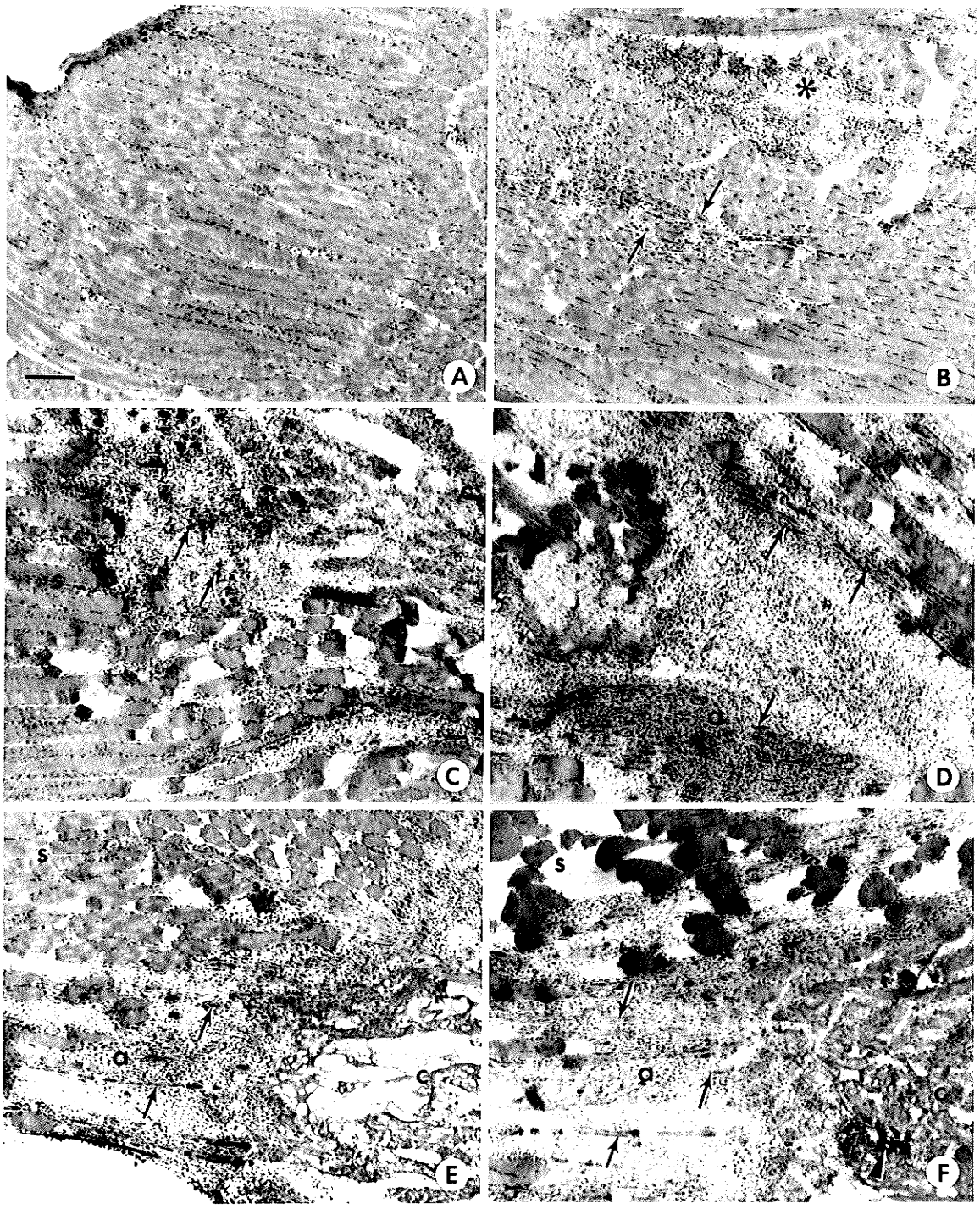
A
B
C
D
E
F
S
a
S
a

FIGURE 5:
Micrographs of longitudinal sections of operated control (A,C,E) and *mdx* (B,D,F) TA from untreated (A,B) and PTU-treated (C-F) mice (A,B,C,F: X250; D,E: X125; bar=50μm). All myotubes are in longitudinal sections.

A: Control untreated TA, 4 days after crush injury shows myotubes containing chains of 5-7 nuclei (arrows).

B: *Mdx* untreated TA, 4 days after crush injury shows myotubes (arrows) that appear longer than in panel A.

C: Control PTU-treated TA exhibits short-medium length myotubes (arrows) in the adjacent zone.

D: *Mdx* PTU-treated TA demonstrates very long myotubes (arrows) lining up parallel with a few surviving fibers.

E: Surviving area of operated control treated TA. The surviving fibers show mainly peripherally nucleated fibers, but one fiber is clearly centrally nucleated (arrowhead). CNI in surviving fields of operated muscle was significantly greater than in the contralateral unoperated control muscle.

F: Surviving area of operated *mdx* treated TA. The distal surviving zone shows more central nuclei in mature fibers close to the adjacent zone, than typical in unoperated contralateral *mdx* TA.

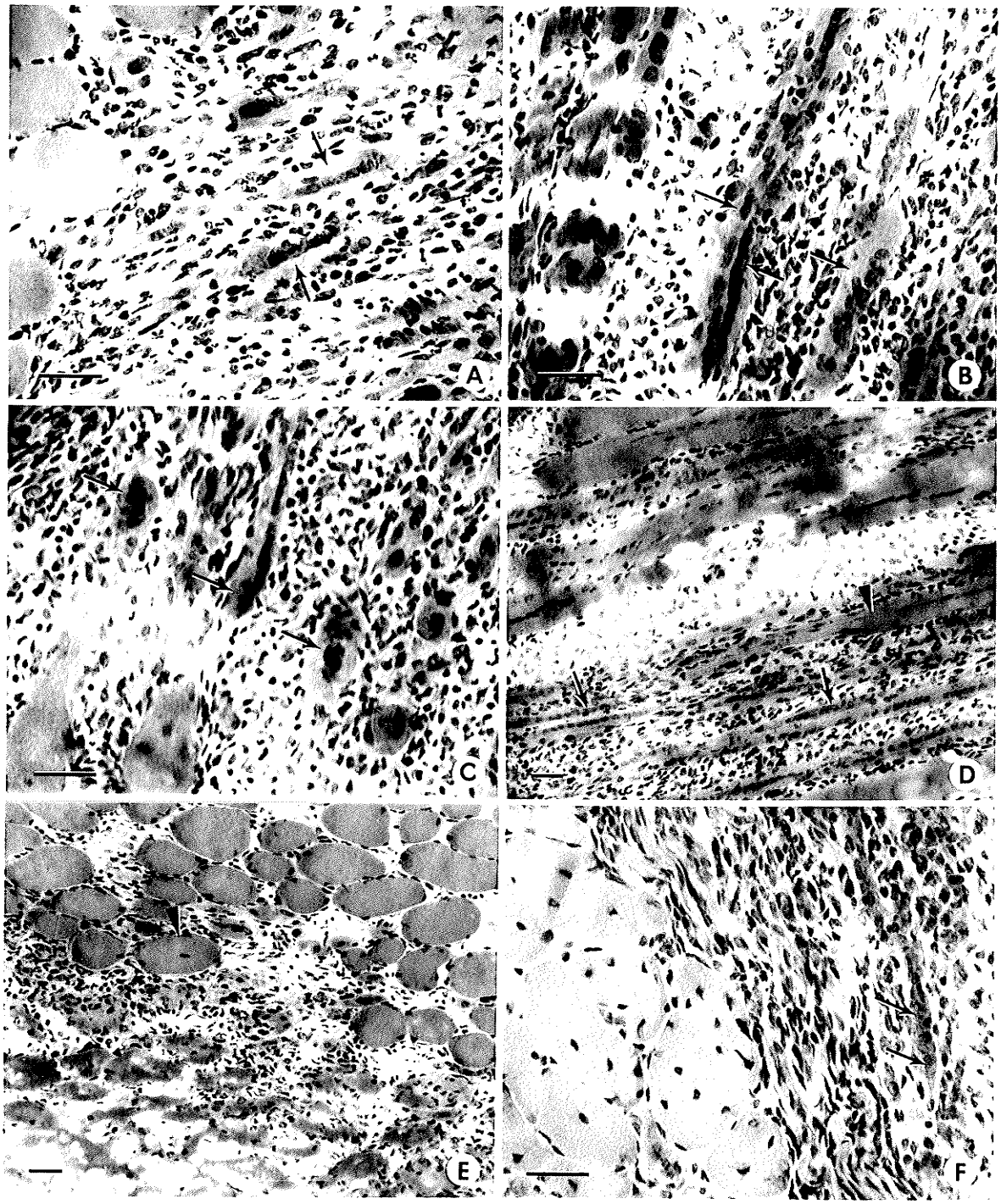
A
B
C
D
E
F

FIGURE 6:

Graphs representing the distribution of fiber diameter (μm) plotted as frequency (%) in the sample population from untreated (black bars) and PTU-treated (shaded bars) mice. While fiber diameter distribution in PTU treatment did not shift the distribution in unoperated control TA (top left panel), the fiber diameter distribution of PTU-treated *mdx* TA was significantly left-shifted (toward smaller diameter, $p<0.01$) from the distribution in untreated *mdx* TA fiber diameters (top right panel). The distribution of fiber diameter was not different between control operated PTU-treated and control operated untreated control TA (bottom left panel). By contrast there is a significant ($p<0.01$) right shift of the distribution of surviving TA fibers in PTU-treated *mdx*, compared to surviving fibers in untreated operated *mdx* TA (bottom left panel). Fibers (427-447 were measured for each group) were evenly sampled from all animals within each group.

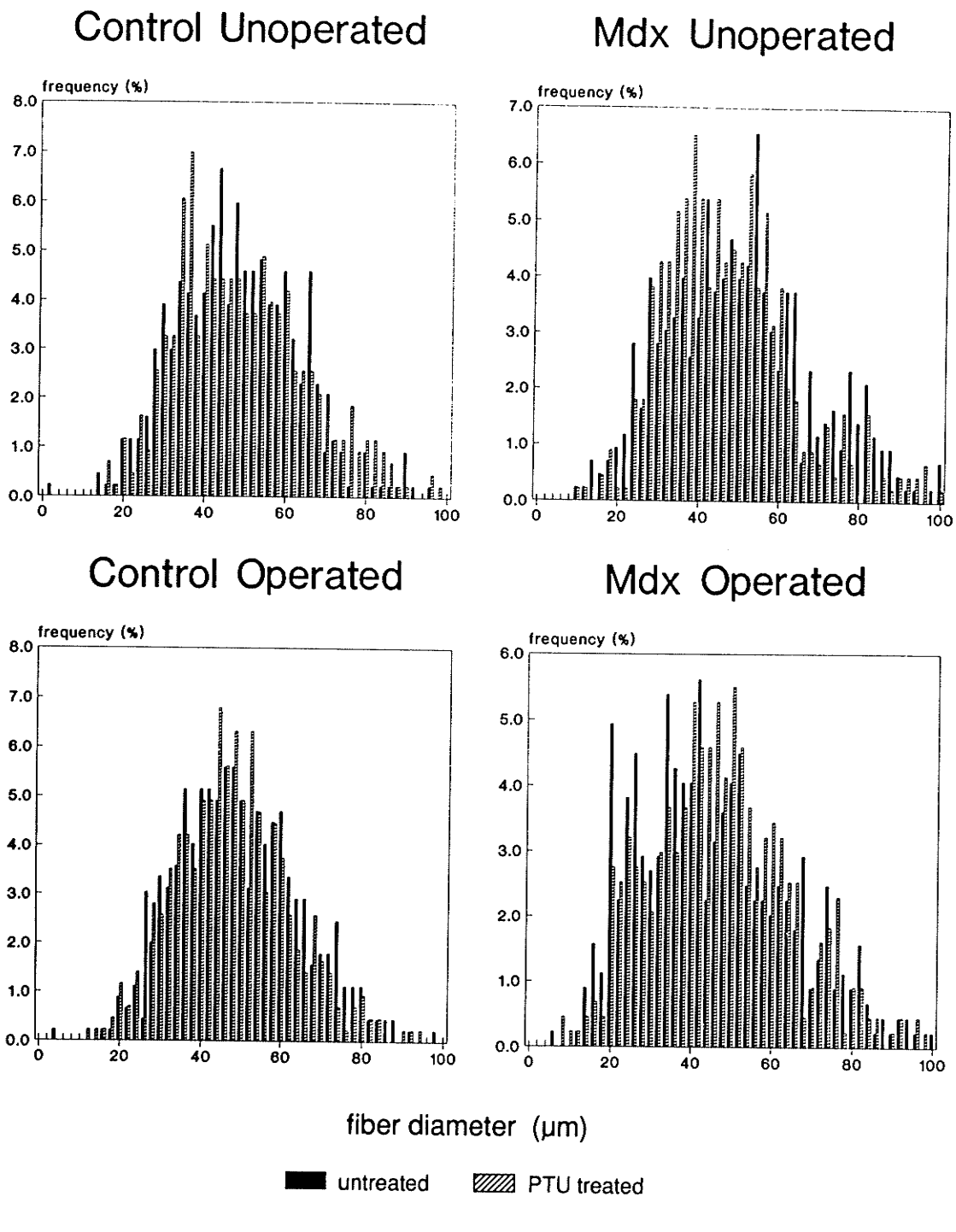
Control Unoperated
frequency (%)
8.0
7.0
6.0
5.0
4.0
3.0
2.0
1.0
0.0
0
20
40
60
80
100
Mdx Unoperated
frequency (%)
7.0
6.0
5.0
4.0
3.0
2.0
1.0
0.0
0
20
40
60
80
100
Control Operated
frequency (%)
8.0
7.0
6.0
5.0
4.0
3.0
2.0
1.0
0.0
0
20
40
60
80
100
Mdx Operated
frequency (%)
6.0
5.0
4.0
3.0
2.0
1.0
0.0
0
20
40
60
80
100
fiber diameter (µm)
untreated
PTU treated

FIGURE 7:
Micrographs of longitudinal sections of control (A) and *mdx* (B-D) diaphragm (A,B,C: X120; D: X240; bar=50μm).

A: Control PTU-treated diaphragm shows some centrally placed nuclei (arrowhead).

B: *Mdx* untreated diaphragm. An area of active dystrophy (star) is present amongst many small myotubes and centrally nucleated myofibers. Adipose tissue deposition (open arrows) is obvious between degenerating fibers.

C: *Mdx* untreated diaphragm in which much degeneration is present. Areas of calcification (open arrows) are obvious between degenerating fibers.

D: Higher power view of *mdx* untreated diaphragm showing small fibers with long chains of central nuclei and active dystrophy (top right).

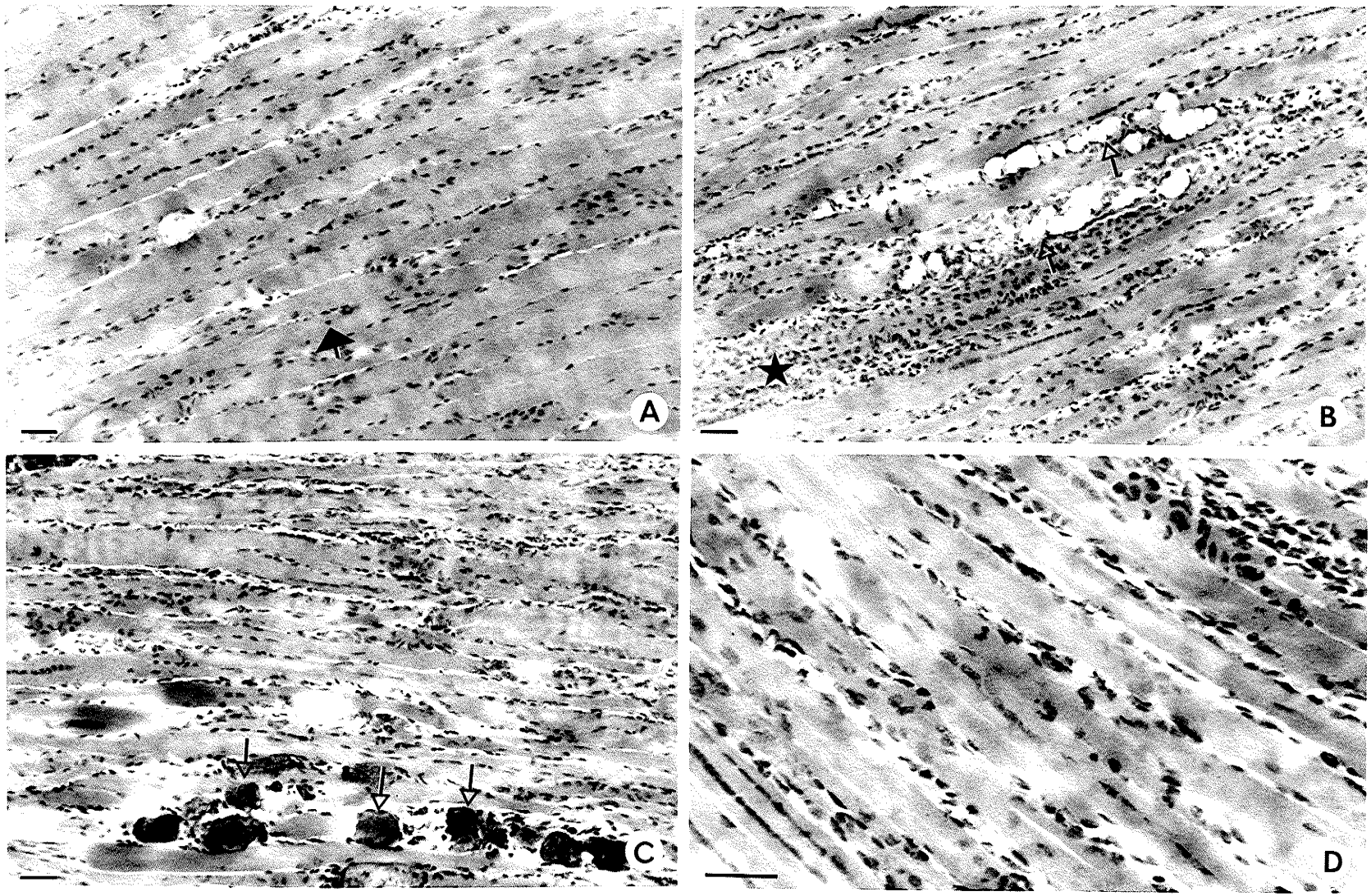
A
B
C
D

FIGURE 8:
Micrographs of control and *mdx* muscle sections stained with the anti-NCAM antibody (HRP-linked) (A,D: X475; B: X430; C: X240; bar=25μm).

A: Negative control: Control treated crushed TA in which the primary antibody was omitted. Moderate background staining is observed. The nucleus of a poly (arrow) exhibits endogenous peroxidase activity.

B: Unoperated *mdx* TA (untreated). NCAM localizes strongly to the NMJ (arrowhead). Light staining of the sarcolemma of some myofibers can also be observed.

C: Operated *mdx* treated TA shows positive staining of what appear to be myoblasts (large arrows), but could also be inflammatory cells of some variety. Some of the probable myoblasts are quite large, while others are small. Polys (small arrows) also stain positively. In this micrograph, cells appear to be lining up and joining with the blunt end of a retracted myofiber.

D: This higher power micrograph of the operated *mdx* treated TA shows probable myoblasts (large arrow) labelled with anti-NCAM. The cytoplasm of the two myofibers in the field appears to be positively labelled also.

A
B
C
D

FIGURE 9:
Micrographs of sections of regenerating areas in *mdx* TA stained with anti-NCAM (HRP-linked) (A), anti-bFGF (FITC-linked) (B), and with a basic fuchsin, methylene blue and Azure II stain (C,D) (A,B,C: X475; D: X240; bar=25μm).

A: NCAM (HRP-linked) in regenerating *mdx* treated TA localizes to the sarcolemma of the blunt end of a retracted myofiber (star). NCAM positive cells (large arrow) appear to distributed within a fan-like array of projections from the sealed end of the disrupted myofiber.

B: Regenerating *mdx* untreated muscle stained for bFGF (FITC-linked). This area is similar to the area in panel A. The end of a retracted myofiber (star) stains strongly with anti-bFGF. A myotube (small arrow) which can be seen joining with the retracted myofiber is not stained. Mononuclear cells (large arrow) stain strongly, and could be myoblasts or inflammatory cells.

C: Regenerating *mdx* treated muscle stained with a basic fuchsin, methylene blue and Azure II stain. stain. Vesicles (large arrow) are present near the blunt end of sealed myofibers. These membranous vesicles fuse to form a new sarcolemma for the damaged cell (Robertson et al., 1990). A spike of cytoplasm can be seen above the arrow. It may be communicating with mpcs or orienting itself so as myotube formation will be in the proper direction.

D: Regenerating *mdx* treated muscle stained with a basic fuchsin, methylene blue and Azure II stain. This represents the next phase in regeneration after the events in C. Myotubes (arrows) have fused with retracted myofibers. The top myofiber (arrow) appears to be branched, a common occurrence in *mdx* muscle.

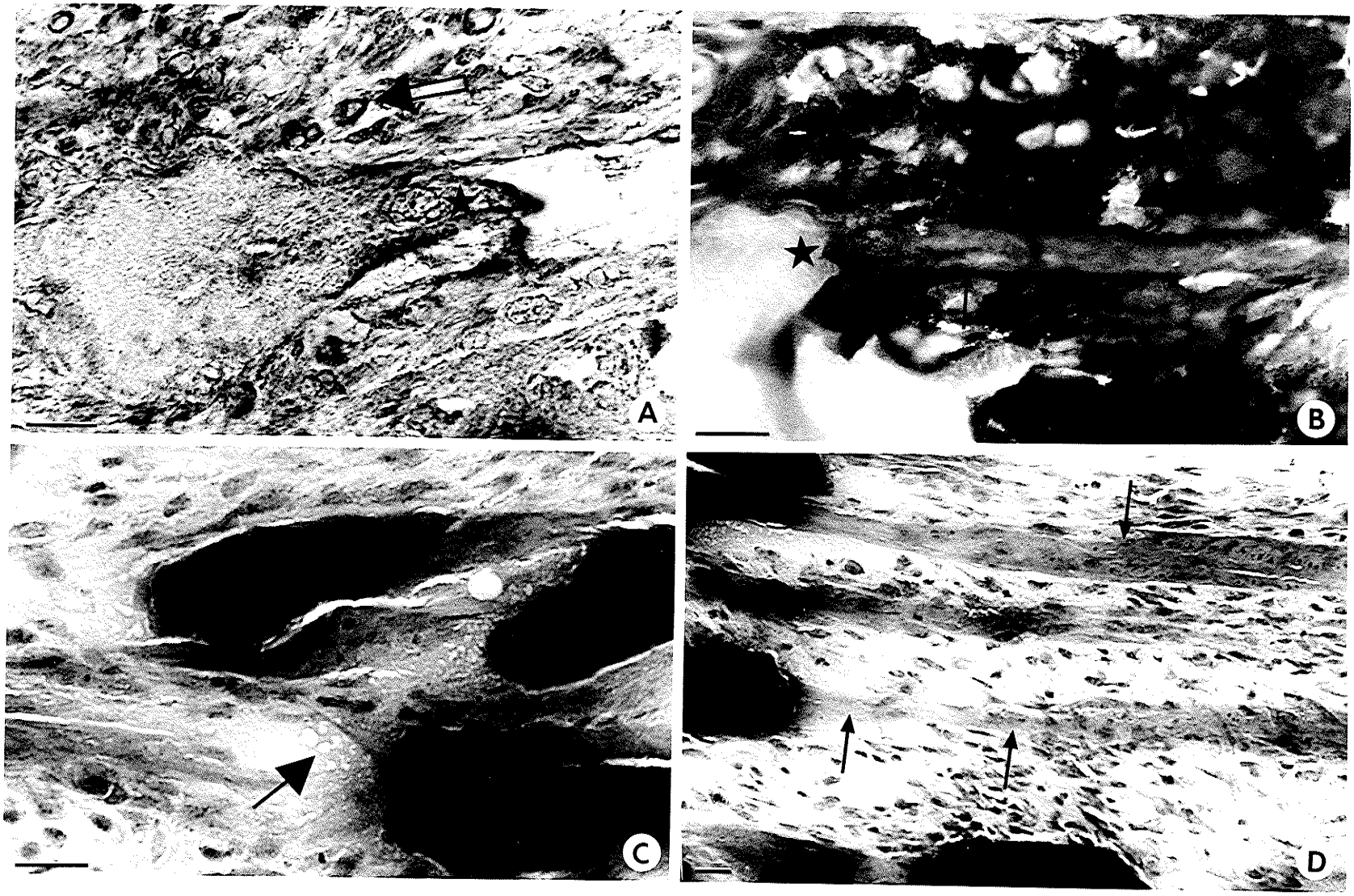
A
B
C
D

FIGURE 10:
Fluorescence micrographs of adjacent zones in control operated TA, double-immunostained for bFGF (A,C) and NCAM (B,D) (X240; bar=50μm).

A and B are the same field viewed under ultra violet light of different wavelengths. Likewise, C and D are the same field. Arrows represent cells stained for NCAM, but not bFGF. Small arrowheads represent cells stained with both anti-NCAM and anti-bFGF. Stars represent degenerating tissue.

A: Basic FGF in control untreated TA.

B: NCAM in control untreated TA.

C: Basic FGF in control PTU-treated TA. There appears to be more positive cells here than in panel A, possibly due to an increased number of dividing mpcs (see discussion). A degenerating area (star) exhibits some positively labelled mononuclear cells.

D: NCAM in control PTU-treated TA. Staining of NCAM is similar in control treated (D) and untreated (B) TA, possibly because non-specific staining of degenerating tissue (star) masks positive mononuclear cells.

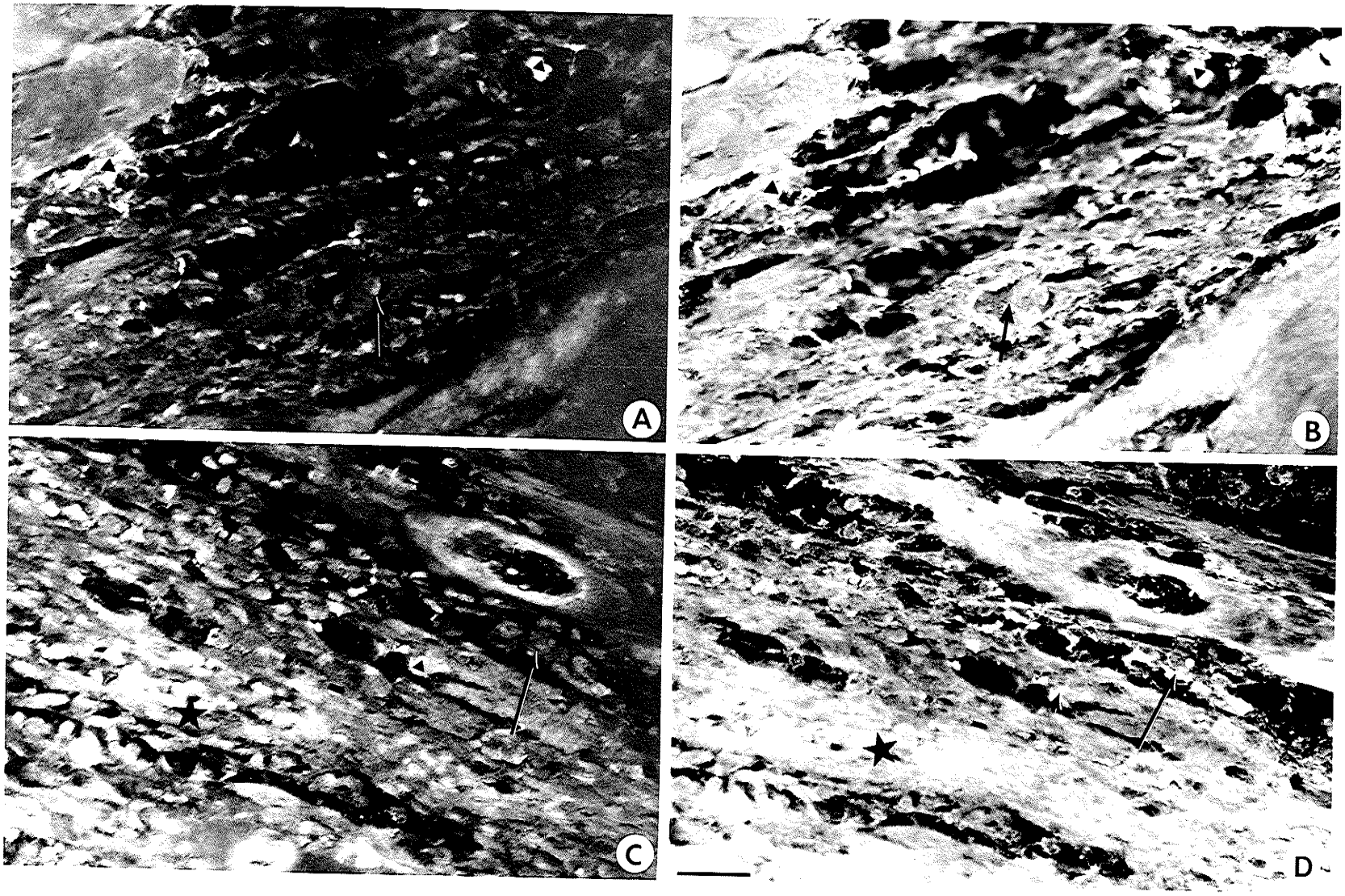
A
B
C
D

FIGURE 11:
Fluorescence micrographs of adjacent zones in *mdx* operated TA double-immunostained for bFGF (A,C) and NCAM (B,D) (X240; bar=50μm).

A and B are the same field viewed under ultra violet light of different wavelengths. Likewise, C and D are the same field. Arrows represent cells stained for NCAM, but not bFGF. Small arrowheads represent cells stained with both anti-NCAM and anti-bFGF. Stars represent degenerating tissue.

A: Basic FGF in *mdx* untreated TA.

B: NCAM in *mdx* untreated TA.

C: Basic FGF in *mdx* PTU-treated TA. More mononuclear cells are stained here than in A.

D: NCAM in *mdx* PTU-treated TA. More staining occurs here than in B, possibly due to an increased number of dividing mpcs cells in treated compared to untreated *mdx* TA.

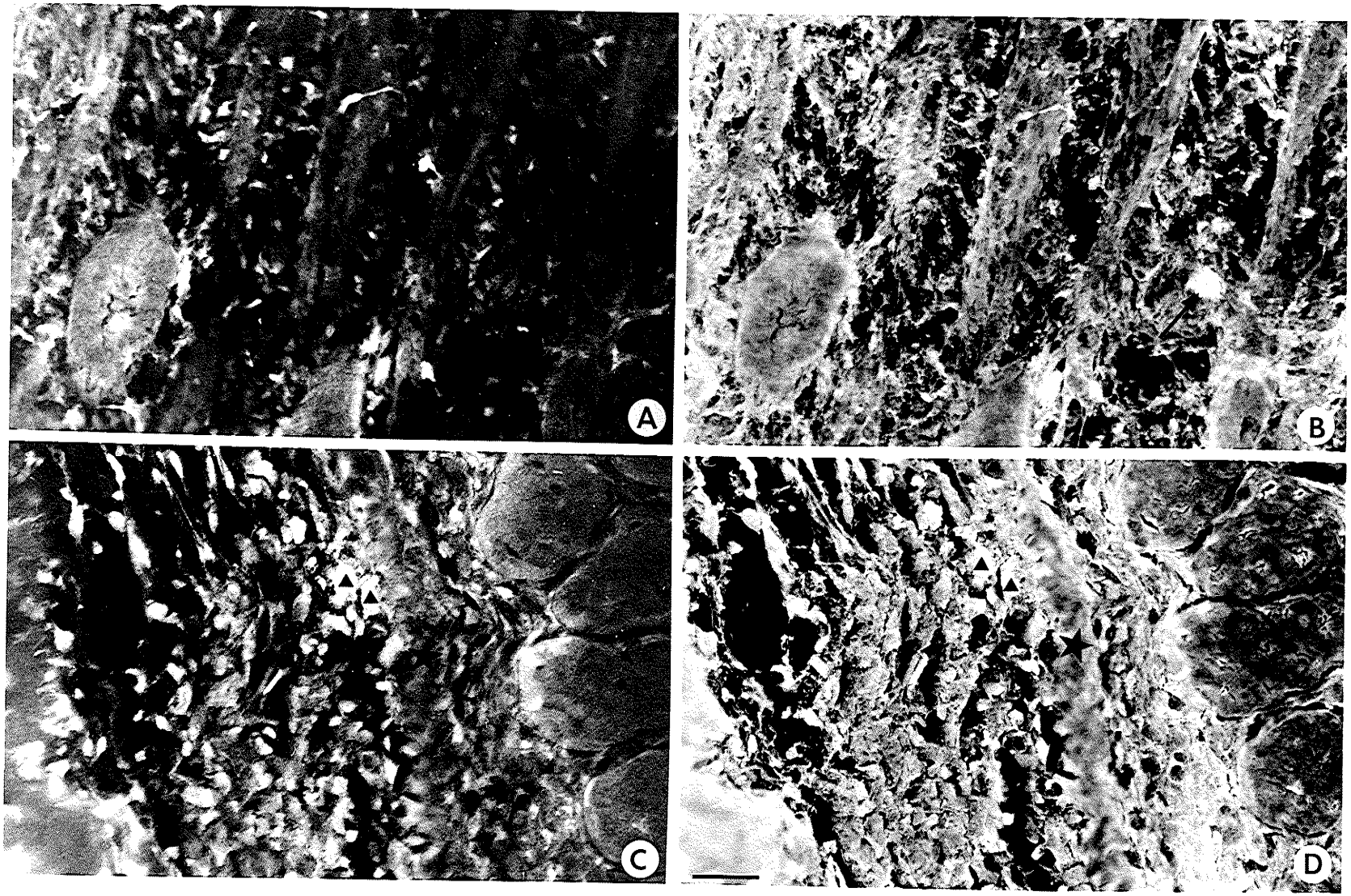
A
B
C
D

FIGURE 12:

Bar graph of double-immunohistochemistry data in the adjacent zone of the operated TA. The proportion of cells that stained for bFGF-only, NCAM-only, or both NCAM and bFGF is given from the total number of fluorescent mononuclear cells counted in control and mdx, treated and untreated groups.

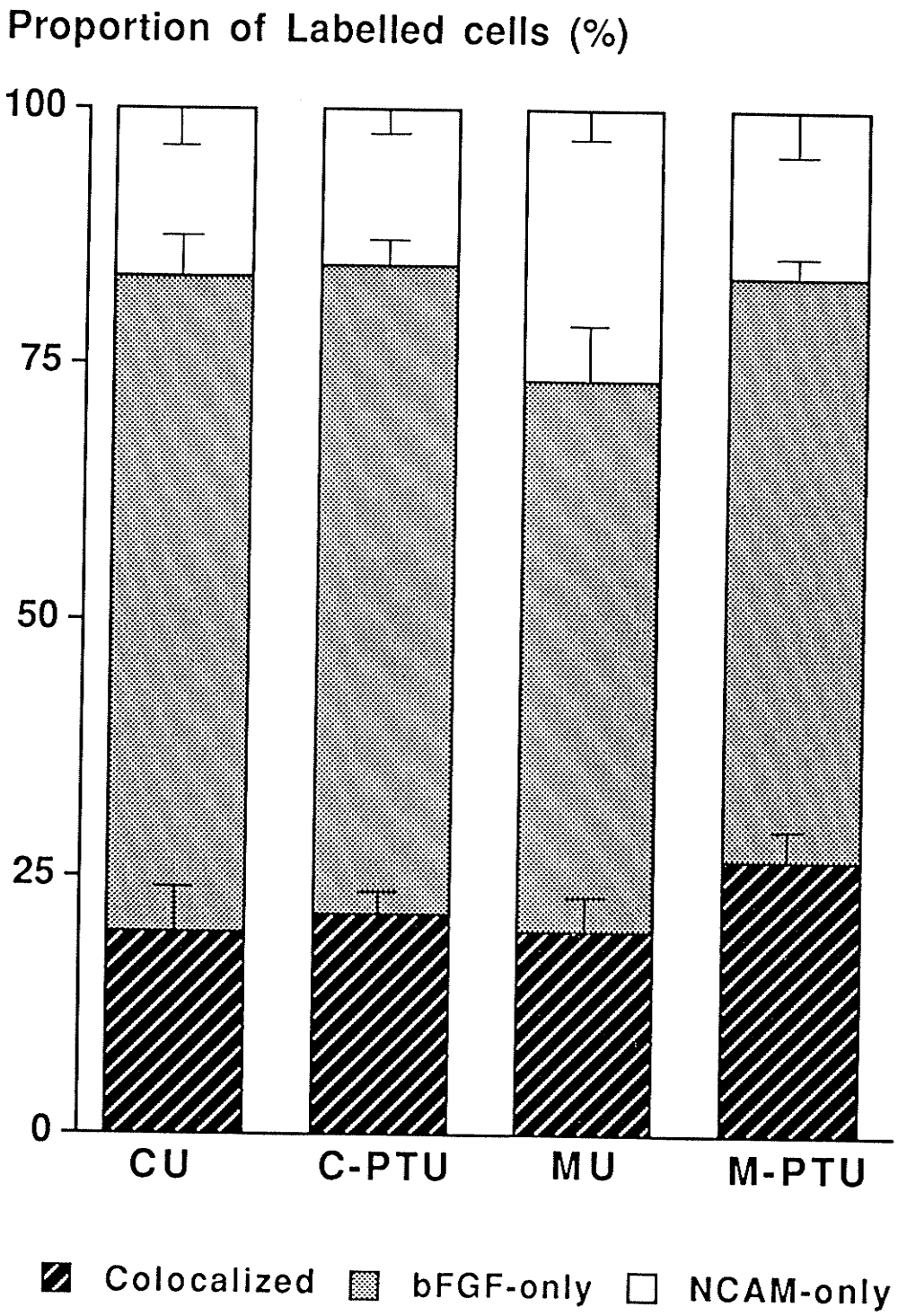
Proportion of Labelled cells (%)
100
75
50
25
0
CU
C-PTU
MU
M-PTU
Colocalized
bFGF-only
NCAM-only

FIGURE 13:
Autoradiographs of *mdx* and control TA sections (A,C: X475; B: X215; D: X120; bar=25μm). In order for a nucleus to be counted as labelled, at least three silver grains had to be located over the nucleus.

A: Unoperated control untreated TA is mostly unlabelled, except for some endothelial cells (arrowhead).

B: The small intestine of a control mouse exhibits staining (open arrows). This confirms uptake of tritiated thymidine.

C: Unoperated *mdx* PTU-treated TA. An area of active dystrophy exhibits many labelled nuclei, some of which may be mpcs (large arrows). A peripherally located nucleus (diamond) in a surviving fiber is labelled, and is probably a satellite cell.

D: Operated control PTU-treated TA. This distal adjacent zone exhibits much labelling of mononuclear cells (large arrow) and myoblasts (small arrows). Notice that not all myotube nuclei are labelled.

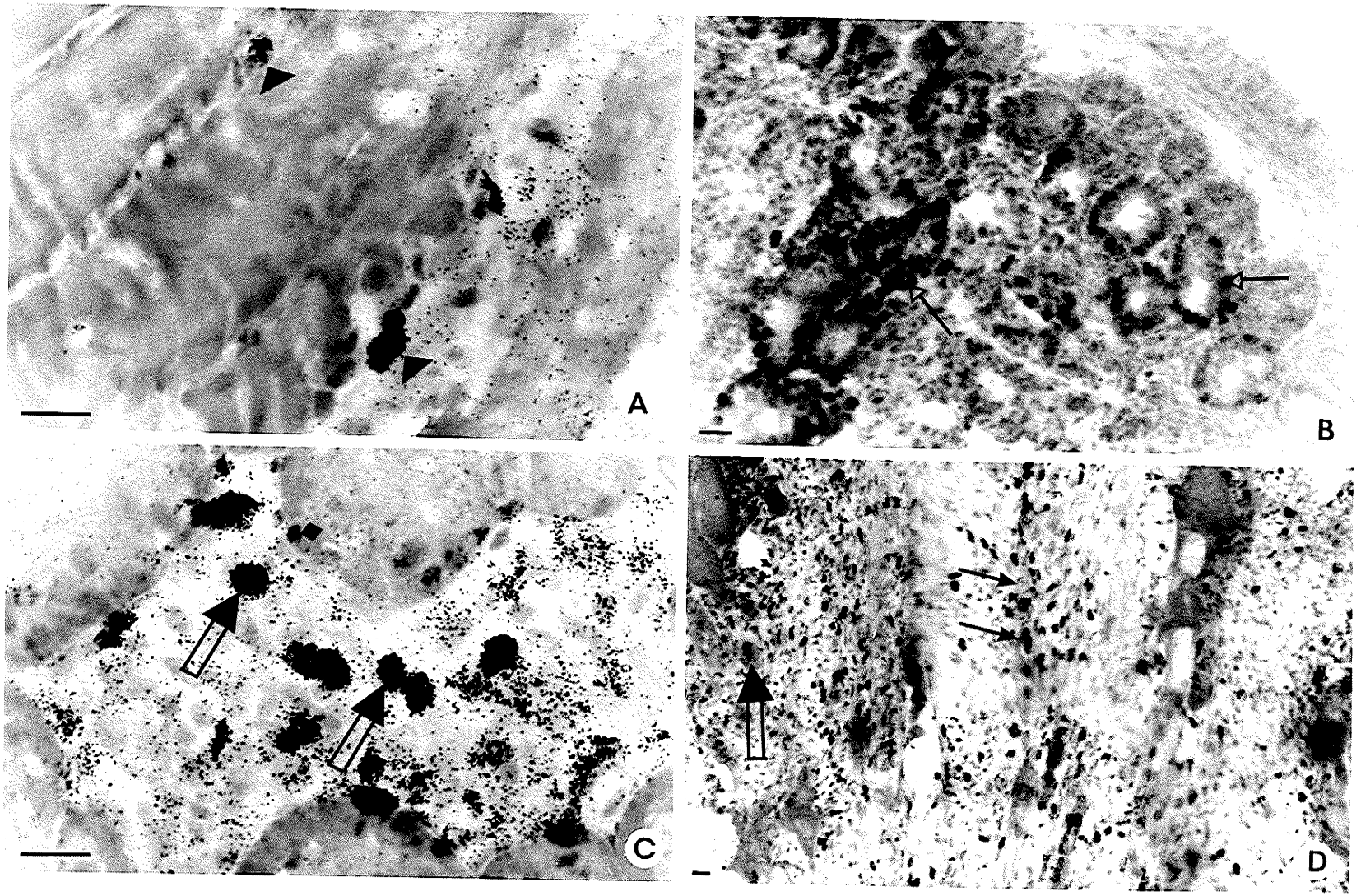
A
B
C
D

FIGURE 14:
Autoradiographs of *mdx* and control sections in operated TA (X475; bar=25μm).

A: Operated *mdx* untreated TA shows labelled cells (arrows) near to surviving muscle. It appears as if the myotubes are connecting with the surviving areas. Notice that not all myotube nuclei are labelled, indicating that they had fused before injection of tritiated thymidine.

B: Operated *mdx* treated TA. Some peripherally located satellite cells (diamonds) are labelled.

C: Operated control untreated TA in which large nuclei are labelled and are probable myoblasts (large arrow). Also, it appears as if myoblasts are lining up (small arrows) in preparation for fusion.

D: Operated control PTU-treated TA shows labelled probable myoblasts (large arrow) and labelled myotube nuclei (small arrows). More labelled mononuclear cells, but less labelled myotube nuclei are present compared to C.

A
B
C
D

TABLE 1: Metabolic and growth parameters of control and *mdx* groups with and without 8 wks of PTU-treatment. Also included is data from *mdx* mice which were PTU-treated or untreated for 4 weeks. Data are mean ± SEM. CU=control untreated, CT=control PTU-treated, MU=*mdx* untreated, MT=*mdx* PTU-treated

Parameter	8 weeks with or without PTU				4 weeks with or without PTU	
	CU	CT	MU	MT	MU	MT
% BODY WEIGHT GAIN (1st 2 runs) [a,d]	249±14 n=7	262±10 n=12	312.5±19.5 n=6	269±5.6[c] n=8	212±12.3 n=7	221±19.8 n=7
FINAL WATER INTAKE (ml/wk)	38.5 n=9	27.4[b] n=13	41.2 n=9	31.7[b] n=12	33.0 n=7	22.9[b] n=7
RESPIRATORY RATE (breaths/min)	171.0±7.9 n=4	148.5±3.8[b] n=4	175.5±2.9 n=4	157.5±7.9[b] n=4	-ND-	-ND-
T.S.H. (mU/L)	0.042±0.007 n=12	0.080±0.012[b] n=10	0.030±0.007 n=8	0.055±0.03[b,c] n=8	-ND-	-ND-
MUSCLE WT (mg)						
soleus [a]	8.7±0.7	8.2±0.5	10.7±0.2	11.5±0.5	10.4±2.1	7.5±0.6
gastrocnemius [a,d]	149.7±2.9 n=4	148.5±4.9 n=9	155.1±4.4 n=4	167.8±5.0 n=3	135.6±9.9 n=5	127.2±3.5 n=4
MUSCLE/BODY WT						
soleus [a]	0.33±0.02	0.30±0.02	0.42±0.001	0.41±0.03	0.35±0.099	0.35±0.06
gastrocnemius [a]	5.55±0.12	5.48±0.18	6.02±0.13	6.00±0.16	5.68±0.53	6.04±0.13

a : indicates significant strain-effect (control versus *mdx*)
b : indicates significant PTU-effect
c : indicates significant interaction between strain and treatment (*mdx* changes with PTU differ from control changes with PTU)
d : indicates significant age-effect (4 wks versus 8 wks treatment)
ND: not done

TABLE 2: Muscle histology parameters measured in UNOPERATED tibialis anterior with or without 8 wks (control & *mdx*) or 4 wks (*mdx*) PTU-treatment. Data are mean ± SEM.
CU=control untreated, CT=control PTU-treated, MU=*mdx* untreated, MT=*mdx* PTU-treated

Parameter	8 wks with or without PTU				4 wks with or without PTU	
	CU n=7	CT n=7	MU n=6-7	MT n=6	MU n=7	MT n=7
ACTIVE DYSTROPHY (prop. area)	---	---	0.04±0.01	0.09±0.02[b]	0.03±0.004	0.06±0.03[b]
DYSTROPHIC FOCI (#/μm^2) [d]	---	---	1.73±0.42	2.23±0.36	3.46±0.30	3.43±0.53
CN:PN RATIO [a,d]	0.03±0.02	0.05±0.02	1.38±0.10	1.34±0.08	0.53±0.04	0.43±0.03
CENTRONUCLEATION INDEX (CNI) [d]	---	---	0.79±0.02	0.80±0.02	0.56±0.03	0.53±0.01
TOTAL NUCLEI PER FIELD						
central [a,d]	6±3	10±5	209±12	197±12	88±8	89±7
peripheral [a,d]	262±22	230±15	155±9	151±10	167±8	205±9[b]
FIBER DIAMETER (μm) [a]	47.1±0.7	48.4±0.8	50.7±0.9	46.3±0.8[b]	-ND-	-ND-

a : indicates significant strain-effect (control versus *mdx*)
b : indicates significant PTU-effect
c : indicates significant interaction between strain and treatment (*mdx* changes with PTU differ from control changes with PTU)
d : indicates significant age-effect (4 wks versus 8 wks treatment)
ND: not done

TABLE 3: Muscle histology parameters measured in OPERATED tibialis anterior with or without 8 wks (control & *mdx*) or 4 wks (*mdx*) PTU-treatment. Data are mean ± SEM.
CU=control untreated, CT=control PTU-treated, MU=*mdx* untreated, MT=*mdx* PTU-treated

Parameter	8 wks with or without PTU				4 wks with or without PTU	
	CU n=6	CT n=7	MU n=6	MT n=6	MU n=5-6	MT n=4
AREA OF CRUSH (μm^2 X 10^{-4})	7.9±0.95	5.6±1.3	5.4±1.5[c]	7.9±1.4[c]	9.9±2.2	9.7±2.2
CN:PN RATIO						
adjacent zone[a,d]	3.4±1.1	3.1±0.9	26.3±12.1	39.6±12.9	7.1±1.1	13.5±5.8
surviving zone						
proximal [a,d]	0.04±0.2	0.1±0.1	4.2±0.6	6.1±1.6	0.69±0.06	0.54±0.07
distal [e]	4.7±8.5	24.9±13.7	49.5±23.2	56.2±32.6	18.9±6.0	4.5±0.49
MYOTUBE DENSITY						
crush zone [d]	3.8±1.8	4.1±2.2	6.2±2.5	4.9±1.9	3.2±1.9	0.25±0.16
adjacent zone [a]	15.7±4.9	19.2±1.9	31.8±5.1	27.0±3.9	35.0±4.2	35.7±2.8
surviving zone[a,d]	1.0±0.6	1.6±0.8	5.8±2.2	2.8±0.9[c]	0.6±0.3	2.2±0.5[c]
FIBER DIAMETER (μm) [a]	48.9±0.7	46.6±0.7	44.4±0.9	46.9±0.9[b]	-ND-	-ND-

a : indicates significant strain-effect (control versus *mdx*)
b : indicates significant PTU-effect
c : indicates significant interaction between strain and treatment (*mdx* changes differ from control changes with treatment) or age and treatment
d : indicates significant age-effect (4 wks differs from 8 wks treatment)
e : indicates significant difference from proximal surviving zone
ND: not done

TABLE 4: Proportions of nuclei (separated by cell type) labelled by silver grains exposed after uptake of tritiated thymidine in cells of the adjacent zone of the operated TA of control and *mdx* mice with and without 8 weeks of PTU-treatment. Data are mean ± SEM.
CU=control untreated, CT=control PTU-treated, MU=*mdx* untreated, MT=*mdx* PTU-treated

Cell Type	CU	CT	MU	MT
4 DAYS RECOVERY:				
POLY NUCLEI: PROXIMAL	0.03 ± 0.01	0.08 ± 0.02	0.04 ± 0.01	0.05 ± 0.02
DISTAL	0.04 ± 0.02	0.02 ± 0.009[b]	0.10 ± 0.04	0.02 ± 0.009[b]
MYOTUBE NUCLEI: PROXIMAL	0.57 ± 0.06	0.58 ± 0.07	0.59 ± 0.09	0.64 ± 0.03
DISTAL	0.68 ± 0.05	0.57 ± 0.07[b]	0.68 ± 0.05	0.54 ± 0.06[b]
TOT. LABELLED NUCLEI: PROX	0.35 ± 0.01	0.33 ± 0.01[a]	0.30 ± 0.02	0.44 ± 0.02[b,c]
DISTAL	0.41 ± 0.02[a]	0.32 ± 0.02[b]	0.33 ± 0.02	0.36 ± 0.02[c]
2 DAYS RECOVERY:				
POLY NUCLEI: PROXIMAL	0.05 ± 0.02[a]	0.29 ± 0.04[b]	0.18 ± 0.03	0.21 ± 0.04[b,c]
DISTAL [e]	0.13 ± 0.04	0.11 ± 0.03	0.10 ± 0.03	0.13 ± 0.03
MYOTUBE NUCLEI: PROXIMAL	0	0	0	0.15 ± 0.08
DISTAL	0.02 ± 0.02	0	0	0.096 ± 0.05
TOTAL LABELLED NUCLEI: PROX	0.50 ± 0.05[a]	0.42 ± 0.03	0.39 ± 0.03	0.45 ± 0.02[c]
DISTAL [e]	0.35 ± 0.04	0.34 ± 0.02	0.30 ± 0.02	0.40 ± 0.03

a: indicates significant strain-effect (control changes differ from *mdx* changes)
b: indicates significant PTU-effect
c: indicates significant interaction between strain and treatment (*mdx* changes with PTU differ from control changes with PTU
e: indicates significant difference between proximal and distal areas

8. BIBLIOGRAPHY

Allbrook D: Skeletal muscle regeneration. Muscle Nerve, 4: 234-245, 1981.

Allen RE, Boxhorn LK: Regulation of skeletal muscle satellite cell proliferation and differentiation by transforming growth factor-beta, insulin-like growth factor I and fibroblast growth factor. J Cell Physiol, 138: 311-315, 1989.

Allen RE, Rankin LL: Regulation of satellite cells during skeletal muscle growth and development. Proc Soc Exp Biol Med, 194: 81-86, 1990.

Anderson JE: Myotube phospholipid synthesis and sarcolemmal ATPase activity in dystrophic (mdx) mouse muscle. Biochem Cell Biol, 69: 835-841, 1991.

Anderson JE, Bressler BH, Ovalle WK: Functional regeneration in the hindlimb skeletal muscle of the *mdx* mouse. J Muscle Res Cell Motil, 9: 499-516, 1988.

Anderson JE, Kakulas BA, Jacobsen PF, Johnsen RD, Kornegay JN, Grounds MD: Comparison of basic fibroblast growth factor in X-linked dystrophin-deficient myopathies of human, dog and mouse. Growth Factors, 9: 107-121, 1993.

Anderson JE, Liu L, Kardami E: Distinctive patterns of basic fibroblast growth factor (bFGF) distribution in degenerating and regenerating areas of dystrophic (*mdx*) striated muscles. Dev Biol, 147: 96-109, 1991.

Anderson JE, Liu L, Kardami E: The effects of hyperthyroidism on muscular dystrophy in the *mdx* mouse: Greater dystrophy in cardiac and soleus muscle. Muscle Nerve, 17: 64-73, 1994.

Anderson JE, Ovalle WK, Bressler BH: Electron microscopic and autoradiographic characterization of hindlimb muscle regeneration in the *mdx* mouse. Anat Rec, 219: 243-257, 1987.

Andersson AM, Olsen M, Zhernosekov D, Gaardsvoll H, Krog L, Linnemann D, Bock E: Age-related changes in expression of the neural cell adhesion molecule in skeletal muscle: a comparative study of newborn, adult and aged rats. Biochem J, 290: 641-648, 1993.

Baird A, Klagsbrun M: The fibroblast growth factor family: An overview. Ann New York Acad Sci, 638: xi-xii, 1991.

Bakker AJ, Head SI, Williams DA, Stephenson DG: Ca^{2+} levels in myotubes grown from the skeletal muscle of dystrophic (*mdx*) and normal mice. J Physiol, 460: 1-13, 1993.

Bandman E: Contractile protein isoforms in muscle development. Dev Biol, 154, 273-283, 1992.

Beilharz MW, Lareu RR, Garrett KL, Grounds MD, Fletcher S: Quantitation of muscle precursor cell activity in skeletal muscle by Northern analysis of MyoD and myogenin expression: Application to dystrophic (*mdx*) mouse muscle. Molec Cell Neurosci, 3: 326-331, 1992.

Bieber FR, Hoffman EP: Duchenne and Becker muscular dystrophies: Genetics, prenatal diagnosis, and future prospects. Clin Perinatol, 17: 845-865, 1990.

Bischoff R: Interaction between satellite cells and skeletal muscle

fibers. Develop, 109: 943-952, 1990.

Bishopric NH, Gahlmann R, Wade R, Kedes L: Gene expression during skeletal and cardiac muscle development. In Fozzard et al., (eds): The Heart and Cardiovascular System. Raven Press, Ltd., New York, pp 1587-1598, 1992.

Blau HM, Webster C, Pavlath GK: Defective myoblasts identified in Duchenne muscular dystrophy. Proc Natl Acad Sci, USA, 80: 4856-4860, 1983.

Bober E, Lyons GE, Braun T, Cossu G, Buckingham M, Arnold HH: The muscle regulatory gene, Myf-6, has a biphasic pattern of expression during early mouse development. J Cell Biol, 113: 1255-1265, 1991.

Braun T, Rudnicki MA, Arnold HH, Jaenisch R: Targeted inactivation of the muscle regulatory gene Myf-5 results in abnormal rib development and perinatal death. Cell, 71: 369-382, 1992.

Bridges LR: The association of cardiac muscle necrosis and inflammation with the degenerative and persistent myopathy of *mdx* mice. J Neurol Sci, 72: 147-157, 1986.

Brooke MH, Fenichel GM, Griggs RC, Mendell JR, Moxley R, Florence J, King WM, Pandya S, Robison J, Schierbecker J, Signore L, Miller JP, Gilder BF, Kaiser KK, Mandel S, Arfken C: Duchenne muscular dystrophy: Patterns of clinical progression and effects of supportive therapy. Neurol, 39: 475-481, 1989.

Brown SC, Stickland NC: Satellite cell content in muscles of large and small mice. J Anat, 183: 91-96, 1993.

Bulfield G, Siller W, Wight P, Moore K: X-chromosome linked muscular dystrophy (*mdx*) in the mouse. Proc Natl Acad Sci USA, 81: 1189-1192, 1984.

Butler-Browne GS, Herlicoviez D, Whalen RG: Effects of hypothyroidism on myosin isozyme transitions in developing rat muscle. FEBS Lett, 166: 77-81, 1984.

Calpan A, Carlson B, Faulkner J, Fischman D, Garrett W: Skeletal muscle. In Woo SLY, Buckwalter JA (eds): Injury and Repair of the Musculoskeletal Soft Tissues. Am Acad of Orthopaedic Surgeons, Park Ridge, Ill., pp 209-281, 1988.

Carlson BN: The regeneration of skeletal muscle - A review. Am J Anat, 137: 119-150, 1973.

Carlson BN: Regeneration of entire skeletal muscles. Fed Proc, 45: 1456-1460, 1986.

Carlson BN, Faulkner JA: The regeneration of skeletal muscle fibers following injury: a review. Med Sci Sports Exerc, 15: 187-198, 1983.

Carnwath JW, Shotton DM: Muscular dystrophy in the *mdx* mouse: Histopathology of the soleus and extensor digitorum longus muscles. J Neurol Sci, 80: 39-54, 1987.

Carpenter S, Karpati G: Muscle development and growth. In Carpenter S, Karpatti G (eds): Pathology of Skeletal Muscle. Churchill Livingstone, New York, pp 1-13, 1984.

Clarke MSF, Khakee R, McNeil PL: Loss of cytoplasmic basic fibroblast growth factor from physiologically wounded myofibers of normal and dystrophic muscle. J Cell Sci, 106: 121-133, 1993.

Clegg CH, Linkhart TA, Olwin BB, Hauschka SD: Growth factor control of skeletal muscle differentiation occurs in G_1-phase and is repressed by fibroblast growth factor. J Cell Biol, 105: 959-956, 1987.

Coulton GR, Morgan JE, Partridge TA, Sloper JC: The *mdx* mouse skeletal muscle myopathy: I. A histological, morphometric and biochemical investigation. Neuropathol Appl Neurobiol, 14: 53-70, 1988.

Covault J, Merlie JP, Goridis C, Sanes JR: Molecular forms of NCAM and its RNA in developing and denervated skeletal muscle. J Cell Biol, 102: 731-739, 1986.

Covault J, Sanes JR: Distribution of NCAM in synaptic and extrasynaptic portions of developing and adult skeletal muscle. J Cell Biol, 102: 716-730, 1986.

Cox GA, Cole NM, Matsumura K, Phelps SF, Hauschka SD, Campbell KP, Faulkner JA, Chamberlain JS: Overexpression of dystrophin in transgenic *mdx* mice eliminates dystrophin symptoms without toxicity. Nature, 364: 725-729, 1993.

d'Albis A, Chanoine C, Janmot C, Mira JC, Couteaux R: Muscle-specific response to thyroid hormone of myosin isoform transitions during rat postnatal development. Eur J Biochem, 193: 155-161, 1990.

d'Albis A, Lenfant-Guyot M, Janmot C, Chanoine C, Weinman J, Gallien CL: Regulation by thyroid hormones of terminal differentiation in the skeletal dorsal muscle: I. Neonate mouse. Dev Biol, 123: 25-32, 1987a.

d'Albis A, Weinman J, Mira JC, Janmot C, Couteaux R: The regulator role of thyroid hormones in myogenesis. Analysis of isoforms of myosin in muscular regeneration. C R Acad Sci III, 305: 697-702, 1987b.

Dangain J, Vrbova G: Muscle development in *mdx* mutant mice. Muscle Nerve, 7: 700-704, 1984.

Davies HL, Jasmin BJ: Direct gene transfer into mouse diaphragm. FEBS Lett, 333: 146-150, 1993.

Davies HL, Whalen RG, Demenueix BA: Direct gene transfer into skeletal muscle *in vivo*: Factors affecting efficiency of transfer and stability of expression. Hum Gene Ther, 4: 151-159, 1993.

Dick J, Vrbova G: Progressive deterioration of muscles in *mdx* mice induced by overload. Clin Sci, 84: 145-150, 1993.

Dickson G, Peck D, Moore SE, Barton CH, Walsh FS: Enhanced myogenesis in NCAM-transfected mouse myoblasts. Nature, 344: 348-351, 1990.

DiMario J, Buffinger N, Yamada S, Strohman RC: Fibroblast growth factor in the extracellular matrix of dystophic (*mdx*) mouse muscle. Science, 244: 688-690, 1989.

DiMario J, Strohman RC: Satellite cells from dystrophic (*mdx*) mouse muscle are stimulated by fibroblast growth factor *in vitro*. Differentiation, 39: 42-49, 1988.

DiMario J, Uzman A, Strohman RC: Fiber regeneration is not persistent in dystrophic (*mdx*) mouse skeletal muscle. Dev Biol, 148: 314-321, 1991.

Draeger A, Weeds AG, Fitzsimons RB: Primary, secondary and tertiary myotubes in developing skeletal muscle: a new approach to the analysis of

human myogenesis. J Neurol Sci, 81: 19-43, 1987.

Dubois JD, Dussault JH: Ontogenesis of thyroid function in the neonatal rat. Thyroxine (T4) and triiodothyronine (T3) production rates. Endocrinol, 101: 435-441, 1977.

Dulhunty AF, Gage PW, Lamb GD: Differential effects of thyroid hormone on T-tubules and terminal cisternae in rat muscles: an electrophysiological and morphometric analysis. J Musc Res Cell Motil, 7: 225-236, 1986.

Dunn JF, Radda GK: Total ion content of skeletal and cardiac muscle in the *mdx* mouse dystrophy: Ca^{2+} is elevated at all ages. J Neurol Sci, 103: 226-231, 1991.

Dupont-Versteegden EE, McCarter RJ: Differential expression of muscular dystrophy in diaphragm verus hindlimb muscles of *mdx* mice. Muscle Nerve, 15: 1105-1110, 1992.

Dusterhoft S, Yablonka-Reuveni Z, Pette D: Characterization of myosin isoforms in satellite cell cultures from adult rat diaphragm, soleus and tibialis anterior muscles. Different, 45: 185-191, 1990.

Edwards RHT, Newhan DJ, Jones DA et al.: Role of mechanical damage in pathogenesis of proximal myopathy in man. Lancet, 1: 548-552, 1984.

Ervasti JM, Campbell KP: Membrane organization of the dystrophin-glycoprotein complex. Cell, 66: 1121-1131, 1991.

Ervasti JM, Ohlendieck K, Kahl SD, Gaver MG, Campbell KP: Deficiency of a glycoprotein component of the dystrophin complex in dystrophic muscle. Nature, 345: 315-319, 1990.

Everts ME, Dorup I, Flyvbjerg A, Marshall SM, Jorgensen KD: Na^+-K^+ pump in rat muscle: effects of hypophysectomy, growth hormone, and thryoid hormone. Am J Physiol, 259: E278-E283, 1990.

Fabbrizio E, Bonet-Kerrache A, Leger JJ, Mornet D: Actin-dystrophin interface. Biochemistry, 32: 10457-10463, 1993.

Feldman JL, Stockdale FE: Skeletal muscle satellite cell diversity: Satellite cells form fibers of different types in cell culture. Dev Biol, 143: 320-334, 1991.

Fenichel GM, Florence JM, Pestronk A, Mendell JR, Moxley RT, Griggs RC et al.: Long-term benefits from prednisone therapy in Duchenne muscular dystrophy. Neurol, 41: 1874-1877, 1991.

Fitzsimons DP, Herrick RE, Baldmin KM: Isomyosin distributions in rodent muscles: effects of altered thyroid state. J Appl Physiol, 69: 321-327, 1990.

Florini JR, Magri KA: Effects of growth factors on myogenic differentiation. Am J Physiol, 256: C701-C711, 1989.

Flucher BE: Structural analysis of muscle development: transverse tubules, sarcoplasmic reticulum, and the triad. Dev Biol, 154: 245-260, 1992.

Fuchtbauer EM, Westphal H: MyoD and myogenin are coexpressed in regenerating skeletal muscle of the mouse. Dev Dynamics, 193: 34-39, 1992.

Gambke B, Lyons GE, Haselgrove J, Kelly AM, Rubinstein NA: Thyroidal and neural control of myosin transitions during development of rat fast and

slow muscles. FEBS Lett, 156: 335-339, 1983.

Gospodarowicz D, Neufeld G, Schweigerer L: Fibroblast growth factor: Structural and biological properties. J Cell Physiol (Supp), 5: 15-26, 1987.

Greenberg CR, Jacobs HK, Halliday W, Wrogemann K: Three years experience with neonatal screening for Duchenne/Becker muscular dystrophy: gene analysis, gene expression and phenotype prediction. Am J Med Genet, 39: 68-75, 1991.

Grounds MD: Towards understanding skeletal muscle regeneration. Path Res Pract, 187: 1-22, 1991.

Grounds MD, Garrett KL, Lai MC, Wright WE, Beilharz MW: Identification of skeletal muscle precursor cells *in vivo* by use of MyoD1 and myogenin probes. Cell Tissue Res, 267: 99-104, 1992a.

Grounds MD, Garrett KL, Beilharz MW: The transcription of MyoD1 and myogenin genes in thymic cells *in vivo*. Exp Cell Res, 198: 357-361, 1992b.

Grounds MD, McGeachie JK: A model of myogenesis *in vivo*, derived from detailed autoradiographic studies of regenerating skeletal muscle, challenges the concept of quantal mitosis. Cell Tiss Res, 250: 563-569, 1987.

Grounds MD, McGeachie JK: A comparison of muscle precursor replication in crush injured skeletal muscle of Swiss and BALB/C mice. Cell Tissue Res, 255: 385-391, 1989.

Grounds MD, McGeachie JK: Skeletal muscle regeneration after crush injury in dystrophic *mdx* mice: An autoradiographic study. Muscle Nerve, 15: 580-586, 1992.

Grumet M, Rutishauser U, Edelman GM: Neural cell adhesion molecule in on embryonic muscle cells and mediates adhesion to nerve cells *in vitro*. Nature, 293: 693-695, 1982.

Gussoni E, Pavlath GK, Lanctot AM, Sharma KR, Miller RG, Steinman L, Blau HM: Normal dystrophin transcripts detected in Duchenne muscular dystrophy patients after myoblast transplantation. Nature, 356: 435-438, 1992.

Guthridge M, Wilson M, Cowling J, Bertolini J, Hearn MTW: The role of basic fibroblast growth factor in skeletal muscle regeneration. Growth Factors, 6: 53-63, 1992.

Haemaelaeinen N, Pette D: The histochemical profiles of fast fiber types IIB, IID and IIA in skeletal muscle of mouse, rat, and rabbit. J Histochem Cytochem, 41: 733-743, 1993.

Hansen-Smith FM, Carlson BN: Cellular responses to free grafting of the extensor digitorum longus muscle of the rat. J Neurol Sci, 41: 149-173, 1979.

Hasty P, Bradley A, Morris JH, Edmondson DG, Venuti JM, Olson EN, Klein WH: Muscle deficiency and neonatal death in mice with a targeted mutation in the myogenin gene. Nature, 364: 501-506, 1993.

Hoffman EP: The animal model of Duchenne muscular dystrophy: Windows on the pathophysiological consequences of dystrophin deficieny. In Mooseker M, Morrow J (eds): Ordering the Membrane-cytoskeleton Trilayer. Academic Press, NY, pp 1-26, 1991.

Hoffman EP, Morgan JE, Watkins SC, Partridge TA: Somatic reversion/suppression of the mouse *mdx* phenotype *in vivo*. J Neurol Sci, 99: 9-25, 1990.

Huard J, Bouchard JP, Roy R, Malouin F, Dansereau G, Labrecque C, Albert N, Richards CL, Lemieux B, Tremblay JP: Human myoblast transplantation: Preliminary results of 4 cases. Muscle Nerve, 15: 550-560, 1992.

Hughes SM, Taylor JM, Tapscott SJ, Gurley CM, Carter WJ, Peterson CA: Selective accumulation of MyoD and Myogenin mRNAs in fast and slow adult skeletal muscle is controlled by innervation and hormones. Develop, 118: 1137-1147, 1993.

Izumo S, Nadal-Ginard B, Mahdavi V: All members of the MHC multigene family respond to thyroid hormone in a highly tissue-specific manner. Science, 231: 597-600, 1986.

Jones GE, Murphy SJ, Watt DJ: Segregation of the myogenic cell lineage in mouse muscle development. J Cell Sci, 97: 659-667, 1990.

Kaminsky P, Klein M, Robin-Lherbier B, Walker P, Escanye JM, Brunotte F, Robert J, Duc M: ^{31}P-NMR study of different hypothyroid states in rat leg muscle. Am J Physiol, 261: E706-E712, 1991.

Kardami E, Fandrich RR: Basic fibroblast growth factor in atria and ventricles of the vertebrate heart. J Cell Biol, 109: 1865-1875, 1989.

Kardami E, Liu L, Doble BW: Basic fibroblast growth factor in cultured cardiac myocytes. Ann New York Acad Sci, 638: 244-255, 1991.

Kardami E, Murphy LJ, Liu L, Padua RR, Fandrich RR: Characterization of two preparations of antibodies to basic fibroblast growth factor which exhibit distinct patterns of immunolocalization. Growth Factors, 4: 69-80, 1990.

Kardami E, Spector D, Strohman RC: Heparin inhibits skeletal muscle growth *in vitro*. Dev Biol, 126: 19-29, 1988.

Karpati G, Acsadi G: The potential for gene therapy in Duchenne muscular dystrophy and other genetic muscle diseases. Muscle Nerve, 16: 1141-1153, 1993.

Karpati G, Carpenter S: Small caliber skeletal muscle fibers do not suffer deleterious consequences of dystrophin gene expression. Am J Med Genet, 25: 653-658, 1986.

Karpati G, Carpenter S, Prescott S: Small-caliber skeletal muscle fibers do not suffer necrosis in *mdx* mouse dystrophy. Muscle Nerve, 11: 795-803, 1988.

Kaufman SJ, George-Weinstein M, Foster RF: In vitro development of precursor cells in the myogenic lineage. Dev Biol, 146: 228-238, 1991.

Khan MA: Corticosteroid therapy in Duchenne muscular dystrophy. J Neurol Sci, 120: 8-14, 1993.

Knudsen KA, McElwee SA, Myers L: A role for neural cell adhesion molecule, NCAM, in myoblast interaction during myogenesis. Dev Biol, 138: 159-168, 1990.

Lee CC, Pons F, Jones PG, Bies RD, Schlang AM, Leger JJ, Caskey CT: *Mdx* transgenic mouse: Restoration of recombinant dystrophin to the dystrophic

muscle. Hum Gene Ther, 4: 273-281, 1993.

Liu L, Doble BW, Kardamin E: Perinatal phenotype and hypothyroidism are associated with elevated levels of 21.5- to 22-kDa basic fibroblast growth factor in cardiac ventricles. Dev Biol, 157: 507-516, 1993.

Lyles JM, Amin W, Bock E, Weill CL: Regulation of NCAM by growth factors in serum-free myotube cultures. J Neurosci Res, 34: 273-286, 1993.

Lyons GE, Moore R, Yahara O, Buckingham ME, Walsh FS: Expression of NCAM isoforms during skeletal myogenesis in the mouse embryo. Dev Dynam, 194: 94-104, 1992.

Marshall PA, Williams PE, Goldspink G: Accumulation of collagen and altered fiber-type ratios as indicators of abnormal muscle gene expression in the *mdx* dystrophic mouse. Muscle Nerve, 12: 528-537, 1989.

Mastaglia FL, Dawkins RL, Papadimitriou JM: Morphological changes in skeletal muscle after transplantation: A light and electron microscopic study of the initial phases of degeneration and regeneration. J Neurol Sci, 25: 227-247, 1975.

Matoba H, Sugiura T, Murakami N: Effect of thyroidectomy on histochemical properties of the extensor digitorum longus and soleus muscles in rats. J Physical Fitness Japan, 31: 189-195, 1982.

Matsumura K, Ervasti J, Ohlendieck K, Kahl SD, Campbell KP: Association of dystrophin-related protein with dystrophin-associated proteins in *mdx* mouse muscle. Nature, 360: 588-591, 1992a.

Matsumura K, Tome FMS, Collin H, Azibi K, Chaouch M, Kaplan JC, Fardeau M, Campbell KP: Deficiency of the 50K dystrophin-associated glycoprotein in severe childhood autosomal recessive muscular dystrophy. Nature, 359: 320-322, 1992b.

Mauro A: Satellite cells of skeletal muscle fibers. J Biophys Biochem Cytol, 9: 493-495, 1961.

McAllister RM, Ogilvie RW, Terjung RL: Functional and metabolic consequences of skeletal muscle remodeling in hypothyroidism. Am J Physiol, 260: E272-E279, 1991.

McGeachie JK, Grounds MD: Initiation and duration of muscle precursor replication after mild and severe injury to skeletal muscle of mice: An autoradiographic study. Cell Tissue Res, 248: 125-130, 1987.

Mege RM, Goudou D, Diaz C, Nicolet M, Garcia L, Geraud G, Rieger F: N-cadherin and N-CAM in myoblast fusion: compared localization and effect of blockade by peptides and antibodies. J Cell Sci, 103: 897-906, 1992.

Mesa LE, Dubrovsky AL, Corderi J, Marco P, Flores D: Steroids in Duchenni muscular dystophy - Deflazacort trial. Neuromusc Dis, 1: 261-266, 1991.

Mezzogiorno A, Coletta M, Zani BM, Cossu G, Molinaro M: Paracrine stimulation of senescent satellite cell proliferation by factors released by muscle or myotubes from young mice. Mech Ageing Dev: 70: 35-44, 1993.

Miller JB, Everitt EA, Smith TH, Block NE, Dominov JA: Cellular and molecular diversity in skeletal muscle development: News from in vitro and in vivo. BioEssays, 15: 191-196, 1993.

Mitchell CA, McGeachie JK, Grounds MD: Cellular differences in the

regeneration of murine skeletal muscle: a quantitative histological study in SJL/J and BALB/C mice. Cell Tissue Res, 269: 159-166, 1992.

Mizuno Y, Nonaka I, Hirai S, Ozawa E: Reciprocal expression of dystrophin and utrophin in muscles of Duchenne muscular dystrophy patients, female DMD-carriers and control subjects. J Neurol Sci, 119: 43-52, 1993.

Moore JW, Dionne C, Jaye M, Swain JL: The mRNAs encoding acidic FGF, basic FGF and FGF receptor are coordinately downregulated during myogenic differentiation. Develop, 111: 741-748, 1991.

Moore SE, Walsh FS: Specific regulation of N-CAM/D2-CAM cell adhesion molecule during skeletal muscle development. EMBO, 4: 623-630, 1985.

Moore SE, Walsh FS: The cell adhesion molecule M-cadherin is specifically expressed in developing and regenerating, but not denervated skeletal muscle. Develop, 117: 1409-1420, 1993.

Moss FP, Leblond CP: Satellite cells as the source of nuclei in muscles of growing rats. Anat Rec, 170: 421-436, 1971.

Muntoni F, Mateddu A, Marchei F, Clerk A, Serra G; Muscular weakness in the *mdx* mouse. J Neurol Sci, 120: 71-77, 1993.

Murphy LJ, Bell GI, Duckworth ML, Friesen HG: Identification, characterization, and regulation of a rat complementary deoxyribonucleic acid which encodes insulin-like growth factor-I. Endocrinol, 121: 684-691, 1987.

Nabeshima Y, Hanaoka K, Hayasaka M, Esumi E, Li S, Nonaka I, Nabeshima YI: Myogenin gene disruption results in perinatal lethality because of severe muscle defect. Nature, 364: 532-535, 1993.

Naidoo PR: EM investigation of myoblast origin in regenerating hamster skeletal muscle explants. J Struct Biol, 109: 160-167, 1992.

Neumeyer AM, DiGregorio DM, Brown RH: Arterial delivery of myoblasts to skeletal muscle. Neurol, 42: 2258-2262, 1992.

Nwoye L, Mommaerts FHM, Simpson DR, Seraydarian K, Marusich: Evidence for a direct action of thyroid hormone in specifying muscle properties. Am J Physiol, 242: R401-R408, 1982.

Ohlendieck K, Campbell KP: Dystrophin-associated proteins are greatly reduced in skeletal muscle from *mdx* mice. J Cell Biol, 115: 1685-1694, 1991.

Olson EN: Interplay between proliferation and differentiation with in the myogenic lineage. Dev Biol, 154: 261-272, 1992.

Olson EN, Brennan TJ, Chakraborty T, Cheng TC, Cserjesi P, Edmondson D, James G, Li L: Molecular control of myogenesis: antagonism between growth and differentiation. Molec Cell Biochem, 104: 7-13, 1991.

Olson EN, Sternberg W, Hu JS, Spizz G, Wilcox C: Regulation of myogenic differentiation by type ß transforming growth factor. J Cell Biol, 103: 1799-1805, 1986.

Olwin BB, Hauschka SD: Cell surface fibroblast growth factor and epidermal growth factor receptors are permanently lost during skeletal muscle terminal differentiation in culture. J Cell Biol, 107: 761-769, 1988.

Ontell M: Muscle satellite cells: A validated technique for light microscopic identification and a quantitative study of changes in their population following denervation. Anat Rec, 178: 211-228, 1974.

Ontell M: Morphological aspects of muscle fiber regeneration. Federation Proc, 45: 1461-1465, 1986.

Ontell M, Hughes D, Bourke D: Morphometric analysis of the developing mouse soleus muscle. Am J Anat, 181: 279-288, 1988.

Ontell M, Kozeka K: Organogenesis of the mouse extensor digitorum longus muscle: A quantitative study. Am J Anat, 171: 149-161. 1987.

Orimo S, Hiyamuta E, Arahata K, Sugita H: Analysis of inflammatory cells and complement C3 in bupivacine-induced myonecrosis. Muscle Nerve, 14: 515-520, 1991.

Papadimitriou JM, Robertson TA, Mitchell CA, Grounds MD: The process of new plasmalemma formation in focally injured skeletal muscle fibers. J Struct Biol, 103: 124-134, 1990.

Partridge TA: Pathophysiology of muscular dystrophy. Br J Hosp Med, 49: 26-36, 1993.

Partridge TA, Morgan JE, Coulton GR, Hoffman EP, Kunkel LM: Conversion of *mdx* myofibres from dystrophin-negative to -positive by injection of normal myoblasts. Nature, 337: 176-179, 1989.

Petrof BJ, Shrager JB, Stedman HH, Kelly AM, Sweeney HL: Dystrophin protects the sarcolemma from stresses developed during muscle contraction. Proc Natl Acad Sci, 90: 3710-3714, 1993.

Pette D, Staron RS: Cellular and molecular diversities of mammalian skeletal muscle fibers. Rev Physiol Biochem Pharmacol, 116: 2-76, 1990.

Pilarska M, Wrzosek A, Pikula S, Famulski KS: Thyroid hormones control lipid composition and membrane fluidity of skeletal muscle sarcolemma. Biochem Biophys Acta, 1068: 167-173, 1991.

Pin CL, Merrifield PA: Embryonic and fetal rat myoblasts express different phenotypes following differentiation *in vitro*. Dev Genet, 14: 356-368, 1993.

Pinney DF, de la Brousse FC, Emerson CP Jr: Molecular genetic basis of skeletal myogenic lineage determination and differentiation. In Genetics of Pattern Formation and Growth Control. Wiley-Liss, Inc., pp 65-89, 1990.

Pinney DF, Pearson-White SH, Konieczny SF, Latham KE, Emerson CP Jr.: Myogenic lineage determination and differentiation: evidence for a regulatory gene pathway. Cell, 53: 781-793, 1988.

Quinn LS, Nameroff M, Holtzer H: Age-dependent changes in myogenic precursor cell compartment sizes: Evidence for the existence of a stem cell. Exp Cell Res, 154: 65-82, 1984.

Reznik M: Origin of myoblasts during skeletal muscle regeneration. Lab Invest, 20: 353-363, 1969.

Roberts P, McGeachie JK, Grounds MD, Smith ER: Initiation and duration of myogenic precursor cell replication in transplants of intact skeletal muscles: An autoradiographic study in mice. Anat Rec, 224: 1-6, 1989.

Robertson TA, Grounds MD, Mitchell CA, Papadimitriou JM: Fusion between myogenic cells *in vivo*: An ultrastructural study in regenerating murine skeletal muscle. J Struct Biol, 105: 170-182, 1990.

Robertson TA, Grounds MD, Papadimitriou JM: Elucidation of aspects of murine skeletal muscle regeneration using local and whole body irradiation. J Anat, 181: 265-276, 1992.

Robertson TA, Maley MAL, Grounds MD, Papadimitriou JM: The role of macrophages in skeletal muscle regeneration with particular reference to chemotaxis. Exp Cell Res, 207: 321-331, 1993.

Rojas CV, Hoffman EP: Recent advances in dystrophin research. Curr Opin Neurobiol, 1: 420-429, 1991.

Rudnicki MA, Braun T, Hinuma S, Jaenisch R: Inactivation of MyoD in mice leads to upregulation of the myogenic HLH gene Myf-5 and results in apparently normal muscle development. Cell, 71: 383-390, 1992.

Rutishauser US: Neural cell adhesion molecule and polysialic acid. In McDonald JA, Mecham RP (eds): Receptors for Extracellular Matrix. Academic Press Inc, San Deigo, CA, pp 131-156, 1991.

Sadeh M: Effects of aging on skeletal muscle regeneration. J Neurol Sci, 87: 67-74, 1988.

Salviati G, Zeviani M, Betto R, Nacamulli D, Busnardo B: Effects of thyroid hormones on the biochemical specialization fo human muscle fibers. Muscle Nerve, 8: 363-371, 1985.

Schmalbruch H: The morphology of regeneration of skeletal muscle in the rat. Tissue Cell, 8: 673-692, 1976.

Schultz E, Albright DJ, Jaryszak DL, David TL: Survival of satellite cells in whole muscle transplants. Anat Rec, 222: 12-17, 1988.

Schweigerer L: Basic fibroblast growth factor: Properties and clinical implications. In Habenicht A (ed): Growth Factors, Differentiation Factors, and Cytokines. Springer-Verlag, pp 42-55, 1990.

Sheard PW, Duxson MJ, Harris AJ: Neuromuscular transmission to identified primary and secondary myotubes: A reevaluation of polyneuronal innervation patterns in rat embryos. Dev Biol, 148: 459-472, 1991.

Sicinski P, Geng Y, Ryder-Cook AS, Barnard EA, Darlison MG, Barnard PJ: The molecular basis of muscular dystrophy in the *mdx* mouse: a point mutation. Science, 244: 1578-1580, 1989.

Simonides WS, van Hardeveld C: The postnatal development of sarcoplasmic reticulum Ca^{2+} transport activity in skeletal muscle of the rat is critically dependent on thyroid hormone. Endo, 124: 1145-1153, 1989.

Smith TH, Block NE, Rhodes SJ, Konieczny SF, Miller JB: A unique pattern of expression of the four muscle regulatory factors proteins distinguishes somitic form embryonic, fetal and newborn mouse myogenic cells. Develop, 117: 1125-1133, 1993.

Snow MH: The effects of aging on satellite cells in skeletal muscles of mice and rats. Cell Tiss Res, 185: 399-408, 1977.

Snow MH: Satellite cell distribution within the soleus muscle of adult mouse. Anat Rec, 201: 463-369, 1981.

Sommerland H, Ullman M, Jennische E, Skottner A, Oldfors A: Muscle regeneration: The effect of hypophysectomy on cell proliferation and expression of insulin-like growth factor-I. Acta Neuropathol, 78: 264-269, 1989.

Stedman HH, Sweeney HL, Shrager JB, Maguire HC, Panettieri RA, Petrof B, Narusawa M, Leferovich JM, Sladky JT, Kelly AM: The *mdx* mouse diaphragm reproduces the degenerative changes of Duchenne muscular dystrophy. Nature, 352: 536-538, 1991.

Stockdale FE: Myogenic cell lineages. Dev Biol, 154: 284-298, 1992.

Stockdale FE, Miller JB, Feldman JL, Lamson G, Hager J: Myogenic cell lineages: Commitment and modulation during differentiation of avian muscle. In Kedes LH, Stockdale FE (eds): Cellular and Molecular Biology of Muscle Development. Alan R Liss, Inc., pp 3-13, 1989.

Stratford-Perricaudet LD, Makeh I, Perricaudet M, Briand P: Widespread long-term gene transfer to mouse skeletal muscles and heart. J Clin Invest, 90: 626-630, 1992.

Swash M, Schwartz M: Histologic and morphometric characteristics of normal muscle. In Swash M, Schwartz M (eds): Biopsy Pathology of Muscle. Chapman Hall, Ltd., London, pp 34-45, 1984.

Tanabe Y, Esaki K, Nomura T: Skeletal muscle pathology in X chromosome-linked muscular dystrophy (*mdx*) mouse. Acta Neuropathol (Berl), 69: 91-95, 1986.

Tapscott SJ, Davies RL, Thayer MJ, Cheng PF, Weintraub H, Lassar AB: MyoD1: A nuclear phosphoprotein requiring a *myc* homology region to convert fibroblasts to myoblasts. Science, 242: 405-411, 1988.

Thompson J, Moore SE, Walsh FS: Thyroid hormones regulate expression of the neural cell adhesion molecule in adult skeletal muscle. FEBS Lett, 219: 135-138, 1987.

Turner PR, Fong P, Denetclaw WF, Steinhardt RA: Increased calcium influx in dystrophic muscle. J Cell Biol, 115: 1710-1712, 1991.

Ullman M, Alameddine H, Skottner A, Oldfors A: Effects of growth hormone on skeletal muscle. II. Studies on regeneration and denervation in adult rats. Acta Physiol Scand, 135: 537-543, 1989.

Ullman M, Oldfors A: Effects of growth hormone on skeletal muscle. I. Studies on normal adult rats. Acta Physiol Scand, 135: 531-536, 1989.

van Heyningen HE; The initiation of thyroid function in the mouse. Endocrinol, 69: 720-727, 1961.

Watt DJ, Morgan JE, Clifford MA, Partridge TA: The movement of muscle precursor cells between adjacent regenerating muscles in the mouse. Anat Embryol, 175: 527-536, 1987.

Webster C, Pavlath GK, Parks DR, Walsh FS, Blau HM: Isolation of human myoblasts with the fluorescence-activated cell sorter. Exp Cell Res, 174: 252-265, 1988.

Webster G, Silberstein L, Hays AP et al.: Fast muscle fibers are preferentially affected in DMD. Cell, 52: 503-513, 1988.

Widner WW, Baldwin M, Terjung RL, Holloszy JO: Effects of thyroid hormone

administration on skeletal muscle mitochondria. Am J Physiol, 228: 1341-1345, 1975.

Widner WW, Holloszy JO: Response of mitochondria of different types of skeletal muscle to thyrotoxicosis. Am J Physiol, 232: C180-C184, 1977.

Wilson SJ, McEwan JC, Sheard PW, Harris AJ: Early stages of myogenesis in a large mammal: Formation of successive generations myotubes in sheep tibialis cranialis muscle. J Mus Res Cell Motil, 13: 535-550, 1992.

Zacharias JM, Anderson JE: Muscle regeneration after imposed injury is better in younger than older *mdx* dystrophic mice. J Neurol Sci, 104: 190-196, 1991.

APPENDIX A

WESTERN BLOTS

I. METHODS

Protein sample preparation

Samples of protein from adult TA muscles (crushed and uncrushed) were prepared by tissue homogenization in cold 2.5 mM Tris buffer (pH=7.2). Tissue was frozen at -70°C and lyophilized in order to obtain the precipitate. The precipitate was dissolved in double-distilled water and the protein concentration was determined by a BioRad protein assay using gammaglobulin as the standard. Each sample was diluted with the appropriate amount of sample buffer (2μg protein/1μL sample buffer) so the same concentration of protein was present in each sample. One hundred microliters of each sample (equivalent to 67μg of protein) was loaded per lane. Prestained broad range molecular weight standards (20μl) (Biorad) were loaded in the first lane, and 1μg of recombinant bFGF was loaded in the second lane.

Gel electrophoresis

Protein preparations were electrophoresed in a 7.5-15% gradient polyacrylamide gel for about 4 hours. The gel was run at 150 volts until the samples were past the stacking gel. The voltage was then raised to 250 volts.

Western blotting

Proteins were transferred from the gel to a nitrocellulose transfer membrane (PVDF filter, 0.45μM pore size, Immobilon-P, Millipore) overnight at 30 volts in cold Towbin buffer (pH=8.3). The next morning, the nitrocellulose membrane was removed from the buffer and rinsed in a 5% milk powder blocking solution for 30 minutes. The primary antibodies (combined anti-NCAM and anti-bFGF) were added to primary diluent (1:500) (see section 4.6.1) and incubated with the membrane for 2 and a half hours. Membranes were rinsed in PBS for 30 mins, the secondary antibodies (anti-mouse HRP and anti-rabbit HRP, Amersham) were added to the solution (1:300) and incubated with the membrane for one and a half hours. The membrane was again rinsed in PBS for 30 mins. A DAB kit (rinsing for 25mins) was used to visualize the proteins linked to HRP. Blots were then examined by densitometry.

Densitometry

The density of staining in dried blots was measured using the Java Program (Jandel Scientific, Corte Madera, CA) and an optical density calibration strip (Kodak). Data was collected in spread sheet, translated into EXCEL 4.2 (Microsoft), plotted against pixel number in the scan of linear intensity (1-260 pixels) and printed using Wordperfect graphics. No statistics were attempted since only 4 blots were run, with varying

amounts of success.

II. RESULTS AND DISCUSSION

Blots using protein samples from protocol 4 (restoration of euthyroid state) were the only ones analyzed.

NCAM: (Figure A): Bands can be observed at approximately 190, 145, 125, and 115kD. Keeping in mind that control untreated (top plot) had twice as much protein loaded in the gel, in general all of the bands were of similar magnitude, except for the 125kD band, which is absent in control mice treated with PTU and left to recover for 2 weeks before crush-injury (middle plot).

A 140kD form of NCAM is predominantly associated with myoblasts, while a 125kD form is predominantly associated with newly formed myotubes and myofibers (Covault et al., 1986). Thus, it appears that fewer new myotubes are present in control treated TA, left to recover thyroid status for 2 weeks after treatment. However, the amount of NCAM associated with myoblasts (125kD) appears approximately the same in all plots. These NCAM results suggest that the control mice have mainly recovered from hypothyrodism.

bFGF: (Figure B): It appears that there are three bands at approximately 30, 28, and 26kD. The higher molecular weight bands are more predominant in *mdx* untreated (third plot) than control untreated (top plot). The *mdx* PTU-treated muscles at 2 weeks after removal of PTU (bottom plot) appear to have less total bFGF than untreated TA (third plot). The control muscles left to recover from PTU-treatment for 2 weeks (second plot) appear to have more high molecular weight bFGF than untreated controls (top plot).

In the hypothyroid heart and skeletal muscle, high molecular weight forms of bFGF are present compared to euthyroid controls (Liu et al., 1993). This appears to be the case in the control muscles that were treated and then untreated for 2 weeks (second plot). This suggests that the control muscles have not completely regained a euthyroid state. However, *mdx* TA (treated for 8 weeks and then untreated for 2 weeks) does not appear to have more high molecular weight bFGF compared to euthyroid controls, and thus must be at least partially recovered.

It is recognized that these densitometry plots include very few muscle samples (a maximum of 2 muscles per group). However, results do suggest that a PTU-treated animals, at least partially regained thyroid function. Also, the process of learning this technique were valuable to the investigator.

TABLE A:

Densitometry plots of NCAM protein amount showing pixel number (1-260) on the x-axis and optical density (OD) on the y-axis. Molecular weight markers are labelled in the top plot and indicate a gradient gel

Top plot: Plot of NCAM protein amount in control untreated TA. Twice as much protein was loaded in the gel lane for this sample compared to the other two samples (middle and bottom plots).

Middle plot: Plot of NCAM protein amount in control TA, PTU- treated for 8 weeks and then left to recover thyroid function for 2 weeks.

Bottom plot: Plot of NCAM protein amount in *mdx* untreated TA.

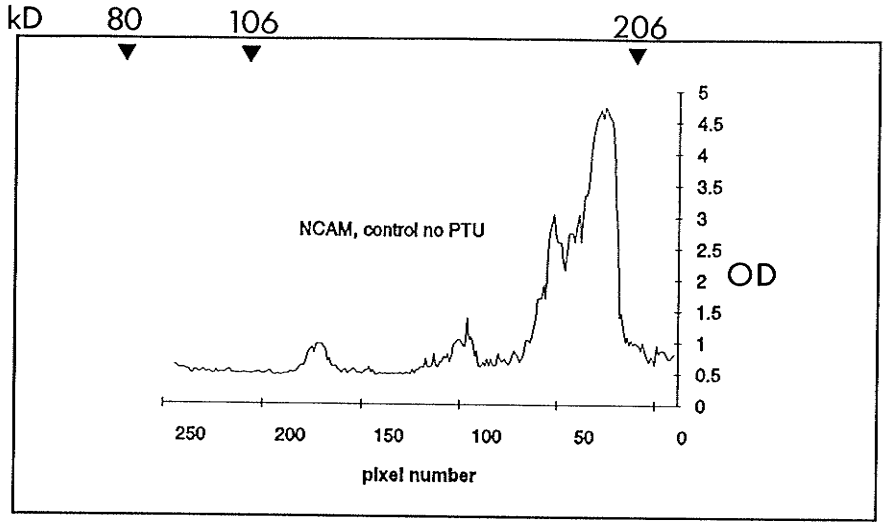
kD
80
106
206
NCAM, control no PTU
OD
5
4.5
4
3.5
3
2.5
2
1.5
1
0.5
0
250
200
150
100
50
0
pixel number

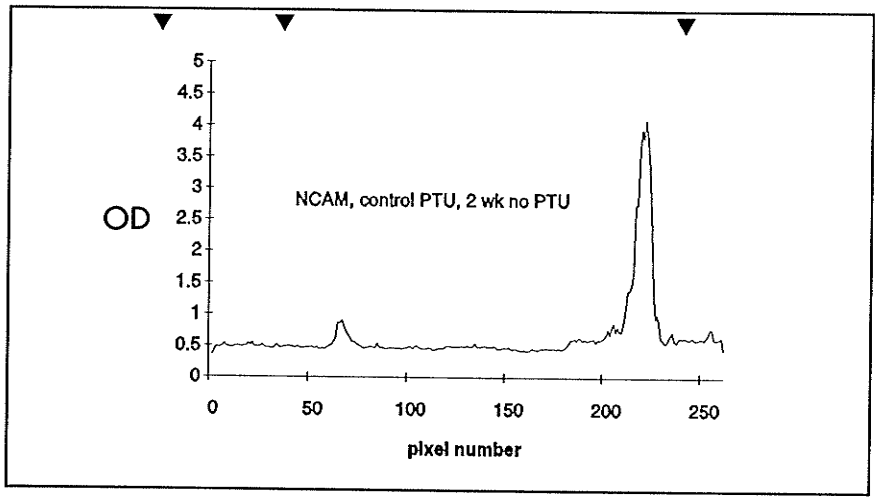
OD
NCAM, control PTU, 2 wk no PTU
5
4.5
4
3.5
3
2.5
2
1.5
1
0.5
0
0
50
100
150
200
250
pixel number

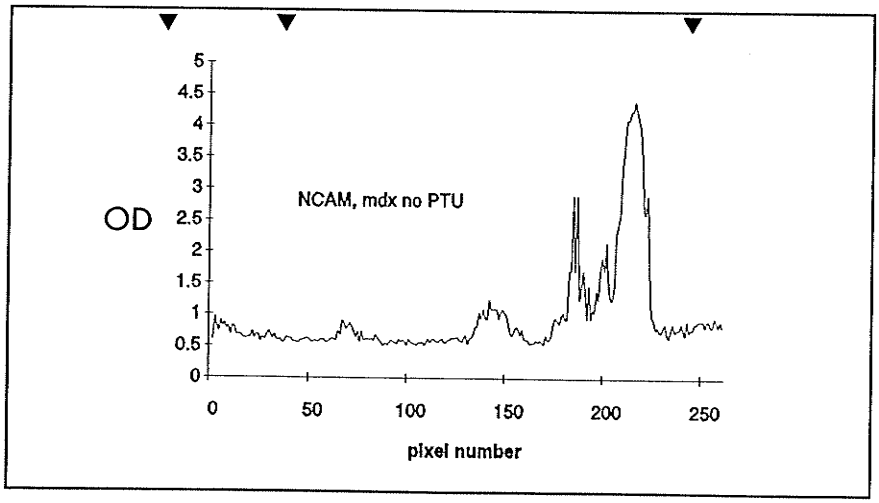
OD
NCAM, mdx no PTU
5
4.5
4
3.5
3
2.5
2
1.5
1
0.5
0
0
50
100
150
200
250
pixel number

TABLE B:

Densitometry plots of bFGF protein amount showing pixel number (1-260) on the x-axis and optical density (OD) on the y-axis. Molecular weight markers are labelled in the top plot and indicate a gradient gel.

Top plot: Plot of bFGF protein amount in control untreated TA.

Second plot: Plot of bFGF protein amount in control TA, PTU- treated for 8 weeks and then left to recover thyroid function for 2 weeks.

Third plot: Plot of bFGF protein amount in *mdx* untreated TA.

Bottom plot: Plot of bFGF protein amount in *mdx* TA, PTU-treated for 8 weeks and then left to recover thyroid function for 2 weeks.

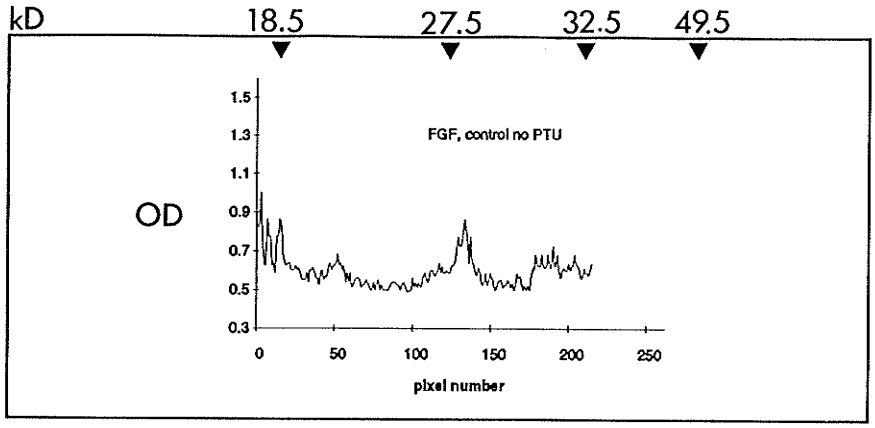
kD
18.5
27.5
32.5
49.5
OD
FGF, control no PTU
1.5
1.3
1.1
0.9
0.7
0.5
0.3
0
50
100
150
200
250
pixel number

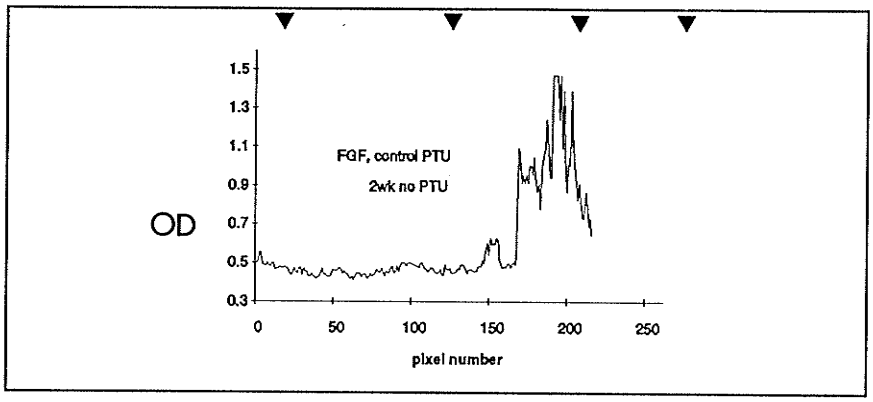
OD
FGF, control PTU
2wk no PTU
1.5
1.3
1.1
0.9
0.7
0.5
0.3
0
50
100
150
200
250
pixel number

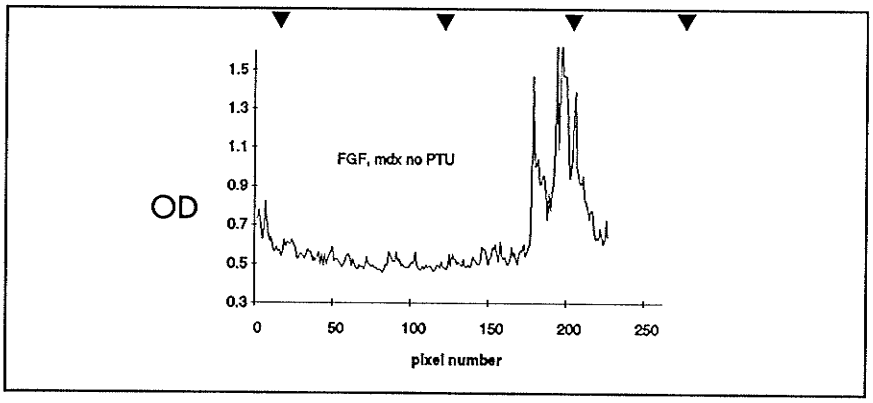
OD
FGF, mdx no PTU
1.5
1.3
1.1
0.9
0.7
0.5
0.3
0
50
100
150
200
250
pixel number

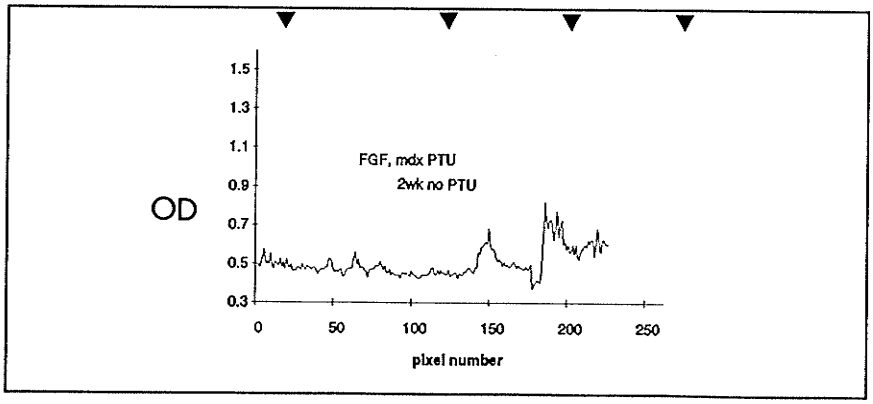
OD
FGF, mdx PTU
2wk no PTU
1.5
1.3
1.1
0.9
0.7
0.5
0.3
0
50
100
150
200
250
pixel number

APPENDIX B

After dystrophic damage, the limb muscles of the mdx mouse recover very effectively compared to muscles in Duchenne muscular dystrophy (DMD) patients. Since thyroid hormone is required for muscle development and integrity, we examined whether a deficiency of the hormone, induced by 0.05% propylthiouracil (PTU) in drinking water over 8 weeks, would be deleterious to the myogenesis and muscle repair in control and mdx mice. Measured metabolic and growth parameters confirmed hypothyroidism in PTU-treated mice. Histological and morphometric techniques were used to study myogenesis and the repair of the tibialis anterior muscle (TA) after crush injury in mdx mice and their nondystrophic controls (C57B1/10ScSn). After 8 weeks, PTU-treated TA from mdx mice had larger crush sites and lower myotube density than TA in untreated mdx mice. In unoperated mdx TA, there was a larger proportionate area of active dystrophy and smaller fiber diameter in PTU-treated than in untreated mdx TA, which suggested that PTU increased the activity of dystrophy as well. In contrast, in control TA neither the regeneration of myotubes or fiber diameter were affected significantly by PTU. Therefore, these results suggest that mdx muscle regeneration is more affected by hypothyroidism than normal muscle repair. This may be due to the larger pool of muscle precursors in mdx than control muscle, and a possible impairment of precursor cell proliferation or fusion during myotube formation.

Key words: hypothyroid • mdx • dystrophy • muscle regeneration • bFGF • NCAM

MUSCLE & NERVE 17:000–000 1994

THE EFFECTS OF ALTERED METABOLISM (HYPOTHYROIDISM) ON MUSCLE REPAIR IN THE mdx DYSTROPHIC MOUSE

L. M. McINTOSH, MD, A.N. PERNITSKY, MD, and J.E. ANDERSON, MD

The mdx mouse is genetically similar to humans with Duchenne muscular dystrophy (DMD) in that muscles in both lack dystrophin,[18] which is crucial to muscle integrity. However, mdx limb muscles respond to muscular dystrophy with an active myoproliferative response[1,16] which appears to stabilize the number of fibers in limb muscles.[1,24]

Although the level of active dystrophy and repair in mdx limb[1–3,12,21] and cardiac[3,8] muscles gradually decreases with age, it is not precisely known what permits dystrophin-deficient mdx muscle to respond so well to dystrophy. Some small caliber myofibers, such as extraocular fibers, are spared from DMD and mdx dystrophy,[21] possibly due to substitution by utrophin.[24] However, the absence of utrophin from large mdx limb muscles, except at neuromuscular junctions,[24] does not account for the successful recovery of limb muscles from dystrophy, in contrast to the progression of DMD.

Thyroid hormone is known to be an important stimulus to metabolic processes and an absolute requirement for muscle cell development and maturation.[11,27] Both fiber size and myosin heavy chain (MHC) expression are under the influence of thyroid status,[19,20,23] as is growth.[11] Recent work in this laboratory has shown that hyperthyroidism in mdx mice appears to increase the amount of dystrophic damage in slow limb muscles and in the

From the Department of Anatomy, University of Manitoba, Winnipeg, Manitoba, Canada.

Acknowledgments: This work was supported by a grant from the Muscular Dystrophy Association of Canada (J.E.A.). L.M. was the recipient of a Thyroid Foundation Summer Fellowship (1992) and a Medical Research Council of Canada Studentship. A.P. was supported by a University of Manitoba Graduate Fellowship. The authors also thank Mr. Roy Simpson for expert photographic assistance.

Address reprint requests to Dr. Judy E. Anderson, Department of Anatomy, University of Manitoba, 730 William Avenue, Winnipeg Manitoba, R3E 0W3, Canada.

Accepted for publication November 1, 1993.

CCC 0148-639X/94/000000-00

(272) Art 11

heart.[7] This was thought to occur in a combined response[7] to an increased expression of fast MHC isoforms in slow-twitch muscles[19] and increased cardiac work during hyperthyroidism.[11] The increase in dystrophic lesions was also detected by basic fibroblast growth factor (bFGF) immunolocalization, which was shown previously to highlight degenerating regions in mdx[3] and human dystrophic muscle.[6]

The present study attempted to explore a second method of altering the mdx phenotype to resemble DMD: the effect of a reduced metabolic rate (induced by hypothyroidism) on myogenesis during mdx mouse muscular dystrophy was examined. As well, we tested whether hypothyroidism had any important effect on muscle repair synchronized by crush injury,[25] which might be more obvious than a gradual perturbation of mdx dystrophy.

MATERIALS AND METHODS

Experimental Animals. mdx dystrophic mice and normal age-matched control mice (C57B1/10ScSn) were bred by brother–sister matings from original breeding pairs[9] and housed according to the Canadian Council on Animal Care in the University of Manitoba Animal Care Facility. Hypothyroidism was induced in 9 control (7 males, 2 females) and 8 mdx dystrophic mice (6 males, 2 females) by treatment with 0.05% propylthiouracil (PTU) in drinking water ad libitum.[11] The mice were treated for the 8 weeks after the onset of dystrophy at 3 weeks of age. Age-matched littermates, 8 controls (all male) and nine mdx mice (3 males, 6 females), were untreated for the same period. Mice were weighed and checked daily during the 8 weeks to monitor any side effects of treatment. Daily water intake was also measured and calculated per mouse.

After 8 weeks of treatment (11 weeks of age), mice were coded and anesthetized (ketamine:rompun 1:1, 0.01 cc per 10 g body weight). Five minutes later, the breathing movements over two periods of 30 s were observed in a double-blind fashion in order to estimate the respiratory rate. Mice were then subjected to a crush injury[25] of the right tibialis anterior muscle (TA). Briefly, skin and fascia were opened over the TA. The belly of TA was gently separated from the tibia and a serrated hemostat was placed around the muscle belly just below the proximal attachment of TA. The clamp was closed (locked to one notch) around the muscle for 5 s and released. The pressure applied by the clamp was therefore consistent, and was given by one investigator. This procedure did not disrupt muscle continuity. Skin was closed with four 5-0 silk sutures and the animals were left to recover.

Four days later, mice were again anesthetized in random coded order, and blood was drawn from the heart for commercial assay (Cadham Provincial Laboratory, Winnipeg, MB) of thyroid stimulating hormone (TSH). The TA muscles from both hindlimbs were bisected longitudinally using a razor blade (through the center of the crush site on the right limb), and rapidly removed from the limb. Muscle halves were oriented in Tissue-Tek OCT compound and frozen in isopentane (−50°C) as left–right pairs for longitudinal cryosectioning (8 μm). Sections were stained with hematoxylin and eosin (H&E). The gastrocnemius and soleus muscles were also removed from the limbs and weighed.

Morphometry. On coded H&E sections, various measures were used to assess the extent of regeneration and dystrophy in defined longitudinal zones of the TA, prior to decoding the sections. In the mdx unoperated (left) TA, the total area of active dystrophy (defined as all degenerating and inflammatory areas in a TA as a proportion of the total muscle area) and the number of dystrophic foci (degenerating and inflammatory areas as a proportion of the total muscle area) were measured. The Sigma Scan program (Jandel Scientific, CA) and a calibrated computerized graphics tablet were used to measure the areas. In the unoperated (left) TA, the centronucleation index (CNI, defined as the number of cells with central nuclei as a proportion of the total number of fibers) was determined in mdx muscles, as a measure of accumulated fiber injury and repair during dystrophy. The total number of central and peripheral nuclei, and the ratio of central-to-peripheral nuclei (CN:PN) in two areas of the unoperated TA were also determined. An Olympus microscope was used to observe and photograph selected fields.

In the operated (right) TA, the crush site, adjacent muscle, and surviving muscle were analyzed in a systematic manner (after Mitchell et al.)[26] at 200× by their distance (preset multiples of one, 200× field = 4.4×10^5 μm^2) from the center of the necrotic crush zone, which was acellular (Fig. 1). Two fields were counted within the crush area in each operated muscle, four in the adjacent area (3 proximal, 1 distal to crush), and three fields in the region of distant surviving muscle (2 proximal, 1 distal to crush). The adjacent and surviving zones were therefore determined by distance from the

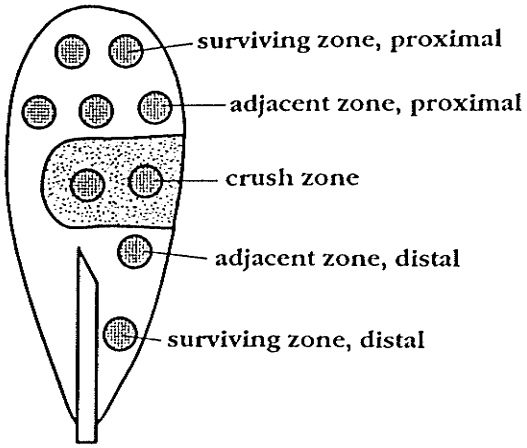

FIGURE 1. This diagram indicates the zones and fields of a typical longitudinal section of the tibialis anterior muscle, taken between proximal origin (top) and distal tendon (bottom). The fields were assessed during morphometric study of myotubes and nucleation. The center of the crushed area (necrotic and acellular) was established under the microscope a 100×, and two 200× fields were located one field apart and horizontally within the crush zone. Fields in the adjacent zone (three proximal, one distal) were sampled at a distance of one field diameter from the crush fields. Two fields of fibers in the surviving zone were sampled one field proximal to the proximal adjacent zone, and one additional field was sampled 1.5 field diameters distal to the distal adjacent zone. These criteria were strictly adhered to, such that zones were determined by the *distance* from the crush, not by the particular cell types prevalent in a region.

crush and not by the cells prevalent in those regions. If there were more than five surviving fibers in a field of "adjacent zone," as defined above, that field was not counted. For statistical analysis, the four adjacent zone fields were pooled, as there was no proximal–distal difference between fields in that zone. However, the distal and proximal fields of the surviving zone were analyzed separately.

The orientation of sections through the crush and adjacent zones (with longitudinally aligned myotubes) was carefully made using phase contrast and correction of block placement during sectioning. Since the TA is a pennate muscle with a central tendon, only fibers on one side of the tendon can be in a longitudinal plane, while fibers on the opposite side of the central tendon will be oblique or cross-sectioned. The fields assessed for morphometry were always in the longitudinally sectioned aspect of the TA.

The numbers of central and peripheral muscle nuclei were counted in each zone of the operated TA, and the CN:PN ratio was determined within the same fields. The number of small myotubes in each field (at 200×) and zone was also counted. Using Sigma Scan and a camera lucida (100×), the area of the necrotic acellular crush zone was outlined and measured.

Fiber diameter was measured from the unoperated TA and from the distal surviving zone of operated TA in both control and mdx mice, again using the calibrated graphics tablet and camera lucida at 100×. At least 100 fibers were sampled from each section along chords perpendicular to the longitudinal axis of each muscle as previously reported for fiber area.[1] Measurements at the smallest diameter of each fiber were recorded. The distribution of fiber diameter was also plotted for each group.

Statistical Analysis. Data (mean ± SEM) for each muscle ($n \geq 6$–7) were determined and those means were grouped and analyzed using a two-way ANOVA. Individual groups were compared using Duncan's multiple range test post hoc where appropriate. A repeated measures ANOVA was used to compare fiber diameter, CN:PN, and CNI between unoperated (left) and operated (right) TA in the four groups. Fiber diameter distributions were compared using chi-square statistics. In all cases, a probability of $P < 0.05$ was used to reject the null hypothesis.

RESULTS

Metabolic and Growth Parameters (Table 1). In order to confirm hypothyroid status, a number of metabolic and growth parameters were measured (water intake, TSH, respiratory rate, body weight gain, muscle weight). These parameters all indicated that hypothyroidism was achieved by treatment with 0.05% PTU for 8 weeks. Increased TSH ($P < 0.01$), lower respiratory rate ($P < 0.01$), and lower water intake ($P < 0.001$) were noted in PTU-treated mice. After only the third week of PTU, the age-related increase in body weight was significantly decreased ($P < 0.05$, ANOVA) compared to normal growth without PTU, especially in mdx mice. In agreement with previous reports,[1,2] mdx mice weighed significantly ($P < 0.02$) ore than their age-matched controls. Weights of the soleus and gastrocnemius muscles were not affected by 8 weeks of PTU treatment, and all mdx muscles were heavier ($P < 0.05$) than muscles in controls, in parallel with their greater body weight. After decoding observations made at the time of tissue preparation, it was noted that the crushed TA from control mice were clearly more hemorrhagic than in mdx untreated TA. In addition, crush sites of mdx PTU-treated muscles were also hemorrhagic, and similar to TA of control mice.

Table 1. Metabolic and growth parameters (body weight gain, final water intake, respiratory rate, thyroid stimulating hormone [TSH] level, and muscle weight) in control and mdx groups with and without 8 weeks treatment with PTU.

	Control untreated	Control PTU-treated	mdx untreated	mdx PTU-treated
Weight gain (%)†	265 ± 12	247 ± 9.2*	302 ± 16	269 ± 5.6*
Water intake (mL/wk)	48.3	35.3*	44.0	35.0*
Respiratory rate (no./min)	171.0 ± 7.9	148.5 ± 3.8*	175.5 ± 2.9	157.5 ± 7.9*
TSH (mU/L)	0.042 ± 0.007	0.080 ± 0.012*	0.030 ± 0.007	0.055 ± 0.03*‡
Muscle weight (mg)				
Soleus†	8.7 ± 0.7	8.2 ± 0.5	10.7 ± 0.2	11.5 ± 0.5
Gastrocnemius†	149.7 ± 2.9	148.5 ± 4.9	155.1 ± 4.4	167.8 ± 5.0

Data are mean ± SEM.
**Indicates significant PTU effect.*
†Indicates significant strain effect (control versus mdx).
‡Indicates significant interaction of strain × treatment.

During handling, the treated mice were noted to be less active than untreated mice. Treated mdx mice did not extend the hindlimb toes, a normal action when slightly lifted above a surface, suggesting some clinical signs of muscle weakness during treatment.

Histology. Unoperated control and mdx muscles were characteristic of previous reports (e.g., see Anderson et al.,[1] Coulton et al.,[10] Dangain et al.[12]). Control muscle fibers exhibited peripheral myonuclei (Fig. 2A). mdx muscle presented foci of active dystrophy, many regenerated fibers, and intact fibers with peripheral nuclei (Fig. 2B). Grossly, no large differences were noted between treated and untreated unoperated muscles from mdx or control mice, in that coded slides were not separable into treatment groups during blinded observations.

Operated control and mdx muscle 4 days after muscle injury showed zones (Fig. 1) typical of crushed muscle.[25,26] Figure 2C–F show areas of necrotic tissue at the crush site, the adjacent region of inflammatory and mononuclear cells plus small regenerating myotubes, and the distant area of surviving muscle fibers and a few myotubes. Double-blind observations by two observers were unable to find differences between slides from untreated (Fig. 2C) and treated (Fig. 2E) control animals. In contrast, the same observers were able to detect two clearly different groups of muscles in the mdx group. After decoding, it was determined that the untreated mdx TA had consistently more myotubes extending further into the crush zone and a smaller crush site (Fig. 2D) than the PTU-treated mdx TA (Fig. 2F).

Myotube formation in the crushed TA of control untreated mice was typical of earlier reports of crush injured muscle.[16,25,26] Short chains of 5–7 nuclei in longitudinal section were found within control myotubes located in the zone adjacent to the crush site (Fig. 3A and C). In untreated mdx TA, myotubes appeared longer and contained many more nuclei (Fig. 3B). PTU-treated mdx TA had fewer and apparently shorter myotubes in the same adjacent zone (Fig. 3D). As well, there were more control fibers with central nuclei in the distal surviving zone (Fig. 3E) than in the contralateral unoperated control TA. In mdx TA (Fig. 3F) surviving fibers appeared to have many central nuclei compared to their contralateral unoperated TA.

Morphometry. *Unoperated TA* (Table 2). The general character of muscle repair from dystrophy was worsened by the PTU treatment. The area of active dystrophy in treated mdx TA was significantly greater ($P < 0.05$) than in untreated mdx TA. However, there was no change in the number of foci of active injury after treatment.

The centronucleation index was not changed by PTU treatment, nor was the CN:PN ratio, although CN:PN, CNI, and the total number of nuclei all detected the effect of dystrophy in muscle ($P < 0.001$). Interestingly, there was a significant correlation ($r = 0.725$, $P = 0.005$, $df = 11$) between body weight and CNI in untreated mdx mice. This correlation was not changed by PTU treatment. Mean fiber diameter in unoperated TA was significantly smaller ($P < 0.01$) in PTU-treated mdx muscle than in untreated mdx TA. The mdx TA also had a larger mean fiber diameter than control TA ($P < 0.01$). PTU treatment did not affect mean fiber diameter or distribution (Fig. 4) in control muscle. However, mdx myofiber diameter distribution was significantly left-shifted with PTU treatment, indicating greater numbers of small myotubes had regenerated from dystrophic injury during the treatment period.

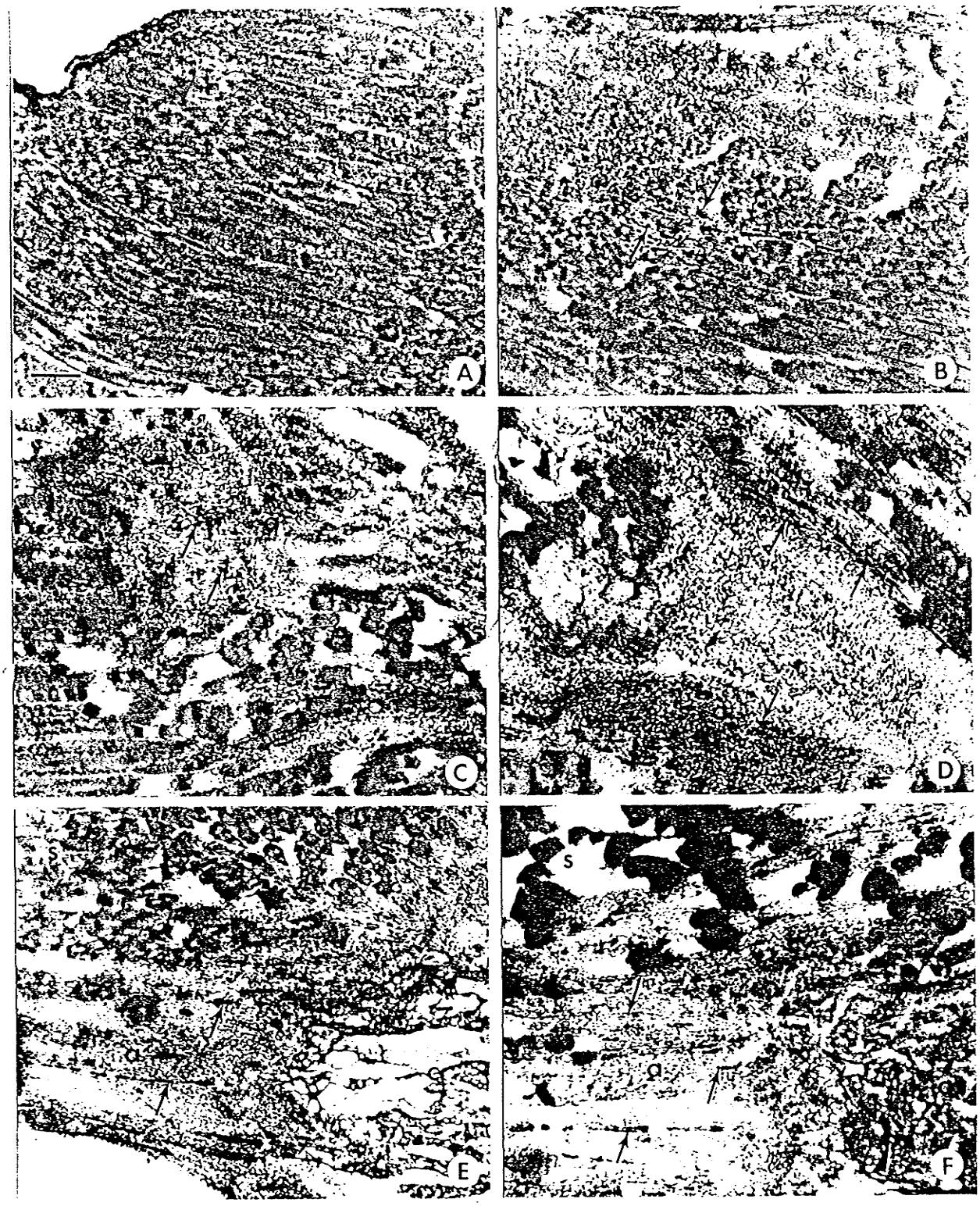

FIGURE 2. Low power micrographs of longitudinal sections of control (A, C, E) and mdx (B, D, F) TA in untreated (A–D) and PTU-treated (E, F) mice. (×4z, bar = 200 μm). While sections may not appear completely longitudinal due to the pennate architecture of TA (see Methods), all myotube and nucleation counts were made only on the side of the tendon where fibers were in longitudinal section. (A) Unoperated, untreated control TA. (B) Unoperated, untreated mdx muscle with centrally nucleated fibers, an area of active dystrophy (asterisk), and an area of recent regeneration containing small myotubes (arrows). In panels (C)–(F), areas of necrosis in the crush site (c), the adjacent zone (a) containing myotubes (arrows), and inflammatory and mononuclear cells, and the distal surviving areas (s) are indicated in the operated TA. (C) Control untreated TA contains a typical necrotic area and short myotubes lining up in the adjacent zone. (D) mdx untreated TA with no obvious necrotic crush area. Many long myotubes are lined up in the adjacent zone. (E) Control PTU-treated TA has a large crush site compared to panel (C). (F) mdx PTU-treated TA also shows a larger area of necrosis in crush zone than in panel D, and an area of calcification (arrowhead) is present. Fewer myotubes extend into the adjacent zone than in untreated mdx operated TA (D).

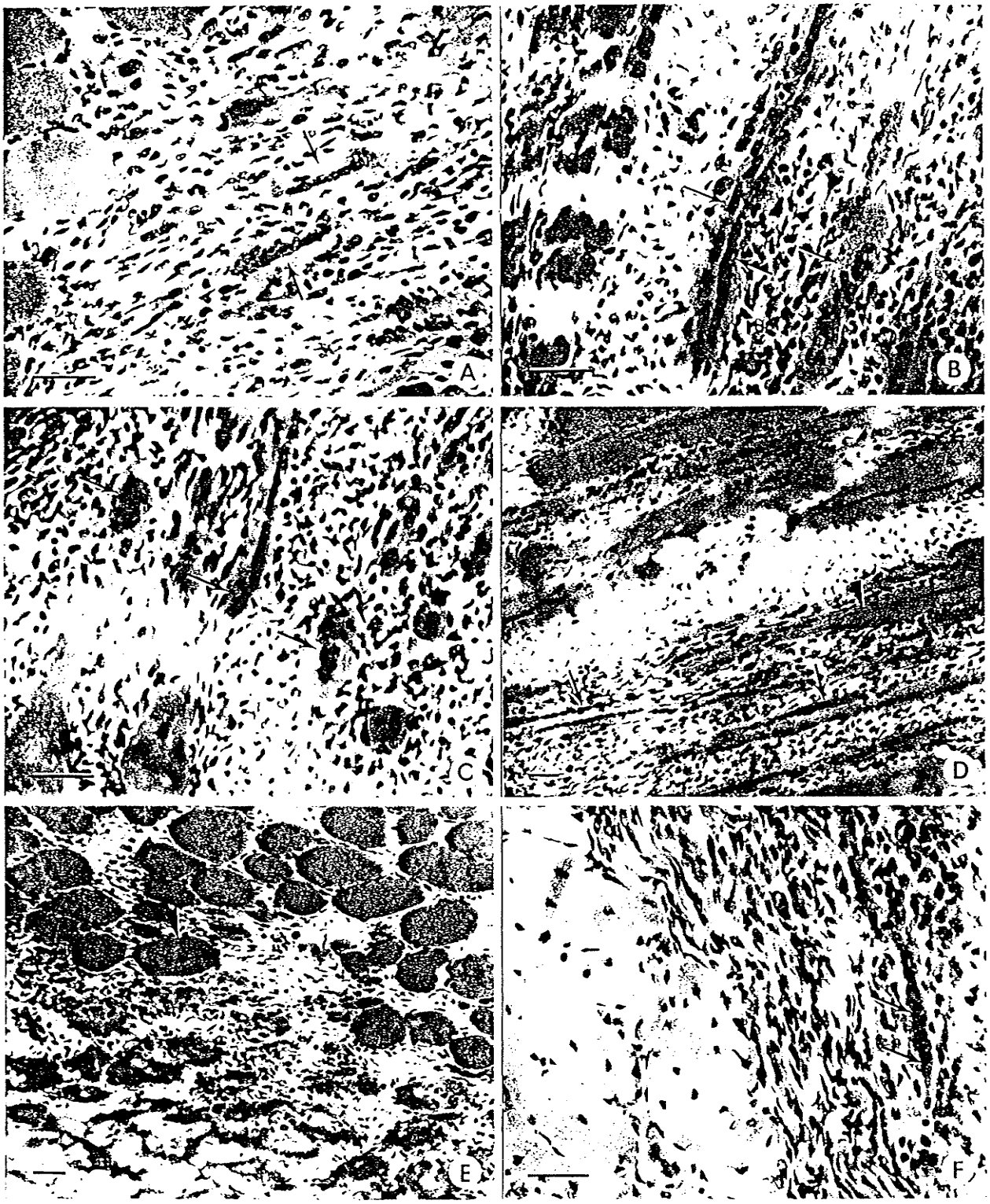

FIGURE 3. Micrographs of longitudinal sections of operated control (A, C, E) and mdx (B, D, F) TA from untreated (A, B) and PTU-treated (C–F) mice. (A, B, C, F: × 210; (D, E: ×105; bar = 50 μm). All myotubes are in longitudinal sections. (A)–(D) show operated TA in the adjacent areas of untreated and treated TA from control and mdx mice. (A) Control untreated muscle 4 days after crush injury shows myotubes containing chains of 5–7 nuclei (arrows). (B) mdx untreated muscle with myotubes that appear (arrows) much longer than in panel (A). (C) Control PTU-treated muscle exhibiting short–medium length myotubes (arrows) in the adjacent zone. (D) mdx PTU-treated TA demonstrates very long myotubes (arrows) lining up parallel with a few surviving fibers (E) And (F) show operated control and mdx surviving areas in PTU-treated TA. (E) The surviving fibers in control TA show mainly peripherally nucleated fibers, but one fiber is clearly centrally nucleated (arrowhead). CNI in surviving fields of operated muscle was typically significantly greater than in the contralateral unoperated control muscle. (F) The distal surviving zone of mdx TA shows more central nuclei in mature fibers close to the adjacent zone than typical in unoperated contralateral mdx TA.

Table 2. Muscle histology parameters (active dystrophy, dystrophic foci, CN:PN ratio, centronucleation index [CNI], total nuclei per field, and fiber diameter) in unoperated tibialis anterior with or without 8-week (control and mdx) PTU treatment.

	Control untreated	Control PTU-treated	mdx untreated	mdx PTU-treated
Active dystrophy (prop. area)	–	–	0.04 ± 0.01	0.09 ± 0.02*
Dystrophic foci (no./μm²)	–	–	1.73 ± 0.42	2.23 ± 0.36
CN:PN ratio†	0.03 ± 0.02	0.05 ± 0.02	1.38 ± 0.10	1.34 ± 0.08
CNI	–	–	0.79 ± 0.02	0.80 ± 0.016
Nuclei field				
Central†	6 ± 3	10 ± 5	209 ± 12	197 ± 12
Peripheral†	262 ± 22	230 ± 15	155 ± 9	151 ± 10
Fiber diameter (μm)†	47.1 ± 0.7	48.4 ± 0.8	50.7 ± 0.9	46.3 ± 0.8*

*Indicates significant PTU effect.
†Indicates significant strain effect.

Operated TA (Table 3): The size of the necrotic crush zone was not different between control and mdx TA. However, the crush zone was increased in area in PTU-treated mdx TA (significant interaction by ANOVA, $P < 0.05$). More myotubes (ANOVA, $P < 0.001$) were observed in mdx crush-injured TA than in control TA, regardless of treatment or zone, 4 days after injury. In general, PTU treatment seemed to reduce the number of myotubes in mdx TA, although changes were only significant in the surviving zone.

The CN:PN ratio in all zones (except for the distal surviving zone) of operated mdx muscles was significantly higher ($P < 0.001$) than in control operated TA. CN:PN was also higher in the distal surviving zones than in the unoperated TA for all groups ($P < 0.001$), suggesting that injury affected the nuclear position in distant fiber segments. The CN:PN in distal surviving muscle was also greater ($P < 0.001$) than in the proximal surviving zone (Fig. 1, Table 3).

DISCUSSION

In this study, the phenotype of mdx dystrophy in

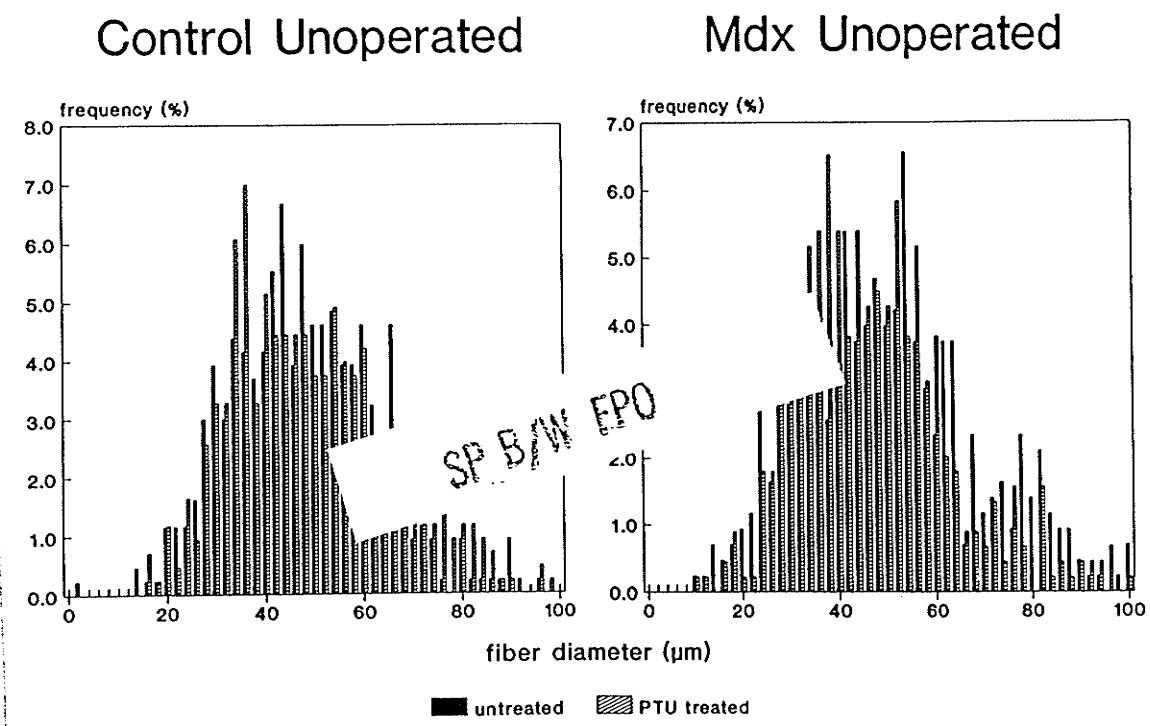

FIGURE 4. Graphs representing the distribution of fiber diameter (μm) plotted as frequency (%) in the sample population from untreated (black bars) and PTU-treated (shaded bars) mice. While fiber distribution in PTU treatment did not shift the distribution in unoperated control TA (left panel), the fiber diameter distribution of PTU-treated mdx TA was significantly left-shifted (toward smaller diameter, $P < 0.01$) from the distribution of untreated mdx TA fiber diameters. Fibers (427–447 were measured for each group) were evenly sampled from all animals within each group.

Table 3. Muscle histology parameters (area of crush, CN:PN ratio, myotube density, and fiber diameter) in operated tibialis anterior with or without 8-week (control and mdx) PTU treatment.

	Control untreated	Control PTU-treated	mdx untreated	mdx PTU-treated
Area of crush ($\mu m \times 10^{-4}$)	7.9 ± 0.95	5.6 ± 1.3	5.4 ± 1.5‡	7.9 ± 1.4‡
CN:PN ratio				
Adjacent zone†	3.4 ± 1.1	3.1 ± 0.88	26.3 ± 12.1	39.6 ± 12.9
Surviving zone				
Proximal†	0.04 ± 0.2	0.1 ± 0.1	4.2 ± 0.6	6.1 ± 1.6
Distal§	4.7 ± 8.5	24.9 ± 13.7	49.5 ± 23.2	56.2 ± 32.6
Myotube density				
Crush zone	3.8 ± 1.8	4.1 ± 2.2	6.2 ± 2.5	4.9 ± 1.9
Adjacent zone†	15.7 ± 4.9	19.2 ± 1.9	31.8 ± 5.1	27.0 ± 3.9
Surviving zone†	1.0 ± 0.6	1.6 ± 0.8	5.8 ± 2.2	2.8 ± 0.9‡

Data are mean ± SEM.
**Indicates significant PTU effect.*
†Indicates significant strain effect.
‡Indicates significant interaction of strain × treatment or age × treatment.
§Indicates significant difference from proximal surviving zone.

hypothyroidism was shifted toward that of DMD, since the dystrophic changes during treatment were more severe than in untreated mdx littermates. However, the change in mdx dystrophy was not as marked as the perturbation by hyperthyroidism which was recently reported by this laboratory.[7] In addition to the effects on dystrophy, the extent of mdx muscle regeneration after crush injury appeared to be delayed by hypothyroidism. The hypothyroid state was confirmed in mice treated for 8 weeks with PTU as described, according to TSH level, growth parameters, and metabolic measurements (water consumption, respiratory rate).

The effects of hypothyroidism on mdx dystrophy were evidenced by an increase in the proportionate area of TA occupied by typical active dystrophy and segmental damage,[1,8,12] CNI was significantly correlated to body weight in all mdx animals, but was not changed by PTU treatment, possibly as mdx TA would have a near-maximal CNI by 11 weeks of age.[21] However, the same absence of change in CNI was seen after PTU treatment for only 4 weeks, suggesting that CNI (as a ratio of fibers) serves only as rough index of accumulated injury and recovery, since the detailed activity of a segmental process may be obscured.

The distribution of fiber diameter offers another profile of muscle regeneration,[28] and dystrophy and repair.[1,34] The effect of hyperthyroidism to shift the profile toward smaller fibers has recently been demonstrated.[7] In the present study, there was also a left shift in fiber diameter distribution in treated mdx TA. This shift indicates that more dystrophic injury had prompted regeneration during PTU treatment, and that the new myotubes remained smaller than in untreated mdx TA.

The short-term sequelae of crush injury and the synchronous regeneration of myotubes were similar to previous reports.[17,25] The use of crush injury during a systemic treatment permitted a focused study of the effects of hypothyroidism on the timing of muscle repair. We also compared those observations in a direct pairwise fashion (by repeated measures ANOVA), to the effects of treatment on the muscular dystrophy in the contralateral mdx limb, to partly account for the between-subjects variation within each group. The density of myotubes in operated mdx TA was consistently and significantly larger than in control operated TA, according to the ANOVA (strain effect, Table 3). This is not in agreement with a previous study,[17] which showed a similar regenerative capacity and cell turnover in mdx and control mice, possibly due to small group sizes in that report.

The influence of hypothyroidism on muscle repair after crush was apparent in three types of double-blinded observation: the gross appearance of muscles, general histopathology, and morphometric assessment. There was more damage at the crush site of PTU-treated than untreated mdx TA. There was also a clear separation of operated mdx muscle sections into groups with either a small or large necrotic crush site and many or fewer myotubes, and these groups were decoded as untreated and PTU-treated mdx TA respectively.

A significant reduction of myotube density after PTU was observed in the surviving zone of operated mdx TA, where new myotubes are fusing to surviving fibers. This suggests that hypothyroid-

ism affects muscle repair during early formation of myotubes, possibly during fusion of muscle precursor cells. The observation of myotubes in treated TA, which appeared shorter and contained fewer nuclei than those in untreated TA, is in agreement with the idea that there may be a delay of fusion-related processes induced by hypothyroidism. mdx myotubes in vitro synthesize greater than normal concentrations of the phospholipids which permit membrane fluidity and could foster membrane fusion;[3] thyroid hormone may interact with that aspect of metabolism.

The reduced density of myotubes in the surviving zone of TA in PTU-treated mdx mice, also indicates that repair from ongoing dystrophy was affected, since that zone had, by definition, survived the crush. However, by 11 weeks of age, the dystrophic process has slowed, and "endogenous" regeneration would play a small part, accounted for by the comparison to untreated mdx muscle. The worsening of dystrophy by PTU treatment also suggests that processes early in myogenesis are regulated by thyroid hormone. Since the inflamed area was larger in hypothyroid than in euthyroid mdx mice, compensation for dystrophy by new fiber formation may have been delayed by PTU.

The finding of central nuclei in control fibers in the surviving zone suggests that a response to injury occurs in fiber segments quite distant from the site of damage. This may be the zone where many new myoblasts and muscle precursors could be localized by careful autoradiography studies. Since the CN:PN ratio in the distal zone was greater than in the proximal surviving zone (Table 3), the proximal origin of the TA blood supply may have a role in the proximodistal feature of fiber response to injury.

Production of new myotubes is dependent on rapid production and fusion of muscle precursors. Thus the difference between regenerative capacity in control and mdx muscles[5,34] may lie in a higher number of muscle precursors in mdx compared to control muscle. DMD muscle also has more satellite cells than normal human muscle,[32] although their capacity for division decreases with age.[33] As many of the peripheral nuclei in older regenerated mdx muscle would be satellite cells, with myonuclei internal in fibers, the proportion of satellite:myonuclei may approach 1:1 in adult mdx TA (as estimated by the counts of total nuclei in older mdx muscle), and would certainly be much greater than in younger mdx or normal muscle. In young normal mouse muscle, satellite cells represent up to 30% of total nuclei within the external lamina (by electron microscopy),[29] while the proportion is typically reduced in adult muscle to as low as 2% depending on the muscle.[13,22,31] Thus, a crush of mdx muscle would stimulate a larger pool of precursor cells than in control TA, such that mdx muscle could respond better than control muscles. Therefore, the scale of PTU-induced changes would be smaller than in mdx muscle, since there are fewer control muscle precursor cells, whether those effects are directly on the precursors, or on their fusion into myotubes.

mdx muscle precursors as a population might also be more activated than control myosatellite cells, due to ongoing dystrophy, and that mobilization could enable faster repair after crush injury. Similarly, more rapid and effective muscle regeneration subsequent to an injury which denervates and devascularizes muscles was noted between the mdx and control strains.[5,34] It is not known whether the proportion of mdx muscle precursors (satellite cells) that respond to injury with DNA synthesis and cell division differs from the control precursor population, but such differences have been reported between species and muscles. Estimates of the satellite cell labeling index with ^{3}H-thymidine in normal muscles are very variable (31% in normal rat muscle;[30] 3.5% in normal mouse TA;[29] about 20% in Swiss and BALB/c mouse TA.[15] The presumably larger number of those satellite cells in mdx muscle (this study and Zacharias and Anderson),[34] and a faster than normal doubling time of ^{3}H-thymidine labelled muscle cells,[1] could underlie the effective recovery from crush injury. Similar explanations of a greater number and density of replicating precursors, and possible faster cell cycling and onset of replication after injury were thought to account for the better regeneration in Swiss than in BALB/c mice, observed in a number of studies.[15,16,26] In any case, the final outcome of repair in mdx muscle might be a better measure for that regeneration, and be more comparable to the outcome of DMD.

Angiogenesis and the connective tissue response are also included in muscle repair. The removal of debris from the site of injury may have been delayed by PTU treatment, since sex, strain, and age differences in phagocytosis are possible.[14] As these processes are modulated in part by basic fibroblast growth factor (bFGF), present in large amounts in mdx muscles[3] and to lesser extent in DMD and canine dystrophy,[6] the role of bFGF in those tissues during early expression of muscle regulatory genes needs to be studied during pro-

cesses such as crush injury and dystrophy. This work tells us about muscle regeneration, and what might inhibit the process. Circumstances that demand muscle repair, such as surgery and dystrophy, should consider the metabolic milieu during treatment. Considering the possibility of myoblast transfer, and occupational and physical therapy treatments of DMD patients, optimal metabolic support of muscle regeneration appears to be crucial to the outcome of treatment.

REFERENCES

1. Anderson JE, Ovalle WK, Bressler BH: Electron microscopic and autoradiographic characterization of hindlimb muscle regeneration in the mdx mouse. *Anat Rec* 1987;219: 243–257.
2. Anderson JE, Bressler BH, Ovalle WK: Functional regeneration in the hindlimb skeletal muscle. *J Muscle Res Cell Motil* 1988;9:499–516.
3. Anderson JE, Lui L, Kardami E: Distinctive patterns of basic fibroblast growth factor (bFGF) distribution in degenerating and regenerating areas of dystrophic (mdx) striated muscles. *Dev Biol* 1991;147:96–109.
4. Anderson JE: Myotube phospholipid synthesis and sarcolemmal ATPase activity in dystrophic (mdx) mouse muscle. *Biochem Cell Biol* 1991;69:835–841.
5. Anderson JE: Dystrophic changes in mdx muscle regenerating from denervation and devascularization. *Muscle Nerve* 1991b;14:268–279.
6. Anderson JE, Kakulas BA, Jacobsen PF, Johnsen RD, Kornegay JN, Grounds MD. Comparison of basic fibroblast growth factor in X-linked dystrophin-deficient myopathies of human, dog and mouse. *Growth Factors* (in press).
7. Anderson JE, Liu L, Kardami E: The effects of hyperthyroidism on muscular dystrophy in the mdx mouse: greater dystrophy in cardiac and soleus muscle. *Muscle Nerve* (in press).
8. Bridges LR: The association of cardiac muscle necrosis and inflammation with the degenerative and persistent myopathy of mdx mice. *J Neurol Sci* 1986;72:147–157.
9. Bulfield G, Siller WG, Wight PAL, Moore KJ: X-chromosome linked muscular dystrophy (mdx) in the mouse. *Proc Natl Acad Sci USA* 1984;81:1189–1192.
10. Coulton GR, Morgan JE, Partridge TA, Sloper JC: The mdx mouse skeletal muscle myopathy: I. A histological, morphometric and biochemical investigation. *Neuropathol Appl Neurobiol* 1988;14:53–70.
11. D'Albis A, Lenfant-Guyot M, Janmot C, Chanane C, Weinman J, Gallien CL: Regulation of thyroid hormones of terminal differentiation in the skeletal dorsal muscle: I. Neonate mouse. *Dev Biol* 1987;123:25–32.
12. Dangain J, Vrbova G: Muscle development of mdx mutant mice. *Muscle Nerve* 1984;7:700–704.
13. Gibson MC, Schultz E: Age-related differences in absolute numbers of skeletal muscle satellite cells. *Muscle Nerve* 1983; 6:574–580.
14. Grounds MD: Phagocytosis of necrotic muscle in muscle isografts is influenced by the strain, age, and sex of host mice. *J Pathol* 1977;153:71–82.
15. Grounds MD, McGeachie JK: A model of myogenesis in vivo derived from detailed autoradiographic studies of regenerating skeletal muscle challenges the concept of quantal mitosis. *Cell Tissue Res* 1987;250:563–569.
16. Grounds MD, McGeachie JK: A comparison of muscle precursor replication in crush injured skeletal muscle of Swiss and BALB/c mice. *Cell Tissue Res* 1989;255:385–391.
17. Grounds MD, McGeachie JK: Skeletal muscle regeneration after crush injury in mdx mice: an autoradiographic study. *Muscle Nerve* 1992;15:580–586.
18. Hoffman EP, Brown RH Jr, Kunkel LM: Dystrophin: the protein product of the Duchenne muscular dystrophy locus. *Cell* 1987;51:919–928.
19. Izumo S, Nadal-Ginard B, Mahdavi V: All members of the MHC multigene family respond to thyroid hormone in a highly tissue-specific manner. *Science* 1986;231:597–600.
20. Izumo S, Nadal-Ginard B, Mahdavi V: The thyroid hormone receptor α gene generates functionally different protein isoforms by alternative splicing, in Roberts R, Schneider MD (eds): *Molecular Biology of the Cardiovascular System.* New York, Liss, 1990, vol 131, pp 111–123.
21. Karpati G, Carpenter S, Prescott S: Small caliber skeletal muscle fibers do not suffer necrosis in mdx mouse dystrophy. *Muscle Nerve* 1988;11:795–803.
22. Kelly AM: Satellite cells in the soleus and extensor digitorum longus muscles of rats. *J Cell Biol* 1975;67:206a.
23. Matoba H, Sugiura T, Murakami N: Effect of thyroidectomy on histochemical properties of the extensor digitorum longus and soleus in rats. *J Phys Fitness Jpn* 1982;31: 189–195.
24. Matsumura K, Ervasti JM, Ohiendieck K, Kahl SD, Campbell KP: Association of dystrophin-related protein with dystrophin-associated proteins in mdx mouse muscle. *Nature* 1992;360:588–591.
25. McGeachie JK, Grounds MD: Initiation and duration of muscle precursor replication after mild and severe injury to skeletal muscle of mice: an autoradiographic study. *Cell Tissue Res* 1987;248:125–130.
26. Mitchell CA, McGeachie JK, Grounds MD: Cellular differences in the regeneration of murine skeletal muscle: a quantitative histological study in SJL/J and BALB/C mice. *Cell Tissue Res* 1992;269:159–166.
27. Nwoye L, Mommaerts WFHM, Simpson DR, Seraydarian K, Marusich M: Evidence for a direct action of thyroid hormone in specifying muscle properties. *Am J Physiol* 1982;242:R401–R408.
28. Ontell M: Muscle fiber necrosis in murine dystrophy. *Muscle Nerve* 1981;4:204–213.
29. Schultz E: A quantitative study of the satellite cell population in postnatal mouse lumbrical muscle. *Anat Rec* 1974; 180:589–596.
30. Snow MH: The effects of aging on satellite cells in skeletal muscles of mice and rats. *Cell Tissue Res* 1977;185:399–408.
31. Snow MH: Satellite cell distribution within the soleus muscle of the adult mouse. *Anat Rec* 1981;201:463–469.
32. Wakayama Y: Electron microscopic study on the satellite cell in the muscle of Duchenne muscular dystrophy. *J Neuropathol Exp Neurol* 1976;35:532–540.
33. Webster C, Blau HM: Accelerated age-related decline in replicative life-span of Duchenne muscular dystrophy myoblasts: implications for cell and gene therapy. *Somat Cell Mol Genet* 1990;16:557–565.
34. Zacharias JM, Anderson JE: Muscle regeneration after imposed injury is better in younger than older mdx dystrophic mice. *J Neurol Sci* 1991;104:190–196.